

11-5-2015

Effect of Mineral and Chemical Admixtures on Durability of Cementitious Systems

Victor Tran

University of South Florida, tran249@yahoo.com

Follow this and additional works at: <http://scholarcommons.usf.edu/etd>

 Part of the [Civil Engineering Commons](#)

Scholar Commons Citation

Tran, Victor, "Effect of Mineral and Chemical Admixtures on Durability of Cementitious Systems" (2015). *Graduate Theses and Dissertations*.

<http://scholarcommons.usf.edu/etd/6040>

This Thesis is brought to you for free and open access by the Graduate School at Scholar Commons. It has been accepted for inclusion in Graduate Theses and Dissertations by an authorized administrator of Scholar Commons. For more information, please contact scholarcommons@usf.edu.

Effect of Mineral and Chemical Admixtures on Durability of Cementitious Systems

by

Victor L. Tran

A thesis submitted in partial fulfillment
of the requirements for the degree of
Master of Science in Civil Engineering
Department of Civil and Environmental Engineering
College of Engineering
University of South Florida

Major Professor: Abla Zayed, Ph.D.
Rajan Sen, Ph.D.
Kyle Riding, Ph.D.

Date of Approval:
October 28, 2015

Keywords: Setting Time, Compressive Strength,
Sulfate Durability, Calorimetry, X-Ray Diffraction

Copyright © 2015, Victor L. Tran

DEDICATION

I would like to dedicate this work to my family and friends. Without their support, I don't know how I would have accomplished the many things in my life.

ACKNOWLEDGEMENTS

I would like to thank everyone who has helped me throughout this study. I would like to thank my advisor, Dr. Zayed, for her help and support during the course of my graduate studies. I would like to thank Dr. Sen for sharing his personal experiences and for the knowledge imparted in class. I would also like to thank Dr. Riding for his time and assistance.

I express my utmost gratitude to my coworkers: Natallia, Jeremy, Andrew, Tanya, and Yuri. Thank you for your help. Natallia, you are a person who I can always go to for help. Jeremy, your help in running these experiments were greatly appreciated. Andrew, your willingness to help, as well as your positive attitude, helped me become a more positive person. Tanya, I will always remember the funny moments during our time together. Yuri, I am truly grateful for all your help. I would also like to thank Tony, Dan, and Tom. Tony, your attitude during this time together helped me greatly. Dan, you were the one who inspired me to pursue graduate school. Your willingness to help made our time together happier and made work such an enjoyable experience. I will never forget that. Tom, our time together was full of fun. It was fun going into work together with you helping, especially when I needed it. I would also like to thank the FDOT for their financial support as well as W.R. Grace for the materials donated in order to conduct this experimental work.

TABLE OF CONTENTS

LIST OF TABLES	iii
LIST OF FIGURES	v
ABSTRACT	ix
CHAPTER 1: INTRODUCTION	1
1.1 Research Objective	1
1.2 Outline of Thesis	2
CHAPTER 2: LITERATURE REVIEW	3
2.1 Introduction	3
2.2 Chemical Admixtures	4
2.3 Mineral Admixtures	6
2.3.1 Metakaolin	7
2.3.2 Silica Fume	11
2.3.3 Fly Ash	13
2.3.4 Blast Furnace Slag	15
CHAPTER 3: MATERIALS AND METHODS	19
3.1 Materials	19
3.1.1 Portland Cement	19
3.1.2 Fine Aggregate	21
3.1.3 Mineral Admixtures	21
3.1.4 Chemical Admixtures	24
3.1.5 Methodology	25
3.1.5.1 Calorimetry/Heat of Hydration	25
3.1.5.2 Mixing Procedure	28
3.1.5.3 Setting Time Determination	28
3.1.5.4 Compressive Strength	31
3.1.5.5 Sulfate Resistance	32
3.1.5.6 Phase Transformation Studies using X-Ray Diffraction	34
CHAPTER 4: RESULTS AND DISCUSSION	35
4.1 Isothermal Calorimetry and Heat of Hydration	35
4.1.1 Effect of Fly Ash Content	49
4.1.2 Effect of Blast Furnace Slag Content	52
4.1.3 Effect of Silica Fume Content	55
4.1.4 Effect of Metakaolin Content	58

4.1.5	Effect of Chemical Admixtures	61
4.2	Setting Time.....	62
4.2.1	Metakaolin	64
4.2.2	Silica Fume	65
4.2.3	Fly Ash.....	66
4.2.4	Blast Furnace Slag	67
4.2.5	Varying SP1 Dosage.....	68
4.2.6	Varying SP2 Dosage.....	69
4.3	Compressive Strength	72
4.3.1	Metakaolin	72
4.3.2	Silica Fume	73
4.3.3	Fly Ash.....	74
4.3.4	Slag	75
4.3.5	Varying SP1 Dosages	76
4.3.6	Varying SP2 Dosages	77
4.4	Sulfate Durability.....	79
4.4.1	Effect of Superplasticizer Type	80
4.4.2	Effect of Metakaolin	81
4.4.3	Effect of Silica Fume	82
4.4.4	Effect of Fly Ash.....	83
4.4.5	Effect of Blast Furnace Slag	84
4.5	XRD Analysis	86
CHAPTER 5: CONCLUSIONS AND FURTHER RESEARCH		89
5.1	Conclusions.....	89
5.2	Recommendations for Future Research	89
REFERENCES		91
APPENDIX A: PERMISSION		100

LIST OF TABLES

Table 1: Chemical Composition of As-Received Cement.....	20
Table 2: Bogue-Calculated Potential Compound Content for As-Received Cement.....	20
Table 3: Cement Phase Content Using QXRD.....	21
Table 4: Chemical Composition of Mineral Admixtures	22
Table 5: Mineral Admixture Phase Content Using QXRD	23
Table 6: Chemical Admixture Composition.....	25
Table 7: Mineral Admixtures Addition Rates for Internal Mixing (w/c= 0.485).....	26
Table 8: Mineral Admixtures Addition Rates for External Mixing (w/c= 0.485).....	26
Table 9: Mineral Admixtures Addition Rates Used in Construction for External Mixing (w/c= 0.42).....	26
Table 10: Chemical Admixtures Additions Rates for External Mixing (w/c= 0.485).....	27
Table 11: Mix Design for Setting Time with Varying Mineral Admixtures	29
Table 12: Mix Design for Setting Time with Varying Chemical Admixtures	30
Table 13: Mix Design for Compressive Strength with Varying Mineral Admixtures	31
Table 14: Mix Design for Compressive Strength for Varying Chemical Admixtures	32
Table 15: Mixture Design for Sulfate Mortar Bars.....	33
Table 16: Heat of Hydration for Binary Cement-Mineral Admixture Combinations using Internal Mixing (w/c= 0.485).....	46
Table 17: Amount of Sand Used for Normal Consistency for Mixtures with Varying Mineral Admixtures	63

Table 18: Amount of Sand Used for Normal Consistency for Mixtures with Varying Chemical Admixtures.....	63
Table 19: Phase Constituents of SW Paste at 1 Day.....	87
Table 20: Phase Constituents of 52% Slag Paste at 1 Day	87

LIST OF FIGURES

Figure 1: Cumulative Particle Size Distribution for Cement and Mineral Admixtures	24
Figure 2: Heat Flow Plot for the OPC Cement Used in this Study	35
Figure 3: Heat Flow for Mixtures Prepared with Mineral Admixtures Normalized by Mass of Cementitious Materials (Internal Mixing, $w/c= 0.485$).....	37
Figure 4: Total Heat for Mixtures Prepared with Mineral Admixtures Normalized by Mass of Cementitious Materials (Internal Mixing, $w/c= 0.485$).....	38
Figure 5: Measured Heat Flow of the OPC/FA Sample Compared to the Control OPC Sample Normalized by the Mass of Cement (Internal Mixing, $w/c= 0.485$)	39
Figure 6: Measured Heat Flow of OPC and OPC/SF Pastes Normalized by Mass of Cement (Internal Mixing, $w/c= 0.485$).....	41
Figure 7: Measured Heat Flow of OPC and OPC/MK Pastes Normalized by Mass of Cement (Internal Mixing, $w/c= 0.485$).....	42
Figure 8: Measured Heat Flow of OPC and OPC/Slag Pastes Normalized by Mass of Cement (Internal Mixing, $w/c= 0.485$).....	45
Figure 9: Measured Heat Flow of Cement and Mineral Admixture Samples Normalized by Mass of Cement (Internal Mixing, $w/c= 0.485$).....	47
Figure 10: Total Heat of Cement and Mineral Admixture Samples Normalized by Mass of Cement (Internal Mixing, $w/c= 0.485$).....	47
Figure 11: Measured Heat Flow of OPC and OPC/Mineral Admixture Pastes Normalized by Mass of Cement (External Mixing, $w/c= 0.42$)	48
Figure 12: Total Heat of Mineral Admixture Samples Normalized by Mass of Cement (External Mixing, $w/c= 0.42$).....	49
Figure 13: Measured Heat Flow of Cement/Fly Ash Pastes Normalized by Mass of Cement (External Mixing, $w/c= 0.485$)	50
Figure 14: Total Heat of Cement/Fly Ash Pastes Normalized by Mass of Cement (External Mixing, $w/c= 0.485$).....	50

Figure 15: Measured Heat Flow of Cement/Fly Ash Pastes Normalized by Mass of Cementitious Materials (External Mixing, w/c= 0.485)	51
Figure 16: Total Heat of Cement/Fly Ash Pastes Normalized by Mass of Cementitious Materials (External Mixing, w/c= 0.485)	51
Figure 17: Measured Heat Flow of Cement/Slag Pastes Normalized by Mass of Cement (External Mixing, w/c= 0.485).....	53
Figure 18: Total Heat of Cement/Slag Pastes Normalized by Mass of Cement (External Mixing, w/c= 0.485)	53
Figure 19: Measured Heat Flow of Cement/Slag Pastes Normalized by Mass of Cementitious Materials (External Mixing, w/c= 0.485).....	54
Figure 20: Total Heat of Cement/Slag Pastes Normalized by Mass of Cementitious Materials (External Mixing, w/c= 0.485)	54
Figure 21: Measured Heat Flow of Cement/Silica Fume Pastes Normalized by Mass of Cement (External Mixing, w/c= 0.485)	56
Figure 22: Total Heat of Cement/Silica Fume Pastes Normalized by Mass of Cement (External Mixing, w/c= 0.485).....	56
Figure 23: Measured Heat Flow of Cement/Silica Fume Pastes Normalized by Mass of Cementitious Materials (External Mixing, w/c= 0.485).....	57
Figure 24: Total Heat of Cement/Silica Fume Pastes Normalized by Mass of Cementitious Materials (External Mixing, w/c= 0.485)	57
Figure 25: Measured Heat Flow of Cement/Metakaolin Pastes Normalized by Mass of Cement (External Mixing, w/c= 0.485).....	59
Figure 26: Total Heat of Cement/Metakaolin Pastes Normalized by Mass of Cement (External Mixing, w/c= 0.485).....	59
Figure 27: Measured Heat Flow of Cement/Metakaolin Pastes Normalized by Mass of Cementitious Materials (External Mixing, w/c= 0.485).....	60
Figure 28: Total Heat of Cement/Metakaolin Pastes Normalized by Mass of Cementitious Materials (External Mixing, w/c= 0.485).....	60
Figure 29: Measured Heat Flow of OPC and OPC/Chemical Admixture Pastes Normalized by Mass of Cement (External Mixing, w/c= 0.485)	61

Figure 30: Measured Total Heat of OPC and OPC/Chemical Admixture Pastes Normalized by Mass of Cement (External Mixing, w/c= 0.485)	62
Figure 31: Mortar Setting Time for Metakaolin Mixtures.....	64
Figure 32: Mortar Setting Time for Silica Fume Mixtures.....	65
Figure 33: Mortar Setting Time for Fly Ash Mixtures	66
Figure 34: Mortar Setting Time for Slag Mixtures.....	67
Figure 35: Mortar Setting Time for Varying SP1 Dosage with No Mineral Admixture Replacement.....	68
Figure 36: Mortar Setting Time for Varying SP1 Dosage for Metakaolin Mixtures.....	69
Figure 37: Mortar Setting Time for Varying SP2 Dosage with No Mineral Admixture Replacement.....	70
Figure 38: Mortar Setting Time for Varying SP2 Dosage for Silica Fume Mixtures.....	70
Figure 39: Mortar Setting Time for Varying SP2 Dosage for Fly Ash Mixtures	71
Figure 40: Mortar Setting Time for Varying SP2 Dosage for Slag Mixtures.....	71
Figure 41: Compressive Strength of Metakaolin Mixtures.....	72
Figure 42: Compressive Strength of Silica Fume Mixtures.....	73
Figure 43: Compressive Strength of Fly Ash Mixtures	74
Figure 44: Compressive Strength of Slag Mixtures.....	75
Figure 45: Compressive Strength of Control Mixtures with Varying SP1 Dosage	76
Figure 46: Compressive Strength of Metakaolin Mixtures with Varying SP1 Dosage	77
Figure 47: Compressive Strength of Control Mixtures with Varying SP2 Dosage	78
Figure 48: Compressive Strength of Silica Fume Mixtures with Varying SP2 Dosage	78
Figure 49: Compressive Strength of Fly Ash Mixtures with Varying SP2 Dosage	79
Figure 50: Compressive Strength of Slag Mixtures with Varying SP2 Dosage	79
Figure 51: Effect of SP on Length Change of Mortar Sample in 5% Na ₂ SO ₄ Solution.....	81

Figure 52: Effect of Metakaolin on Length Change of Mortar Sample in 5% Na ₂ SO ₄ Solution.....	82
Figure 53: Effect of Silica Fume on Length Change of Mortar Sample in 5% Na ₂ SO ₄ Solution.....	83
Figure 54: Effect of Fly Ash on Length Change of Mortar Sample in 5% Na ₂ SO ₄ Solution.....	84
Figure 55: Effect of Slag on Length Change of Mortar Sample in 5% Na ₂ SO ₄ Solution	86
Figure 56: XRD Analysis of 52% Slag at Time of Disintegration and the Control	88

ABSTRACT

Mineral and chemical admixtures are used today in almost all concrete mixtures to improve concrete fresh and hardened properties, and to enhance concrete durability. In this study, four mineral and four chemical admixtures were investigated: namely, metakaolin (MK), silica fume (SF), Class F fly ash (FA), blast-furnace slag (BFS), two high-range water reducers (SP), water reducer/retarder (WRD), and air-entrainer (AEA). The objective of this study is to assess the effects of commonly used mineral and chemical admixtures on the durability of the cementitious system. Two durability issues were addressed in this study: the potential of the cementitious system to generate heat, and sulfate durability. The properties studied here included heat of hydration (HOH) measurements using isothermal calorimetry, setting properties, compressive strength, and expansion on exposure to a sodium sulfate solution. X-ray diffraction was used to characterize the as-received materials and explain failure trends.

The findings of this study indicate that silica fume inclusion sustains superior durability in comparison to the other mineral admixtures considered here. Replacement levels as low as 10% outperformed the other admixtures studied. Fly ash showed improvement in the workability of the mixes, but had the lowest compressive strength results and might pose challenges when the rate of strength gain is critical. However, Class F fly ash mixtures showed better performance than unblended mixtures when exposed to a sulfate source. Metakaolin mixes showed higher heat evolution among all the mixtures studied here. This can potentially lead to durability concerns, especially when temperature rise is a design concern. Blast-furnace slag also improved the

workability of the mixes and the later compressive strength, but had mixed performances when examined for sulfate durability.

CHAPTER 1: INTRODUCTION

1.1 Research Objective

The objective of this research is to investigate the effects of mineral and chemical admixtures, commonly used in Florida structures, on durability. Durability issues addressed here include the potential of the cementitious mixtures to generate heat, and aspects of sulfate durability. In this research, four mineral admixtures were studied: metakaolin, silica fume, Class F fly ash and blast-furnace slag, in addition to four chemical admixtures: two high-range water reducers, water reducer/retarder, and an air-entrainer. Measurements of HOH were determined on plain paste as well as binary systems of mineral admixture, with and without chemical admixtures. Setting time was determined on mortar samples following ASTM C807-13 [1] while hardened properties were determined using compressive strength measurements following ASTM C109-13 [2]. Sulfate durability was determined by length change in a Na_2SO_4 solution according to ASTM C1012-12 [3]. HOH is an important concept to assess as it identifies the potential of a specific cementitious system to contribute to concrete temperature rise, a parameter that is responsible for thermal stresses and higher potential of cracking in massive elements. Setting time determination is an important concept to consider because it notify the contractor, the time, in which to remove formwork. Compressive strength is important in that it determines the strength capacity of the mixture. Sulfate resistance is important to consider for any mixture that will come in contact with water, in which the sulfate ions permeate through concrete and possibly cause expansion and/or strength loss. The temperature rise, setting time, compressive strength, and sulfate resistance of a mixture can be determined by the cement properties, as well as properties modifications through

the use of mineral and chemical admixtures. This work is supported in part by the Florida Department of Transportation and US Department of Transportation study on the “Effect of Chemical and Mineral Admixtures on Performance of Florida Structural Concrete” and “Long-Life Slab Replacement Concrete”. Therefore parts of this write-up are shared with previously submitted reports to the funding agency. “The opinions, findings and conclusions expressed in this publication are those of the author and not necessarily those of the Florida Department of Transportation or the U.S. Department of Transportation”. Approval from the FDOT are presented in Appendix A.

1.2 Outline of Thesis

Chapter 2 presents a summary of the state of knowledge of mineral and chemical admixtures on heat of hydration (HOH), sulfate durability, and fresh and hardened properties of the cementitious system. Chapter 3 outlines the materials and methodologies used throughout this study. Chapter 4 presents the findings and discussion of the experimental trends. Chapter 5 presents the conclusions, as well as recommendations for future research.

CHAPTER 2: LITERATURE REVIEW

2.1 Introduction

In the past decades, cement characteristics have changed significantly. The driving force for many of the current changes is to increase the early strength of concrete. The change encompasses chemical as well as physical properties. Mineralogical changes include substantial increase in tricalcium silicate content while physical changes include substantial increase in cement fineness by about a factor of 3 [4].

Concrete mixtures nowadays incorporate several chemical and mineral admixtures. While mineral admixtures are less evolving, there are several chemical admixtures that continue to be introduced in the market on regular basis. These additions can be possibly problematic due to the existing potential of undesirable interaction between the different components in the concrete mixture.

Once water is added to Portland cement, hydration of cement initiates immediately. Cement hydration is exothermic in nature and can be divided into 5 stages, which are typically referred to in the literature as dissolution, dormant, acceleration, deceleration and steady state. The reactions are chemical and diffusion controlled. Hydration of tricalcium aluminate is primarily controlled by calcium sulfates phases [5]. Insufficient amounts of calcium sulfate can result in setting problems such as flash set. Several forms of calcium sulfates that are present in Portland cement include anhydrite, hemihydrate and gypsum; they have different solubilities and therefore their availability and contribution to hydration kinetics can be different.

The SO_3/A_2O_3 ratio in Portland cement is critical to optimize in order to control the hydration of C_3A and subsequently the hydration of C_3S to ensure proper setting of concrete mixtures. For chemical and mineral admixtures, incompatibility issues can arise when their presence within a specific cementitious system affect the ratio through increasing either the sulfates or the aluminates without making proper adjustments [6], [7], [8].

It is therefore important to assess the effects of different chemical and mineral admixtures combination on the physical properties of the cementitious system in addition to their effect on its durability. Durability in the current study focuses on the potential of the cementitious system to generate heat and its performance upon exposure to a sodium sulfate environment.

2.2 Chemical Admixtures

While chemical admixtures are now an integral component of concrete mixtures, scientific data on many chemical admixtures and their interaction with the cementitious system is not readily available. This is partially due to the proprietary nature of the chemical formula and the continuous introduction of new admixtures. The review presented here will primarily focus on the chemical admixtures used in this research; namely, air-entraining admixtures, water reducing and retarding admixtures and superplasticizers

Air-entraining admixtures [AEA] are typically incorporated in concrete mixtures primarily to introduce a small and well distributed air system, capable of protecting concrete during freezing and thawing cycles. The admixture works on the air-water interface to reduce the surface tension of water at the interface and stabilizes air bubble. Air-entraining admixtures also improve workability. They are made of a hydrocarbon chain with a polar anionic head. The active compound most commonly used in AEAs, vinsol resin, is known to have a retarding effect on C_3S and an accelerating effect on C_3A hydration. It has been reported [8] that AEAs interact with the

soluble alkalis in cement, with the result of enhancing the formation of the air-void system. This implies that for a given air content, a lower air-entraining dosage could be used in a high alkali cement versus a low alkali cement [9], [10]. In combination with WRAs, there is a tendency to entrain more air at a given AEA dosage. However, it has been reported that the spacing factor is increased and the air void diameter is increased which can result in a less effective system for freeze-thaw protection.

Water-reducing admixtures (WRA) are used to reduce the water content for a given slump or increase workability without increasing water demand in concrete [11]. There are several types of WRAs but the focus here is on Type D (water-reducer/retarder) and Type F (high-range water-reducer) as defined by ASTM C494-13 [12]. The most common components of WRA-Type D are lignosulfonates, hydroxycarboxylic acid and sugar. While lignosulfonates and sugar delay setting and entrain air [13], hydroxycarboxylic acid does not, if used at normal dosage. Due to their retarding tendency, a lower early tensile strength is expected [14]

WRAs have been reported to affect the hydration of Portland cement [8], [15], [16], [17]. Studies using isothermal calorimetry indicated WRAs retards C_3S hydration while accelerates C_3A reaction. The effectiveness of WRDs appears to be dependent on cement fineness and tricalcium aluminate content and mineralogy. Also, the rate of dissolution of calcium sulfates in Portland cement was noted to be affected by the amount of WRDs used. In conclusion, the literature indicates that WRDs interaction with Portland cement depends on the mineralogy and phase content of cements.

In order to control retardation effects in Type D-WRAs, triethanolamine (TEA) is commonly incorporated in its formulations [10]. TEA increases the rate of reaction of sulfates with

aluminates but possibly retards silicates hydration with a decrease in the ultimate strength [7], [10], [18].

Type F high-range water reducers (superplasticizers) are more effective in reducing mixing water while improving concrete flow properties. Heikal et al. [19] investigated the effect of the dosage of 0.00, 0.50, 0.75, 1.00, and 1.50 % of polycarboxylate superplasticizer on setting time. It was determined that increasing the dosage lead to an increase in the initial setting times of paste. The initial setting time was measured using electrical conductivity-time curves. Heikal et al. also investigated the effect of the polycarboxylate superplasticizer dosage on 10% silica fume paste. It was found that up to 0.75% of the dosage, the initial setting time increases, after which the initial setting time decreases. Puertas et al. [20] investigated the effect of the dosage of 0, 0.3, 0.5, 0.7, and 1% polycarboxylate superplasticizer on paste setting time. It was determined that increasing the dosage led to an increase in setting times. The setting time of 0, 0.3, 0.5, and 0.7 was 5 h 26 min, 9 h 17 min, 16 h 42min, and 23 h 26 min, respectively. The 1% dosage was not determined. The setting time results corresponds with the results from calorimetry in that the superplasticizer retard initial cement hydration. It is shown that as the admixture dosage increased, the time of the first peak increased with the 0% dosage having its first peak at 1.2 hr. and the 1% dosage having its first peak at 7.7 hr. Jang et al. [21] investigated the effect of polycarboxylate superplasticizer on setting time of a 50% fly ash and 50% slag paste mixture. It was determined that increasing levels of superplasticizer dosage lead to an increased in setting time. The 4% dosage increased the setting time by 70 min.

2.3 Mineral Admixtures

Mineral admixtures used in this study are: Class F fly ash, metakaolin, silica fume and blast-furnace slag. They are classified as pozzolanic and cementitious. Pozzolans are materials

that have high amorphous content but can also include crystalline phases. The amorphous content is typically aluminosilicates with the exception of silica fume where the amorphous content is predominately amorphous silica. The fineness of pozzolanic materials can be similar to Portland cement, as in the case of class F fly ash, or much finer as the case of silica fume. Pozzolans react with cement hydration product, calcium hydroxide, to form calcium silicate hydrate. A pozzolanic reaction is therefore a lime consuming reaction [22].

Blast furnace slag (BFS), unlike pozzolanic materials, does not require lime for its hydration. However, the reaction is very slow and requires an activator. When incorporated in concrete mixture, BFS reacts similar to pozzolanic materials and consumes lime. BFS hydration products are calcium silicate hydrates and calcium aluminate hydrate compounds. Mineral admixtures are known to reduce permeability and therefore improve long term durability of concrete. They also increase concrete ultimate strength though the early strength might be lower than unblended concrete. In the next few sections, a literature review on each mineral admixture used in this study will be presented.

2.3.1 Metakaolin

When kaolinite clay is calcined at elevated temperatures, pozzolanic metakaolin (MK) forms with a high amorphous silica and alumina content [23], [24], [25], [26]. Incorporation of metakaolin in the cementitious system consumes lime to form C-S-H, C-A-H and C-A-S-H [27], [28]. At replacement rates of up to 30% by weight of cement, metakaolin has an accelerating effect on cement hydration. Additions of metakaolin above 30% can delay the final setting [27]. Increased formation of C-S-H results in increased compressive strength, while removal of CH results in a lower pH of the pore solution. Ambroise et al. reported that the highest compressive strengths are achieved at 10% cement replacement level, with 20% replacement level pastes having

similar compressive strengths to that of the OPC paste. Similar results were obtained for mortar [27]. Other researchers have similarly reported 10% replacement to be optimal for maximizing compressive strength [29], [30]. MK has been shown to be effective in reducing concrete expansion due to alkali-aggregate reaction [26], [31] as well as due to external sulfate attack [32], [33].

Brooks et al. [34] had investigated the concrete setting time of 5, 10, and 15% replacement metakaolin and found that for the setting times, 10% had the longest setting time of 9.24 hr. The setting time increases from 5 to 10% metakaolin and then decrease afterwards. There appears to be little difference in setting times when the replacement level is increased to 15%, which has a setting time of 9.31 hr. The 5% replacement had a setting time of 8.82 hr. At all levels of replacement, the final setting time increased compared to the control mixture which had a setting time of 7.7 hr. Li and Ding [35] investigated the setting time of paste at a 10% replacement level of metakaolin and found that the final setting time was shorter than the control. It was determined that the final setting time of the metakaolin mixture was 2 hr 12 min while the setting time of the control mix was 3 hr 27 min. The differences in setting time by the two studies can be attributed to the w/c ratio of both studies. The study by Brooks et al. investigated setting times of mixtures while maintaining the same w/c ratio. On the other hand, Li and Ding investigated the setting time of paste at a normal consistency. This difference can be attributed to the higher water demand as the replacement level was increase to ensure a proper hydration of cement.

Poon et al. [36] investigated the effect of metakaolin at a 5, 10, and 20% replacement level at 2 different w/c ratio of 0.3 and 0.5 on concrete compressive strength. It was found that 10% metakaolin had the highest compressive strength at all test age for both w/c ratio. The 28 day compressive strength for 10% metakaolin was 116.8 and 66.2 MPa for the w/c ratio of 0.3 and 0.5,

respectively. The replacement level of 20% metakaolin showed a decrease in compressive strength for all test ages at both w/c ratio compared to 10% metakaolin. Wild et al. [37] investigated the replacement levels of 0, 5, 10, 15, 20, 25, and 30% metakaolin. It was determined that the optimum level of metakaolin for these mixes was at a replacement level of 20% at a w/c ratio of 0.45. It was found that at all test ages, the 20% replacement level had the highest compressive strength. Metakaolin contributes to compressive strength in that it is a highly reactive pozzolans. According to Wild et al. [37], there are three factors that influence the effect of metakaolin to compressive strength: the filler effect, the acceleration of cement hydration, and the pozzolanic reaction with CH. Kadri et al. [38] investigated two metakaolins with different surface areas at a 10% replacement level. It was determined that the metakaolin with the higher specific surface had a relative strength of 1.2 compared to the control from 7 to 56 days. The metakaolin with the smaller specific surface had a relative strength of 1.1 to the control. Li and Ding [35] investigated 10% replacement by metakaolin and found an increase in strength of 8 MPa for the 28 day compressive strength. Roy et al. [39] investigated the effect of metakaolin at a replacement level ranging from 0 to 22.5%. It was determined that at a replacement level of 22.5%, the 28 day compressive strength was 97.82 MPa, which is higher than that of the control mixture of 91.00 MPa.

Al-Akhras [32] investigated the effect of metakaolin replacement levels ranging from 0 to 15% on sulfate expansion at a w/c ratio of 0.5 and 0.6. Each specimen was non-air entrained and exposed to a sulfate environment after 28 days of an initial moist curing. The results showed that the increasing replacement levels led to an increase in sulfate resistance for both w/c ratio. The 10 and 15% metakaolin at a w/c ratio of 0.5 reached maximum sulfate expansion after 18 months, having a value of 0.10 and 0.07%, respectively. At a w/c ratio of 0.6, the 10 and 15% metakaolin had an expansion value of 0.13 and 0.10%, respectively. The initial cracking for the 10 and 15%

metakaolin at a w/c ratio of 0.5 was 300 and 360 day, respectively. The initial cracking for the 10 and 15% metakaolin at a w/c ratio of 0.6 was 260 and 310 day, respectively. The 5% metakaolin mix showed a lesser improvement in sulfate durability compared to the 10 and 15% mixes, reaching a max expansion at 0.17 and 0.2% and having the initial cracking occurring at 240 and 200 days at a w/c ratio of 0.5 and 0.6, respectively. According to Al-Akhras, the increase in sulfate durability can be attributed to the replacement of cement with metakaolin, the pozzolanic reaction, and the filler effect. The replacement of cement is also known as the dilution effect as using the pozzolans will reduce the cement content, meaning a reduction in the amount of C_3A , as well as formation of CH. When cement reacts with water, the C_3S and C_2S react to form C-S-H and CH, which decreases permeability because of the discontinuous pore structure, but since CH is more soluble, it can dissolve when in contact with water to increase porosity. The pozzolans then reacts and consumes CH to form secondary C-S-H to lower the permeability of the concrete by filling in pores. The filler effect of metakaolin also plays a role in that its finer particle size can fill in the gap between the bigger cement particles. This allows for a dense pore structure that lowers the permeability of the mix. Courard et al. [33] investigated the effect of 5, 10, 15, and 20% replacement level of metakaolin on the sulfate durability of mortars. It was determined that for all replacement levels of metakaolin, each mixture showed relatively no difference from each other. It appears that after 50 weeks, all metakaolin samples showed a less than 1 mm/m of variation in length, while the control mixture had around 5 mm/m. Mardani-Aghabaglou et al. [40] compared the results of fly ash, metakaolin, and silica fume at a 10% replacement level for sulfate durability. It was found that metakaolin had the second best result in sulfate durability after silica fume. Khatib and Wild [41] investigated the effect of metakaolin on the sulfate durability using 2 different types of cement having a high and intermediate C_3A content of 11.7 and 7.8%,

respectively. The results showed that for the high C_3A cement, the control, as well as the 5 and 10% metakaolin mixtures, showed disintegration between 40 and 70 days of sulfate exposure. The metakaolin mixtures with the intermediate C_3A cement showed a slower but similar trend to the high C_3A cement and had no disintegration after 550 days.

2.3.2 Silica Fume

Silica fume (SF), is another pozzolanic material which is produced as a by-product of making silicon metal. The particles have a spherical morphology and a mean particle size of at least an order of magnitude less than Portland cement [22].. Silica fume is known to accelerate the hydration of tricalcium silicate and aluminate [42], [43].

Brooks et al. [34] had investigated the concrete setting time of 5, 10, and 15% replacement silica fume and found that the final setting time of 15% silica fume had the longest setting time of 10.9 hr. The mixture of 5 and 10% silica fume had a final setting time of 8.38 and 8.72 hr, respectively. At all levels of replacement, the final setting time was increased as the control mixture had a setting time of 7.7 hr. Rao et al. [44] investigated the paste setting time of replacement level ranging from 0 to 30% silica fume. It appears that silica fume did not have an effect on final setting times.

Toutanji et al. [45] investigated the effect of silica fume on the compressive strength of paste and mortars at a w/c ratio ranging from 0.22 to 0.34. It was determined that silica fume did not have an effect on compressive strength for paste mixtures. For mortar mixture, increasing replacement levels of silica fume lead to an increase in strength. All w/c ratio ranging from 0.22 to 0.34, the replacement level of 25% had the highest compressive strength. The 16% silica fume mixtures had the second highest strength for all w/c ratios, with the control mixtures having the least. Rao [44] investigated the effect of silica fume on compressive strength and found that the

optimum silica fume replacement level was within the range of 17.5 and 22.5%. Mohamed [46] investigated the effect of silica fume on compressive strength for different curing conditions. The curing conditions tested was air-cured, a 7 day water-cured, and 28 day water-cured. For all curing conditions, the optimum level of replacement if 15% silica fume. Erdem and Kirca [47] investigated the replacement levels of 5, 10, and 15% silica fume on compressive strength. For a binder content of 500, 550, 650, and 700 kg/m³, the optimum replacement level of silica fume was 15%, and for a binder content of 600 kg/m³, the optimum level was 10%. According to Erdem and Kirca[47], improvements in compressive strength of mixes containing silica fume can be explained by the chemical and physical effects of silica fume. The pozzolanic reaction between the amorphous silica and calcium hydroxide forms more calcium-silicate-hydrate gel. The silica fume particles improve the packing at the interfacial transition zone, thus reducing the size of the pores with formation of a denser microstructure. Roy et al. [39] investigated silica fume at a replacement level ranging from 0 to 22.5%. The experiment showed that increasing the replacement levels of silica fume decreases the compressive strength from 0 to 15% but increases at 22.5%. For the 28 day compressive strength, all replacement level of silica fume had a lower compressive strength than the control mixture. The mixture containing 15% silica fume had the lowest compressive strength of 64.89 MPa compared to the control mixture of 91.00 MPa. Gesoğlu et al. [48] investigated the replacement level of 5, 10, and 15% silica fume and found the optimum level of 10% having the highest compressive strength.

Hooton [49] investigated the effect of the replacement levels of 10 and 20% silica fume on sulfate durability. It was determined that the silica fume mixtures expanded less than that of the sulfate-resisting portland cement (SRPC) with the 20% replacement level having the best results. The SRPC and all silica fume mixtures passes the proposed ASTM criteria of 0.1% expansion at

1 year. After 1.7 years, the SRPC failed the 0.1% criteria while the silica fume continued even after 5 years. Kunther et al. [50] investigated the effect of the replacement level of 6 and 12% silica fume on sulfate durability and found that the increased in level led to a decrease in length change. According to Kunther et al. it can be attributed to the high Ca/Si ratio in the 6% silica fume mixture and the low Ca/Si ratio in the 12% silica fume mixture. The high Ca/Si mixture showed a high sulfate concentration within the first mm, while the low Ca/Si mixture showed a lower sulfate binding. Cohen and Bentur [51] investigated the sulfate durability of Type I and V cement containing silica fume. The results showed that for the Type I cement, after 140 days in a sulfate solution, the silica fume mixture showed an expansion of 0.09% versus the control mixture of 0.83%. The results are more profound in the Type I cement mixture because the Type V cement perform well, even without the pozzolans additions.

2.3.3 Fly Ash

The most commonly used pozzolanic material, Class F fly ash, is a by-product of coal combustion in power plants. FA improves workability due to its particle morphology. However, its carbon content can hinder the effectiveness of AEAs. In general, its particle fineness is similar to that of Portland cement. Its amorphous content is aluminosilicates and silicates and it can contain non-reactive crystalline phases such as mullite, hematite, magnetite and quartz. Kocak and Nas [52] had investigated the paste setting time for 5, 10, 15, 20, and 25% replacement fly ash and found that the setting time had increased by 2, 4, 4, 7, and 13% of the control mix, respectively. Brooks et al. [34] investigated the concrete setting time of 10, 20, and 30% replacement fly ash and found that the final setting time of 30% fly ash had the longest setting time of 11.6 hr. 10 and 20% fly ash had a final setting time of 8.93 and 9.37 hr, respectively.

Fan et al. [53] investigated the effect of fly ash on compressive strength and found that as the replacement level of fly ash increases, the compressive strength decreases. From the results, there appears to be minimal change in compressive strength from 5 to 15% replacement. Liu et al. [54] noted that the decrease in strength is due to fly ash having little effect on the chemical activity at early ages. Poon et al. [55] investigated the effect of fly ash at a replacement level of 0, 25, and 45% at a w/c ratio of 0.24 and 0.19. It was determined that at both w/c ratio, the increased replacement levels of fly ash decreases compressive strength at the test age of 7 and 28 days. The mixture of 25% fly ash at a w/c ratio of 0.19 had the highest compressive strength at 90 days, having a 3 MPa increased compared to the control mixture. Roy et al. [39] investigated fly ash at a replacement level ranging from 0 to 30%. It was determined that increasing the replacement levels of fly ash decreases the compressive strength. For the 28 day compressive strength, all replacement level of fly ash had a lower compressive strength than the control mixture. The mixture containing 30% fly ash had the lowest compressive strength of 36.66 MPa. Gesoğlu et al. [48] investigated replacement levels of 20, 40, and 60% fly ash and found that increasing the fly ash content of the mixture would lead to a decrease in strength. Tangpagasit et al. [56] investigated the effect of packing and pozzolanic reaction on the compressive strength of fly ash in mortars. It was determined that the mean particle size of fly ash plays an important role in the compressive strength of mortars in that the increased in size leads to a decrease in strength. The fly ash, which had a mean particle size of 3.3 μm had an 87.0% strength of the control mixture while the 200 μm had a 64.8% strength. It was determined that the pozzolanic reaction of fly ash increases as the fineness increases. In addition, the packing effect of fly ash has more effect on early-age strength while the pozzolanic reaction had more effect on later-age strength.

Kandasamy and Shehata [57] investigated the effect of a high calcium fly ash on sulfate durability. It was determined that the mixture containing 40% fly ash broke before the 4 month period, while the 20% fly ash mixture broke slightly later. According to Kandasamy and Shehata, this result can be attributed to the reactive alumina content as well as the free lime contained in the fly ash. Ghafoori et al. [58] investigated the replacement levels of 15, 20, 25, and 30% fly ash of a Type V cement at three different cementitious content, 333, 374, and 416 kg/m³. For the cementitious content of 333 kg/m³, the 15% replacement level showed the best improvement in expansion, having a 13.7% decrease in expansion from the control mixture. Subsequent replacement levels showed an increased in expansion, with having the 30% replacement level showing the worst results, having a 3.4% increase in expansion from the control mixture. For the cementitious content of 374 kg/m³, the 20% replacement showed the best results, having a 14.8% decrease in expansion than the control and having the 30% replacement at a 3.7% increase. For the cementitious content of 416 kg/m³, the 30% replacement showed the best result of a 13.3% decrease in expansion and having the 15% replacement at a 4.1% decrease. According to Ghafoori, the gain in sulfate resistance can be attributed to the chemical and mechanical effect. The chemical effects include the consumption of free lime, reduction of aluminates from the replacement of cement, and the formation of calcium silicate hydrates. The mechanical effect refers the formation of ettringite compound that will acts as fillers to reduce the amount of sulfates penetrating into the concrete.

2.3.4 Blast Furnace Slag

BFS is a by-product of iron production from its ore. It is cementitious though it requires an alkali activator. It is also slow reacting. Kourounis et al. [59] investigated the paste setting of slag for 0, 15, 30, and 45% slag and found that the setting time increases as the slag content increases.

The final setting time of 0, 15, 30, and 45% slag was 185, 210, 240, and 260 min, respectively. Brooks et al. [34] investigated the concrete setting of 20, 40, and 60% slag and found that the setting time of 60% slag was the longest. The setting time of 20 and 40% slag was 12.9 and 17.8 hr, respectively. At all levels of replacement, the final setting time was increased as the control mixture had a setting time of 7.7 hr.

Menendez [60] investigated the effect of slag on compressive strength at a replacement level of 10, 20, and 35%. It was determined that at the 28 day test age, the 10, 20, and 35% slag had similar compressive strength of 39.5 to 40.9 MPa, showing no difference between the slag content. The control mixture at 28 days showed a compressive strength of 45.1 MPa which was higher than all slag mixtures. It was only at the 90 day test age, that the slag mixture had a higher compressive strength than the control having a 50.9 MPa for the 35% level versus the 46.8 MPa. Aldea et al. [61] investigated the effect of slag on compressive strength at a replacement level of 25, 50, and 75%. At a replacement level of 25% slag, the concrete showed an optimal compressive strength for both normal and steam curing. Gesoğlu et al.[48] investigated the replacement level of 20, 40, and 60% slag and found the optimum level of 40% having the highest compressive strength.

Ekolu and Ngwenya [62] investigated the effect of slag on sulfate durability on mortars immersed in a 28g/L and 50g/L Na₂SO₄ solution. It was shown that as the replacement levels of slag increase, the sulfate resistance also increase. It was determined that for the sample stored in 28g/L Na₂SO₄ solution, the expansion at 460 days for 0, 30, 50, and 70% slag was 0.28, 0.7, 0.01, and 0.00%, respectively. For the sample stored in 50g/L Na₂SO₄ solution, the results showed that the 50 and 70% replacement levels having an expansion of less than 0.1% even up to 600 days. Kandasamy and Shehata [57] investigate the replacement levels of 20, 30, and 40% slag for sulfate

durability. It was determined that the mixtures containing 30 and 40% slag enhance sulfate durability by having the expansion of 0.043 and 0.037 at the 6 month testing period, respectively. Both mixtures had an expansion of less than 0.1 after 1 year. The 20% slag mixture had an expansion of 0.069 after 6 months and 0.209 after 1 year. This shows that increasing the slag content will increase sulfate durability. According to Kandasamy and Shehata, even though slag contains alumina, its sulfate durability is attributed to its ability to incorporate Al^{3+} ions into its C-S-H. Yu et al. [63] studied the replacement levels of 0, 40, and 70% slag on sulfate durability immersed in concentration of 3, 10, and 30 g/L Na_2SO_4 solution. For all concentration of sulfate solution, the 70% slag mixture performed better than the 40% slag in that it lasted longer before failure. For slag sample in 3 g/L Na_2SO_4 solution, the slag had a lower expansion rate than the control mix. The concentration of 10 g/L Na_2SO_4 solution had the slag mixtures showing a faster expansion rate than the control while the 30 g/L Na_2SO_4 solution had the slag mixture following the same trends as the control. For the 40% slag mortars, the samples in the 10 and 30 g/L Na_2SO_4 solution showed similar trend until the 112 day in which the samples rapidly expanded until breakage at 133 and 147 day, respectively. For the 70% slag mortars, up until the 150 day, the expansion showed similar trend in all different concentration of Na_2SO_4 then the samples rapidly expanded until breakage at 240 and 150 day respectively. Ogawa et al. [64] investigated 40% mass replacement of an unmodified slag as well as a novel slag, which the chemical composition was optimized, on sulfate durability. The control mixture as well as the unmodified slag show expansion after 8 and 25 weeks, respectively. There was no further testing as both mixtures experienced breakage before the 38 week testing. The novel slag showed excellent results even after 104 weeks. Ogawa et al. [65] investigated how to improve sulfate durability on mixtures containing high alumina slag. From the results, it appears that when the alumina content of slag is

low, sulfate expansion is less when the alumina content is high, regardless of a low C_3A content in the cement. The addition of limestone powder and the increase in calcium sulfate content appears to improve sulfate durability in high alumina slag. The slag mixture with the addition of 4 and 8% limestone powder showed that the time in which the expansion was 0.1% was extended to 18 months. The 8% limestone addition showed similar results to the 4%, which showed that there is a limit to the addition of limestone to improve sulfate resistance. According to ASTM C989-13 [66], slag cement will decrease the C_3A content in cement therefore decreasing the permeability as well as CH content. High alumina content can have a negative effect at low slag replacement levels. Slag at a replacement level of 60 to 95% had high sulfate resistance, regardless of the Al_2O_3 content. High alumina slag negatively affects sulfate resistance when blended in low percentage of 50% or less.

CHAPTER 3: MATERIALS AND METHODS

This chapter presents the experimental methodology and materials used to study the effects of incorporating mineral and chemical admixtures on cementitious systems properties.

3.1 Materials

A Type I/II Portland cement was used for all mixtures prepared in this study. Mineral admixtures were Class F fly ash, silica fume, metakaolin and blast furnace slag. The chemical admixtures studied here were: two high-range water-reducers conforming to ASTM C494-13 – Type F [12] as well as ASTM C1017 -13– Type II [67], a water reducing/retarding admixture conforming to ASTM C494 -13– Type D [12], and an air-entraining admixture conforming to ASTM C260-10 [68].

3.1.1 Portland Cement

Table 1 shows the elemental oxide composition of Type I/II Portland cement used in this study as determined through X-ray fluorescence spectroscopy (XRF) according to ASTM C114-11b [69]. The corresponding potential compounds composition determined using ASTM C150-12 [70] are presented in Table 2.

Table 1: Chemical Composition of As-Received Cement

	Type I/II cement (%)
SiO ₂	20.40
Al ₂ O ₃	5.20
Fe ₂ O ₃	3.20
CaO	63.10
MgO	0.80
SO ₃	3.60
Na ₂ O	0.10
K ₂ O	0.38
TiO ₂	0.28
P ₂ O ₅	0.12
Mn ₂ O ₃	0.03
SrO	0.08
Cr ₂ O ₃	0.01
ZnO	<0.01
LOI	2.8
Total	100.1

*= Test conducted by an external certified laboratory

Table 2: Bogue-Calculated Potential Compound Content for As-Received Cement

Phase	Without Limestone Correction	With Limestone Correction
C ₃ S	52	50
C ₂ S	19	19
C ₃ A	8	8
C ₄ AF	10	9
C ₄ AF+2C ₃ A	26	26
C ₃ S+4.75C ₃ A	92	89

It has long been established that mineralogical composition of Portland cements is very critical in predicting concrete performance. Mineralogical analysis of Portland cement was conducted using x-ray diffraction and Rietveld analysis (HighScore Plus 3.1). The results are presented in Table 3.

Table 3: Cement Phase Content Using QXRD

Cement Phase	Source	SW
C ₃ S (%)	Rietveld	52.0
C ₂ S (%)	Rietveld	20.7
C ₃ A (%)	Rietveld	10.2
C ₄ AF (%)	Rietveld	5.7
Gypsum	Rietveld	4.4
Hemihydrate	Rietveld	1.6
Anhydrite	Rietveld	0.2
Calcite	Rietveld	2.1
Lime	Rietveld	0.1
Portlandite	Rietveld	2.0
Quartz	Rietveld	0.9

3.1.2 Fine Aggregate

Silica sand conforming to ASTM C778-13 [71] graded sand was used throughout this study.

3.1.3 Mineral Admixtures

The mineral admixtures used throughout this study are metakaolin, fly ash, silica fume, and slag. Metakaolin is a derived from the mineral kaolinite. Fly ash is a by-product from the combustion of coal. Silica fume is a by-product from the carbothermic reaction in the production of silicon and ferrosilicon alloys. Slag, or blast furnace slag, is a by-product from iron or steel making. The chemical oxide composition of each mineral admixture, determined through X-ray fluorescence are shown in Table 4. As mineral admixtures derive their pozzolanic activity primarily through their amorphous content, mineralogical analysis of the crystalline phases in mineral admixtures was conducted and the amorphous content subsequently quantified through using titanium dioxide as an internal standard at 10 weight percent. The results are depicted in

Table 5 where it can be seen that the amorphous content of all mineral admixtures is above 95% except for Class F fly ash where the amorphous content is in the low 70s.

Table 4: Chemical Composition of Mineral Admixtures

	Slag	Metakaolin	Silica Fume	Fly Ash (Class F)	Cement
SiO ₂	35.15	51.29	92.9	55.48	20.40
Al ₂ O ₃	14.25	44.16	0.31	27.46	5.20
Fe ₂ O ₃	0.48	0.49	0.1	6.7	3.20
CaO	41.45	<0.01	0.78	0.99	63.10
MgO	5.21	0.14	0.18	0.88	0.80
SO ₃	1.86	<0.01	<0.01	0.05	3.60
Na ₂ O	0.22	0.26	0.1	0.29	0.10
K ₂ O	0.32	0.27	0.52	2.28	0.38
TiO ₂	0.5	1.12	<0.01	1.47	0.28
P ₂ O ₅	0.01	0.06	0.09	0.21	0.12
Mn ₂ O ₃	0.22	<0.01	0.04	0.02	0.03
SrO	0.05	0.01	0.01	0.09	0.08
Cr ₂ O ₃	<0.01	0.01	<0.01	0.03	0.01
ZnO	<0.01	<0.01	0.05	0.01	<0.01
BaO	0.07	<0.01	<0.01	0.15	--
LOI	0.04	1.4	4.55	3.83	2.8
Total	99.83	99.2	99.63	99.93	100.1

*=Test conducted by an external certified laboratory

Table 5: Mineral Admixture Phase Content Using QXRD

Mineral Admixture	Mineral Phase	Amount (wt. %)
Class F Fly Ash	Mullite	16.1
	Hematite	1.6
	Magnetite	1.1
	Quartz	9.0
	Amorphous	72.2
Metakaolin	Mullite	1.0
	Illite	0.7
	Quartz	0.3
	Amorphous	98.0
Blast Furnace Slag	Melilite	1.3
	Merwinite	0.1
	Quartz	1.4
	CaO	0.1
	Calcite	0.4
	Amorphous	96.7
Silica Fume	Silicon Carbide	2.0
	Crystobalite	0.3
	Quartz	1.9
	Amorphous	95.8

Particle size analysis of the as-received materials was also conducted. It is already established in literature that cementitious materials particle size distribution has a significant effect on strength development, heat of hydration, and sulfate durability. Particle size analysis was conducted using HORIBA Instruments LA-950 laser scattering particle size analyzer and the results are presented in Figure 1. Silica fume was not measured because a dry process was used in examining the samples which was not suitable to examine silica fume due to its particles agglomeration. As the data indicates, metakaolin is the only mineral admixture, excluding silica fume, with finer particle size distribution than cement. Fly ash and slag are very similar in their particle distribution to the as-received cement.

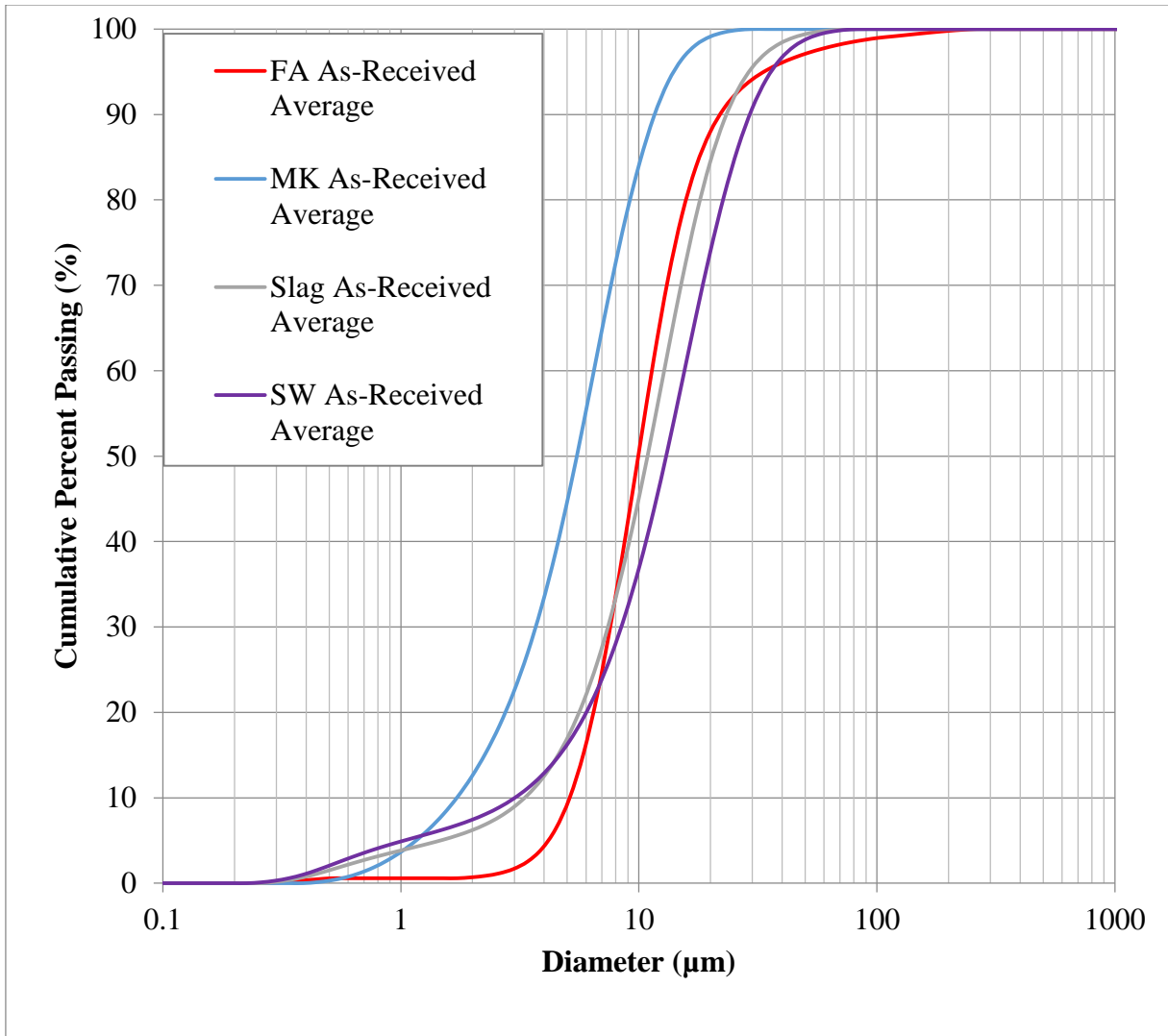


Figure 1: Cumulative Particle Size Distribution for Cement and Mineral Admixtures

3.1.4 Chemical Admixtures

Two high-range water-reducing admixtures (superplasticizers), a water-reducing/retarding admixture, and an air-entraining admixture were used in this study. The composition of the chemical admixtures are presented in Table 6 as obtained from the manufacturer's specifications.

Table 6: Chemical Admixture Composition

Admixture	Component	Percent (max)
High-Range Water-Reducing Admixture (SP1)	5-chloro-2-methyl-2H-isothiazol-3-one	0.0-1.0
	Proprietary Polyacrylate	30-50
	Carbohydrate Mist	2.0-5.0
	Water	50-100
High-Range Water-Reducing Admixture (SP2)	Polyacrylate Aqueous Solution	43-47
	Water	*
	Sodium gluconate	*
Air-Entraining Admixture (AEA)	Sodium dodecylbenzenesulfonate	1-10
Water-Reducing/Retarding Admixture (WRA)	Molasses	10-25
	Sulfate liquors and Cooking liquors	25-50
	Triethanolamine	1-10

* Data not provided by manufacturer

3.1.5 Methodology

3.1.5.1 Calorimetry/Heat of Hydration

Heat of hydration measurements were performed following Method A and B, internal and external mixing, of ASTM C1702-09 [72]. Heat flow measurements with external mixing protocol were performed using iCal-8000 calorimeter produced by Calmetrix. As for internal mixing, all the measurements were performed at the isothermal temperature of 23°C. Internal mixing was performed using TAM air isothermal calorimeter with 8 channels.

Paste samples for as-received cement were prepared with 3.3750 g of cement and 1.6370 g of water at a water to cement (w/c) ratio of 0.485. For cement-mineral admixture combinations, a portion of the cement mass was substituted by an equal mass of mineral admixture. For chemical admixtures, solutions of required concentrations were prepared volumetrically in order to minimize errors in measuring small amounts of admixture. Chemical admixtures were added to cement together with the mixing water. Mineral and chemical admixture addition rates are listed

in Table 7-10. Very limited data is available regarding the composition of chemical admixtures. Material safety data sheets (MSDS) were used to ascertain the active compounds of each admixture.

Table 7: Mineral Admixtures Addition Rates for Internal Mixing (w/c= 0.485)

Mineral Admixture	Cement Replacement (w/o)
Fly Ash, Class F	21
Metakaolin	10
Silica Fume	8
Slag	52

Table 8: Mineral Admixtures Addition Rates for External Mixing (w/c= 0.485)

Mineral Admixture	Cement Replacement (w/o)		
Fly Ash, Class F	10	-	30
Metakaolin	-	21	30
Silica Fume	10	21	30
Slag	10	21	30

Table 9: Mineral Admixtures Addition Rates Used in Construction for External Mixing (w/c= 0.42)

Mineral Admixture	Cement Replacement (w/o)
Fly Ash, Class F	21
Metakaolin	10
Silica Fume	8
Slag	52

Table 10: Chemical Admixtures Additions Rates for External Mixing (w/c= 0.485)

Chemical Admixture	Addition Rate (ml/100 kg cement)
AEA	46
WRA	300
SP1	200
SP2	397

After measuring out the required amount of dry cementitious materials and water or chemical admixture solutions, the ampules were placed in the calorimeter, and the system was allowed to reach thermal equilibrium. Then, water or solution was injected into the vial, and the paste was mixed constantly for 60 seconds. Heat flow measurements were collected for 7 days. Heat flow and cumulative heat of hydration were normalized per gram of cement in the sample, both for chemical and mineral admixtures. In the case of mineral admixtures, where different percent replacement was used for each admixture, normalizing the measurements per gram of cement rather than per gram of cementitious material eliminated this variable and allowed the admixtures to be compared based on their effect on cement hydration.

For external mixing, the mixing of the cement paste was following the mixing procedure described in [73] with the IKA WERKE mixer using the kitchen blade accessory for a total of 7 min. WRA was added to the mixing water. After combining water and cementitious materials, paste was mixed for 1 minute prior to addition of AEA, after which it was mixed for an additional 2 minutes (elapsed time: 3 min). The mixture was then rested for 2 minutes (Elapsed time: 5 min). After the rest period, superplasticizer was added to the mixture, and the sample was mixed for an additional 2 minutes (elapsed time: 7 min) at 1200 rpm rather than the stated 2000 rpm as reported by Muller et al. [73]. If there was no chemical admixture used, the same procedure was followed.

3.1.5.2 Mixing Procedure

Mortars were prepared following ASTM C109-13 [2] and mixed according to the procedure for mixing mortars following ASTM C305-14 [74]. The cementitious materials were mixed in with the cement before touching the water. The chemical admixture were weighed out in separate containers and a portion of water is added to each to ensure that all of the admixtures will be added to the mix, of which the majority is allocated to the WRA. The procedures are as presented:

1. Add all of the WRA/Water mixing to the mixing bowl.
2. Add the cementitious to the water and start the mixer at speed 1 for 30 s. (30 s)
3. Add the quantity of sand over a 30 s period at speed 1 with the last 5 s for the addition of the AEA. (60 s)
4. Stop the mixer and change to speed 2 and mix for 30 s. (90 s)
5. Stop the mixer and let stand for 90 s with the first 15 s to scrape down the sides for any mortar. (180 s)
6. Add the SP and continue mixing at speed 2 for 60 s. (240 s)

3.1.5.3 Setting Time Determination

Setting time was determined following ASTM C807-13 [1] using a modified vicat apparatus. Before each setting time determination, normal consistency was determined by varying the amount of sand to achieve a penetration target of 20 ± 4 mm after 30 s. Once normal consistency was determined, setting time was determined as the time when a penetration of 10 mm or less was achieved. The mixtures design is presented in the following tables.

Table 11: Mix Design for Setting Time with Varying Mineral Admixtures

Mix ID	Cement (g)	MK (g)	FA (g)	SF (g)	Slag (g)	Sand (g)	Dosage (ml/100 kg)				Water (g)
							AEA	WRA	SP1	SP2	
SW+SP1	750	-	-	-	-	2235	2.5	110	155	-	370
SW+SP2	750	-	-	-	-	2150	2.5	110	-	110	370
10MK	675	75	-	-	-	1985	2.5	110	155	-	370
20MK	600	150	-	-	-	1435	2.5	110	155	-	370
10SF	675	-	-	75	-	2100	2.5	110	-	110	370
10FA	675	-	75	-	-	2175	2.5	110	-	110	370
21FA	592.5	-	158	-	-	2100	2.5	110	-	110	370
30FA	525	-	225	-	-	2100	2.5	110	-	110	370
21Slag	592.5	-	-	-	158	2175	2.5	110	-	110	370
30Slag	525	-	-	-	225	2175	2.5	110	-	110	370
52Slag	360	-	-	-	390	2225	2.5	110	-	110	370

Table 12: Mix Design for Setting Time with Varying Chemical Admixtures

Mix ID	Cement (g)	MK (g)	FA (g)	SF (g)	Slag (g)	Sand (g)	Dosage (ml/100 kg)				Water (g)
							AEA	WRA	SP1	SP2	
SW+170SP1	750	-	-	-	-	2255	2.5	200	170	-	369.4
SW+170SP2	750	-	-	-	-	2150	2.5	200	-	170	369.2
10MK+170SP1	675	75	-	-	-	2050	2.5	200	170	-	369.4
10SF+170SP2	675	-	-	75	-	2175	2.5	200	-	170	369.2
21FA+170SP2	592.5	-	157.5	-	-	2175	2.5	200	-	170	369.2
52Slag+170SP2	360	-	-	-	390	2275	2.5	200	-	170	369.2
SW+100SP1	750	-	-	-	-	2235	2.5	200	100	-	369.7
SW+100SP2	750	-	-	-	-	2150	2.5	200	-	100	369.6
10MK+100SP1	675	75	-	-	-	2000	2.5	200	100	-	369.7
10SF+100SP2	675	-	-	75	-	2125	2.5	200	-	100	369.6
21FA+100SP2	592.5	-	157.5	-	-	2175	2.5	200	-	100	369.6
52Slag+100SP2	360	-	-	-	390	2250	2.5	200	-	100	369.6

3.1.5.4 Compressive Strength

Mortar cubes were prepared and tested following ASTM C109-13 [2]. Compressive strength tests were conducted on 2-in cube specimen. Testing ages were 1, 3, and 28 days, of which after the 1-day test, the mortar cubes were submerged in a saturated lime solution until testing at 3 and 28 days. The w/cementitious ratio was maintained constant for all mixtures. Mixture designs are presented in the tables below.

Table 13: Mix Design for Compressive Strength with Varying Mineral Admixtures

Mix ID	Cement (g)	MK (g)	FA (g)	SF (g)	Slag (g)	Sand (g)	Dosage (ml/100 kg)				Water (g)
							AEA	WRA	SP1	SP2	
SW+SP1	740	-	-	-	-	2035	2.5	110	155	-	353.9
SW+SP2	740	-	-	-	-	2035	2.5	110	-	110	353.9
10MK	666	74	-	-	-	2035	2.5	110	155	-	353.9
21MK	585	155	-	-	-	2035	2.5	110	155	-	353.9
10SF	666	-	-	74	-	2035	2.5	110	-	110	353.9
10FA	666	-	74	-	-	2035	2.5	110	-	110	353.9
21FA	585	-	155	-	-	2035	2.5	110	-	110	353.9
30FA)	518	-	222	-	-	2035	2.5	110	-	110	353.9
21Slag	585	-	-	-	155	2035	2.5	110	-	110	353.9
30Slag	518	-	-	-	222	2035	2.5	110	-	110	353.9
52Slag	355	-	-	-	385	2035	2.5	110	-	110	353.9

Table 14: Mix Design for Compressive Strength for Varying Chemical Admixtures

Mix ID	Cement (g)	MK (g)	FA (g)	SF (g)	Slag (g)	Sand (g)	Dosage (ml/100 kg)				Water (g)
							AEA	WRA	SP1	SP2	
SW+170SP1	740	-	-	-	-	2035	2.5	200	170	-	353.3
SW+170SP2	740	-	-	-	-	2035	2.5	200	-	170	353.1
10MK+170SP1	666	74	-	-	-	2035	2.5	200	170	-	353.3
10SF+170SP2	666	-	-	74	-	2035	2.5	200	-	170	353.1
21FA+170SP2	584.6	-	155.4	-	-	2035	2.5	200	-	170	353.1
52Slag+170SP2	355.2	-	-	-	384.8	2035	2.5	200	-	170	353.1
SW+100SP1	740	-	-	-	-	2035	2.5	200	100	-	353.6
SW+100SP2	740	-	-	-	-	2035	2.5	200	-	100	353.5
10MK+100SP1	666	74	-	-	-	2035	2.5	200	100	-	353.6
10SF+100SP2	666	-	-	74	-	2035	2.5	200	-	100	353.5
21FA+100SP2	584.6	-	155.4	-	-	2035	2.5	200	-	100	353.5
52Slag+100SP2	355.2	-	-	-	384.8	2035	2.5	200	-	100	353.5

3.1.5.5 Sulfate Resistance

Mortar bars were prepared and tested following ASTM C1012-12 [3]. Per specification, a compressive strength of 2850 psi or higher is required for initial comparator readings. If the compressive strength has not reached the requirement of 2850 psi, the mortar bars and cubes are stored in a saturated lime solution. After the initial readings, the mortar bars are to be stored in a 5% Na₂SO₄ solution. Measurements are to be taken at 1, 2, 3, 4, 8, 13, 15 weeks as well as 4, 6, 9, and 12 months. After each readings, the used solution is to be discarded and a freshly prepared solution is used. The same w/cementitious ratio was used for all mixtures.

Table 15: Mixture Design for Sulfate Mortar Bars

Mix ID	Cement (g)	MK (g)	FA (g)	SF (g)	Slag (g)	Sand (g)	Dosage (ml/100 kg)				Water (g)
							AEA	WRA	SP1	SP2	
SW	740	-	-	-	-	2035	-	-	-	-	359
SP1	740	-	-	-	-	2035	2.5	110	155	-	353.9
SP2	740	-	-	-	-	2035	2.5	110	-	110	353.9
10SF	666	-	-	74	-	2035	2.5	110	-	110	353.9
30Slag	518	-	-	-	222	2035	2.5	110	-	110	353.9
52Slag	355.2	-	-	-	384.8	2035	2.5	110	-	110	353.9
70Slag	222	-	-	-	518	2035	2.5	110	-	110	353.9
10MK	666	74	-	-	-	2035	2.5	110	155	-	353.9
20MK	592	148	-	-	-	2035	2.5	110	155	-	353.9
21FA	584.6	-	155	-	-	2035	2.5	110	-	110	353.9

3.1.5.6 Phase Transformation Studies using X-Ray Diffraction

XRD analysis was also conducted on mortar bars that had disintegrated during the duration of the test. Two samples were taken from bars: inner and outer. The sample was collected where fracture occurred, separating the inner core from the surface layer as the latter could be easily separated. Liquid nitrogen was then added to the sample and place in a vacuum to slow/stop hydration. Samples were then ground and passed through a No. 325 sieve and mixed with corundum at 20 weight percent for phase quantification. Again, Rietveld analysis was conducted for the quantification of the hydration products and anhydrous phases using ASTM C1365-11 [75].

CHAPTER 4: RESULTS AND DISCUSSION

4.1 Isothermal Calorimetry and Heat of Hydration

An important aspect of concrete durability, especially for mass elements, is the heat generated due to the chemical reaction between cement and water. The reaction is exothermic in nature thus potentially leading to significant temperature rise. It is well established that high temperature differentials is an important factor in thermal stress generation and therefore concrete cracking potential. In the current study, isothermal calorimetry was used in assessing the effectiveness of mineral admixtures in decreasing the heat of hydration in the cementitious systems containing silica fume, blast-furnace slag, metakaolin and Class F fly ash. A typical heat flow profile for a cementitious system is characterized by five distinctive stages (Figure 2) [22].

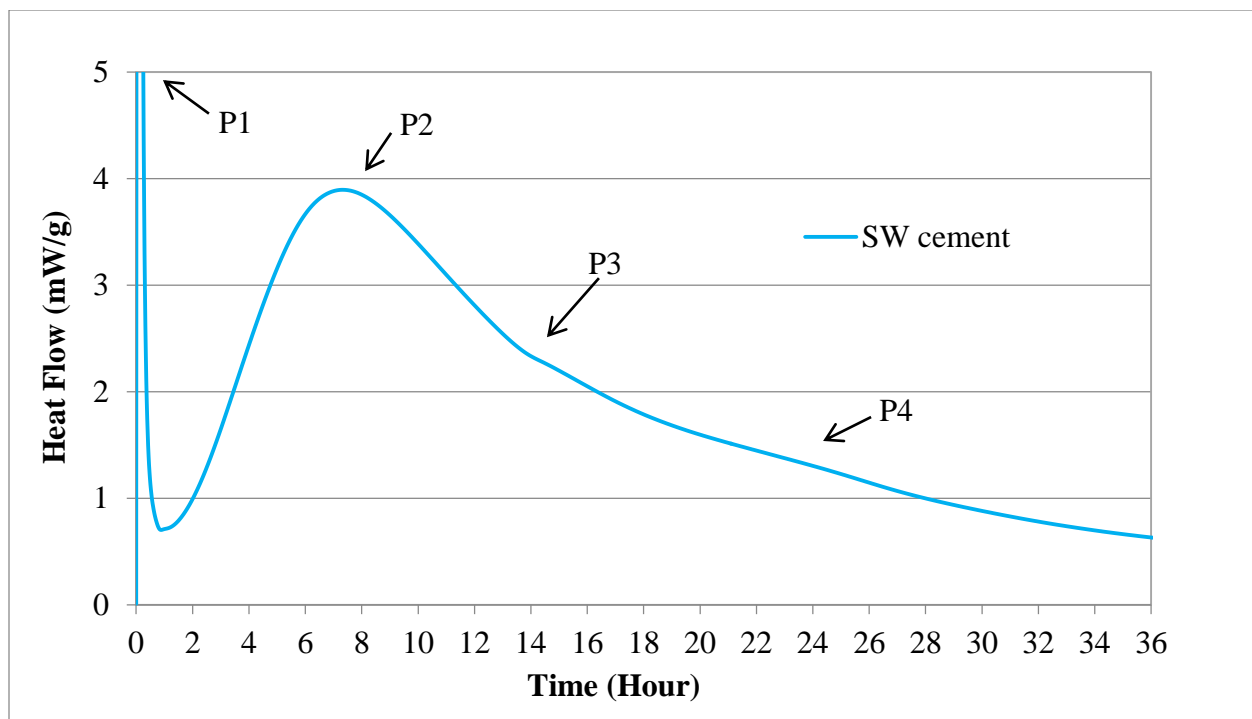


Figure 2: Heat Flow Plot for the OPC Cement Used in this Study

During the first stage, peak (P1), which occurs immediately after water is added to cement, ionic dissolution takes place with the highest rate of heat release. This is followed by the dormant period, which extends for few hours, then another high rate of heat release defining the acceleration stage and the occurrence of the C_3S main hydration peak (P2). Usually, by the time P2 occurs final set has already occurred. For properly sulfated cement, P3, occurs on the descending part of the main hydration peak in the deceleration stage of hydration. Some cements show P4, though the nature of this diffused peak has not been resolved in the literature [76]–[80].

Additions of mineral admixtures affect cement both physically and, in the case of reactive materials, chemically. The main physical effects identified in the literature are dilution and heterogeneous nucleation [81]. Figures 3 and 4 present the heat flow and total heat plots for mineral admixture samples normalized by the total mass of cementitious materials. While these plots are useful to predict compressive strength of the mixtures, they do not allow direct comparison between admixtures since each was used at a different replacement level. It has been recognized that normalizing heat flow and total heat by the mass of cement alone is more appropriate for evaluating the effect of mineral admixtures on cement hydration kinetics [82]. This normalization procedure has been applied to the data presented in Figures 5-12 as well as Table 16.

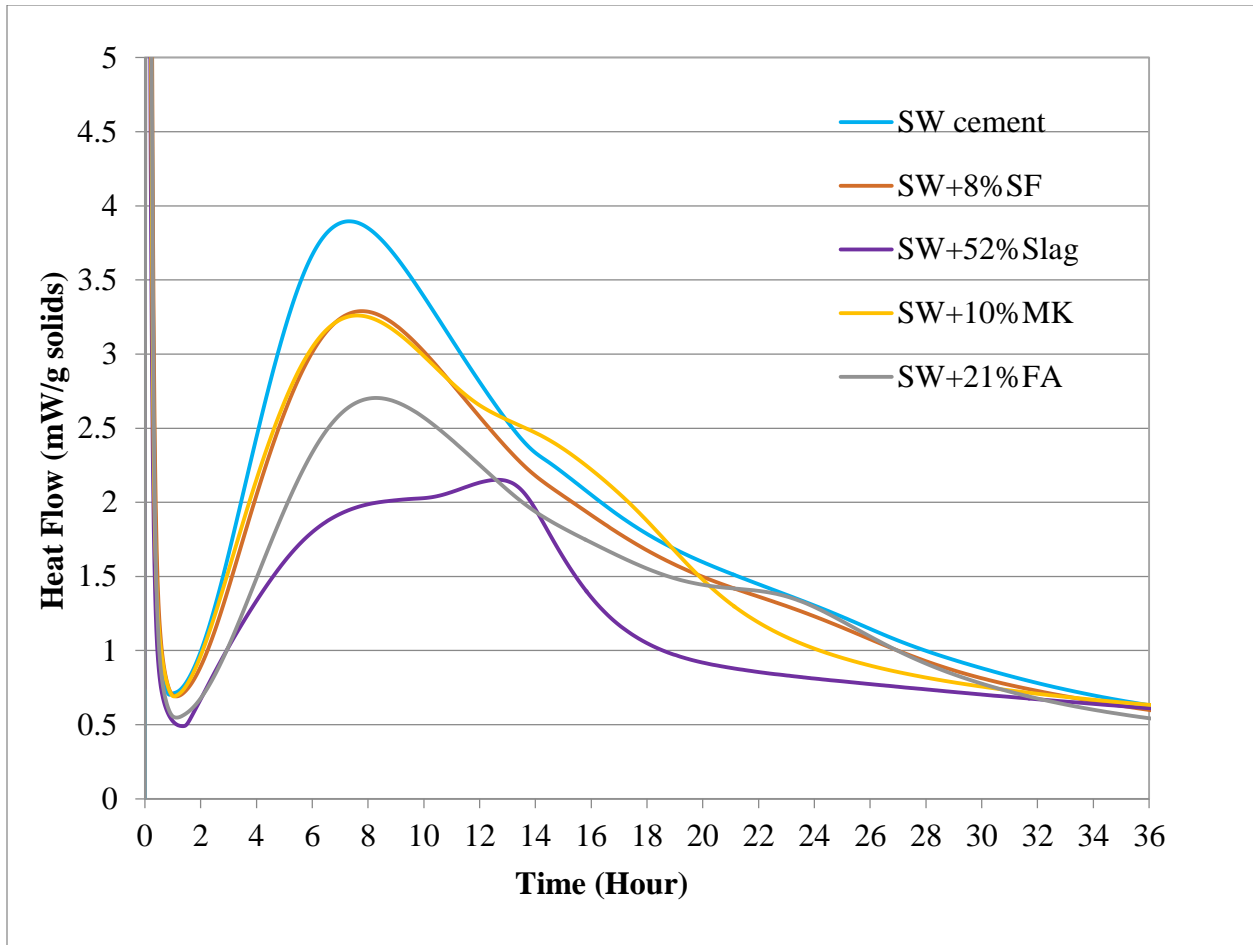


Figure 3: Heat Flow for Mixtures Prepared with Mineral Admixtures Normalized by Mass of Cementitious Materials (Internal Mixing, w/c= 0.485)

For the heat flow and total heat normalized per gram of binder, the trends show that the total heat in the cementitious system decreases with incorporating mineral admixtures. It is interesting to note that at 10% metakaolin, the cementitious system at 7 days show a total heat comparable to the control mixture.

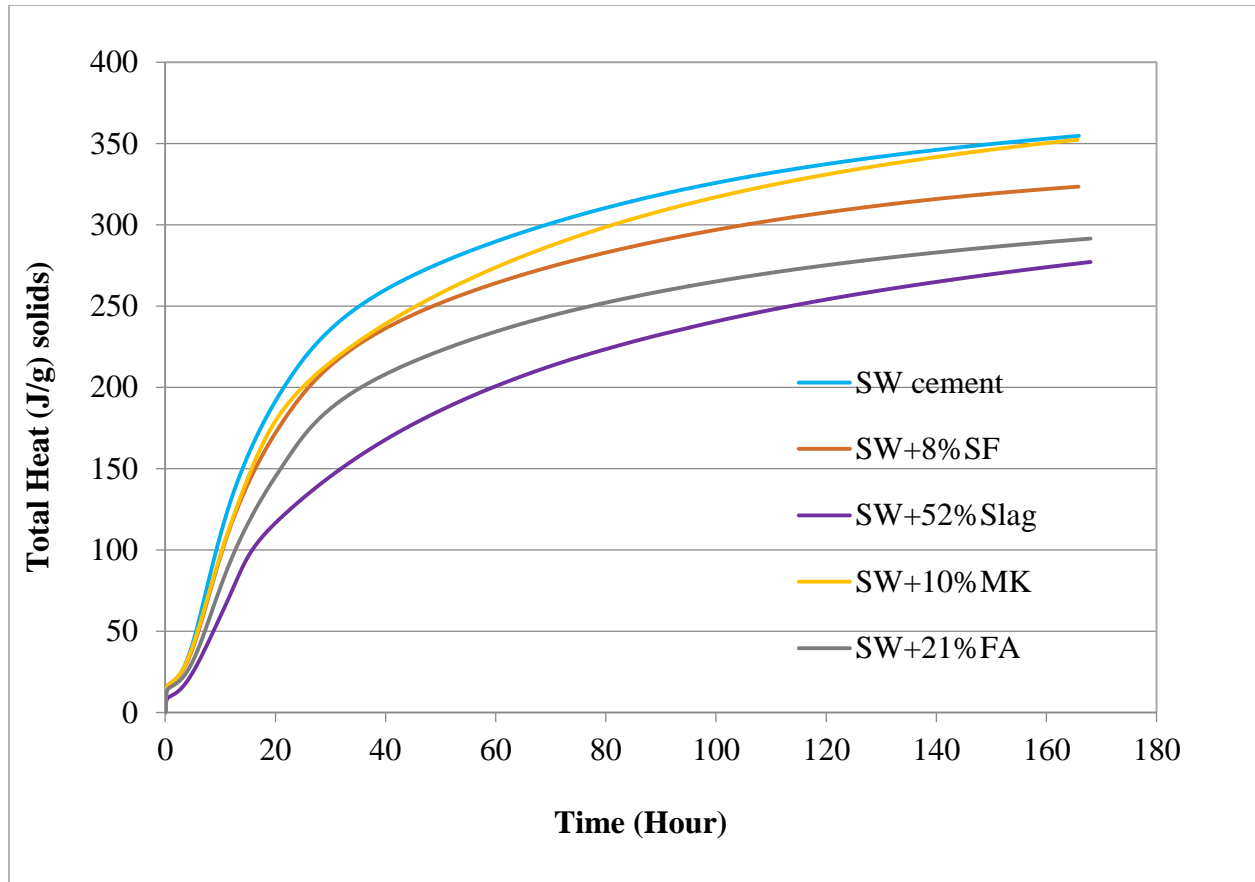


Figure 4: Total Heat for Mixtures Prepared with Mineral Admixtures Normalized by Mass of Cementitious Materials (Internal Mixing, w/c= 0.485)

As can be seen in Figure 5, addition of Class F fly ash did not have a significant effect on the length of the induction period, as expected [17]. Incorporation of FA results in a lower slope in acceleration stage. Also, the main peak position appears to shift to longer time. It has been demonstrated that the effect of fly ash on the length of the induction period depends on the cement replacement level. High-volume fly ash mixes (Class F) experience significant retardation [82], [83], while at lower replacement levels (20%) there is no significant increase of the induction period [17].

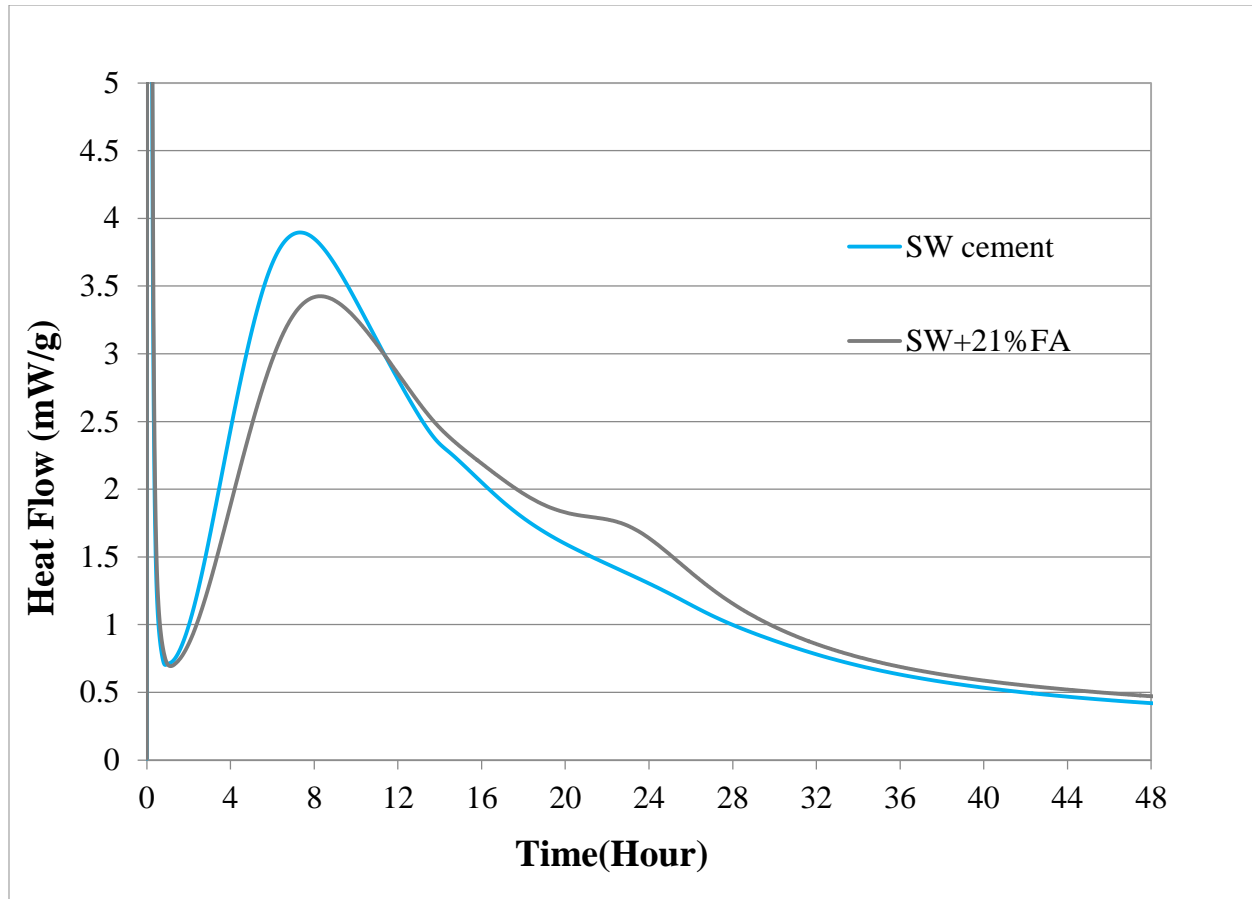


Figure 5: Measured Heat Flow of the OPC/FA Sample Compared to the Control OPC Sample Normalized by the Mass of Cement (Internal Mixing, w/c= 0.485)

This retardation can be attributed to the dilution effect [82], [84]–[86]. The sulfate depletion point is not affected by the fly ash addition as it occurs at the same time both in the OPC paste and paste prepared with fly ash. Again, this was expected as Class F fly ash does not affect sulfate consumption rate [17]. The results indicate that addition of fly ash itself, excluding the dilution effect, did not impact hydration kinetics of cement. This is in line with the conclusions made by others that Class F fly ash does not have a significant effect on hydration [86], [87].

There is a peak that occurs around 24 hours. This peak has been observed by Quennoz and Scrivener [78] in C_3S - C_3A -gypsum systems, although they were not able to explain it by XRD or microscopy analysis. They observed that the intensity and timing of this peak was dependent on

the water/solids (w/s) ratio. As the w/s increased, the intensity of the peak decreased and it occurred at later time. A more pronounced third peak in the fly ash sample may be due to the beginning of the fly ash reaction. The fly ash used in this study had a moderate amorphous content (72%). Frias et al. [88] have shown that although its reactivity is very low, fly ash does show some pozzolanic activity at 1 day.

Based on the heat flow plot presented in Figure 5, a delay in the final setting time of the fly ash sample is expected. Considering the total heat normalized by the mass of cementitious material, Figure 4, it is expected that the compressive strength of the fly ash samples will be lower than that of OPC up to 7 days.

Neither accelerating nor retarding effect was observed with silica fume addition in this study, as illustrated in Figure 6. Apart from a slight decrease in the intensity of the main hydration peak, both the heat flow and the total heat plot of the silica fume sample followed the control heat of hydration profile. The data also show that for the silica fume paste there is an increase in rate of heat flow during the first stage of hydration indicating possible effect of silica fume on enhancing C_3A hydration. There is no clear agreement in the literature regarding the effect of SF on the hydration kinetics. Lilkov et al. [89] demonstrated that SF begins to hydrate during the first hour after contact with water. Frias et al. [88] reported that pozzolanic activity of SF was double that of MK at 2 hours. Acceleration of the alite hydration by SF has been reported earlier by Wu and Young [42]. Wu and Young observed that the presence of SF increases the duration of stage 1 (initial hydrolysis) of alite and decreases the induction period. Cheng-Yi and Feldman [43] concluded that in addition to C_3S , C_3A hydration is also accelerated by the presence of SF.

Langan et al. [90] confirmed the accelerating effect of SF on cement hydration, but only at high w/c ratios. They reported a retarding effect at low w/c ratios. This effect was attributed to the

absorption of water by silica fume, which at low w/c ratios would reduce the water available for reaction with cement particles [90]. On the contrary, Kadri and Duval [91] observed acceleration of hydration process with addition of silica fume at low w/c ratios. With respect to the total heat of hydration (HOH), they observed an increase in HOH with 10% cement replacement by SF. However, at 30% replacement level, HOH was decreased. Zelic et al. [92] concluded that the acceleration of early-age cement hydration by SF is strictly due to the filler effect and contribution from the pozzolanic reaction could only occur after 3 days.

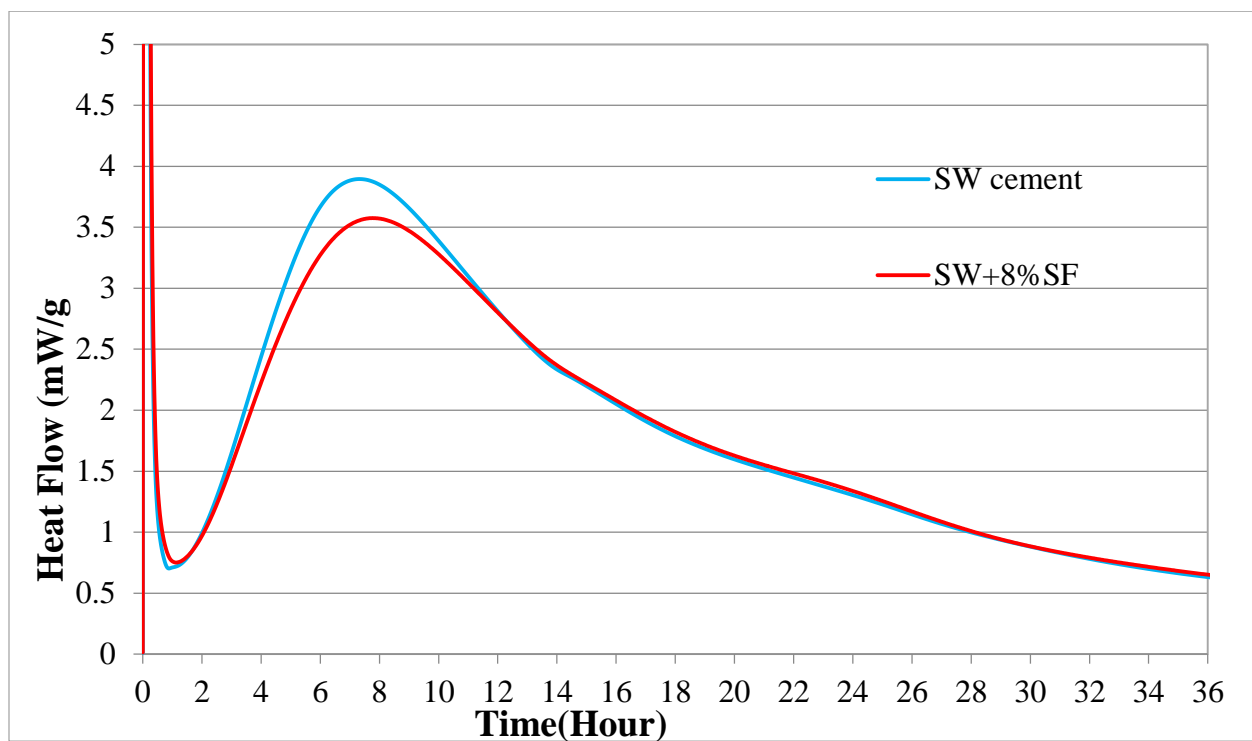


Figure 6: Measured Heat Flow of OPC and OPC/SF Pastes Normalized by Mass of Cement (Internal Mixing, w/c= 0.485)

It has been reported that due to its fine particle size, silica fume requires addition of superplasticizer even at high w/c ratios for proper dispersion [93]. As previously indicated, large agglomerations were observed in the silica fume sample during particle size determination. Manual mixing inside the calorimeter, even at w/c ratio of 0.485, was not sufficient to disperse

these agglomerates, which most likely were too large to accelerate hydration through heterogeneous nucleation. It appears that the dilution effect, which would have resulted in retardation, was offset by the pozzolanic reaction of silica fume. The degree of silica fume reaction was most likely reduced by its agglomeration.

Addition of metakaolin was expected to have a measurable effect on cement hydration. Initial reaction of MK (during the first 50 hours) is very rapid [94], with measurable pozzolanic activity reported as early as after 2 hours of hydration [88]. Since reactivity of metakaolin is related to its amorphous content [23], [25], MK used in this study was expected to be highly reactive due to its 98% amorphous content.

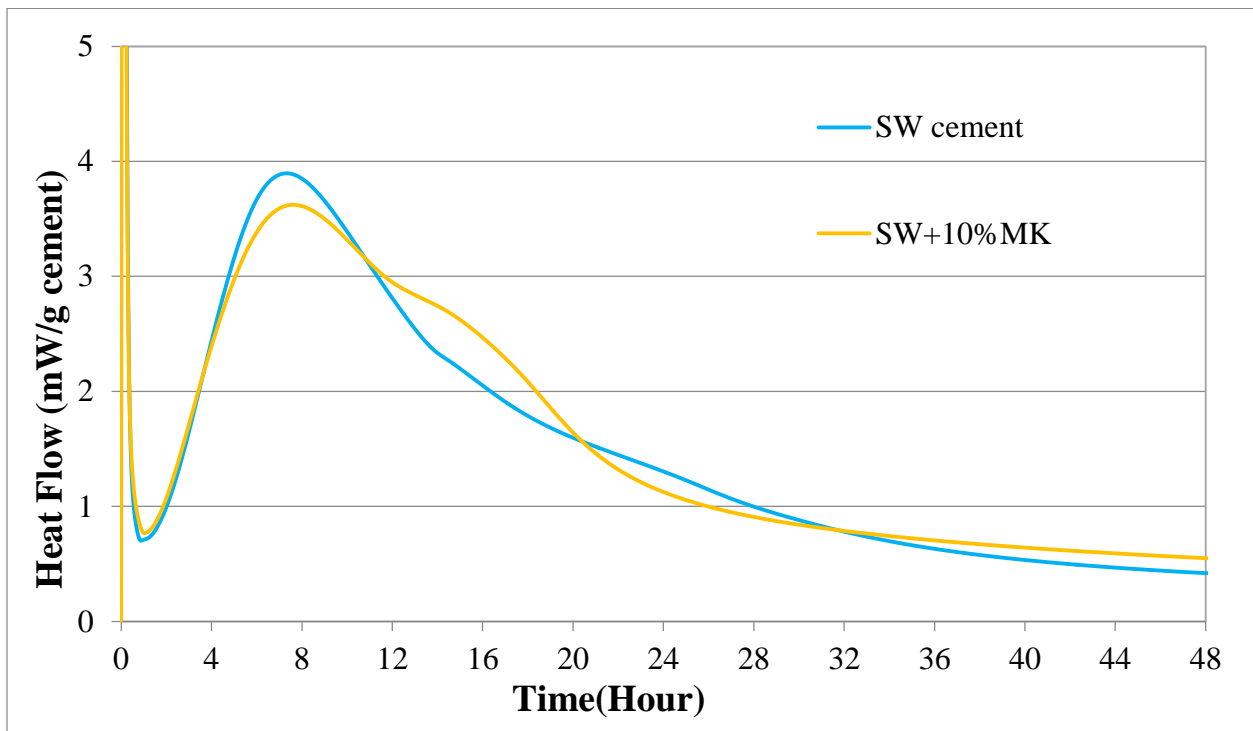


Figure 7: Measured Heat Flow of OPC and OPC/MK Pastes Normalized by Mass of Cement (Internal Mixing, w/c= 0.485)

In the first 15 minutes, MK showed higher reactivity than the control mix; however, the hydration rate of the OPC/MK sample during stage 3 of hydration was very similar to that of the OPC sample (Figure 7). Addition of MK did not have an effect on the timing of the main hydration

peak, although its intensity was slightly reduced. Many researchers have reported an accelerating effect of metakaolin on cement hydration both in terms of intensity and timing of the main peak [77], [95]–[97] which is contrary to the observations of this study. Lagier and Kurtis [77] have shown that this accelerating effect is strongly dependent on the fineness of metakaolin: as fineness increases, so does acceleration of cement hydration. The metakaolin used in this project had similar fineness (14.97 m²/g) to the low-fineness metakaolin (11.1 m²/g) used by Lagier and Kurtis [77], which did not show a significant accelerating effect on the main hydration peak. They also concluded that accelerating effect of metakaolin is much more pronounced on the C₃A hydration, while C₃S reaction is only slightly affected which is in agreement to the results here. The presence of agglomerates that were not sufficiently dispersed by manual mixing is also possible, which would have affected hydration behavior.

As for the sulfate depletion peak, it shifted from 14 hours in OPC paste to 12 hours in OPC/MK sample and the intensity of the peak is also increased which could indicate acceleration of C₃A hydration, as reported by Lagier and Kurtis [77]. The mechanism of the C₃A acceleration is not well understood. It is generally proposed that hydration is accelerated because metakaolin provides additional nucleation sites [77], [96]. It is interesting to note that the 24 hour peak disappears with addition of metakaolin. Antoni et al. [96] suggested that it merged with the third peak. However, the researchers were not able to determine whether or not aluminates contained in metakaolin participate in the reaction with sulfates at this point. If they do, then the shift in the sulfate depletion point can be attributed to the lower SO₃/Al₂O₃ ratio in the cementitious system.

Since metakaolin contained 44.16 % Al₂O₃ and no sulfates, 10% cement replacement by metakaolin effectively reduced the SO₃/Al₂O₃ ratio in the paste from 0.69 (OPC) to 0.40 (OPC/MK-90/10). Since sulfate balance has been identified as one of the main reasons for

admixture incompatibility [6], [15], addition of other admixtures that accelerate aluminate-sulfate reaction to the OPC/MK mixture or an increase in the ambient temperature may result in an undersulfated condition. Further investigation is needed to determine if such conditions will lead to abnormal setting and strength gain behavior in the OPC/MK mixtures and also to explore different mixing procedures on the heat profile.

The OPC/MK mixture appeared to reach steady state faster than the OPC sample, and its heat flow at this stage was higher as well. This can be explained by the reaction of metakaolin with CH to produce additional C-S-H. Comparing the total heat normalized by the mass of cementitious materials, compressive strength of the OPC/MK mixture is expected to be lower at earlier age due to the relatively low acceleration of the early C_3S reactions by metakaolin.

There is little data available for the early-age reactivity of BFS. It has been reported that the reactivity of slag depends on its amorphous content, temperature history, with higher temperature and faster quenching rates producing more reactive materials, fineness, chemical composition and alkali concentration in the mixture as hydration of slag is alkali- and sulfate-activated [98], [99]. Dissolution of slag releases alkalis into the pore solution, ensuring a continuous reaction of slag into the later ages [13]. Escalante et al. [100] work, using selective dissolution, shows that slag reactivity increases with an increase in its amorphous content. The first measurements were performed at 3 days. Feng et al. [101] also observed an accelerating effect of slag addition on cement hydration. The degree of hydration was determined via SEM point counting technique. Again, the first measurement was conducted at 3 days. The authors also compared degree of reaction of slag and Class F fly ash and determined that reactivity of slag was much higher than that of fly ash.

Since it was determined that the slag used in this project has an amorphous content of approximately 97%, it was expected to be highly reactive. Addition of slag resulted in a significant increase in heat evolution compared to the OPC sample. In terms of the silicate reaction, Figure 8 shows a reduced induction period for the OPC-slag sample, increased intensity of the main hydration peak as well as a shift of the peak maximum to the right by approximately 1 hour. Kocaba [80] showed that effect of slag on OPC hydration depends on the mineralogical composition of cement. She reported acceleration of the C_3S reaction based on the isothermal calorimetry results with addition of 40% slag for one cement, and retardation of the C_3S reaction for two other cements, although the degree of alite hydration was determined to be the same for all three of these systems. No explanation was offered for this phenomenon.

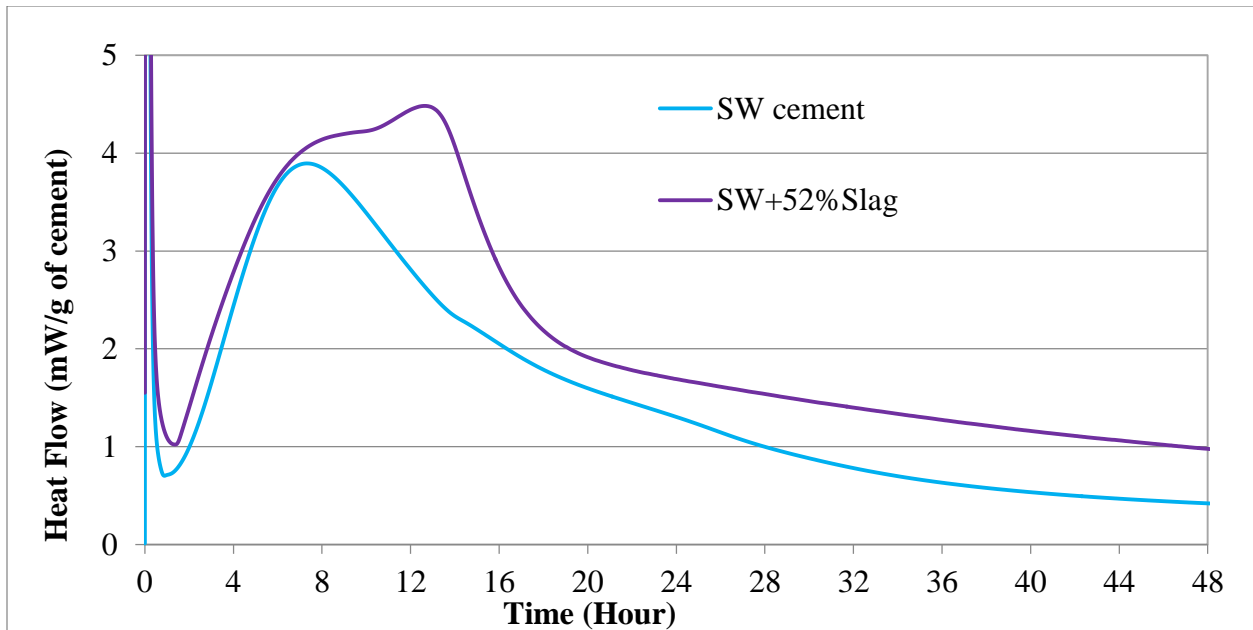


Figure 8: Measured Heat Flow of OPC and OPC/Slag Pastes Normalized by Mass of Cement (Internal Mixing, w/c= 0.485)

As for the aluminate reaction, sulfate depletion peak is shifted to the left, with a significant increase in intensity. Brunet et al. [102] reported that aluminates in slag had higher reactivity compared to the silicates, which can explain the observed shift of the sulfate depletion peak to an

earlier time. Kocaba [80] attributed the acceleration of the aluminate reaction to the filler effect (heterogeneous nucleation). At steady state, heat flow of the OPC-slag sample remained consistently higher than that of the OPC control sample, which point to a continuous reaction of slag itself. The heat of hydration profile identifies the significance of slag incorporation in the paste mixture on the sulfates/aluminates interaction. It is therefore expected that for sulfate durability studies, this interaction might potentially be of significance.

Table 16 and Figures 9 and 10 present the heat measurements for all the OPC-mineral admixture combinations. Addition of slag resulted both in the highest heat flow and the highest total heat of all the samples, including OPC control paste. There is a significant increase in total heat with slag addition as early as 1 day and persistent up to 7 days. The total heat of OPC/MK and OPC/FA samples at 7 days was slightly higher than that of the OPC sample, while no difference was observed between OPC and OPC/SF, most likely due to particle agglomeration as discussed above.

Table 16: Heat of Hydration for Binary Cement-Mineral Admixture Combinations using Internal Mixing (w/c= 0.485)

Mix ID	Mineral Admixture	w/o Cement Replacement	1-Day HOH (J/g cement)	3-Day HOH (J/g cement)	7-Day HOH (J/g cement)
SW	None	0	211	302	354
SW+10%MK	Metakaolin	10	217	320	393
SW+8%SF	Silica fume	8	210	302	353
SW+21%FA	Class F Fly Ash	21	214	340	370
SW+52%Slag	Slag	52	269	450	578

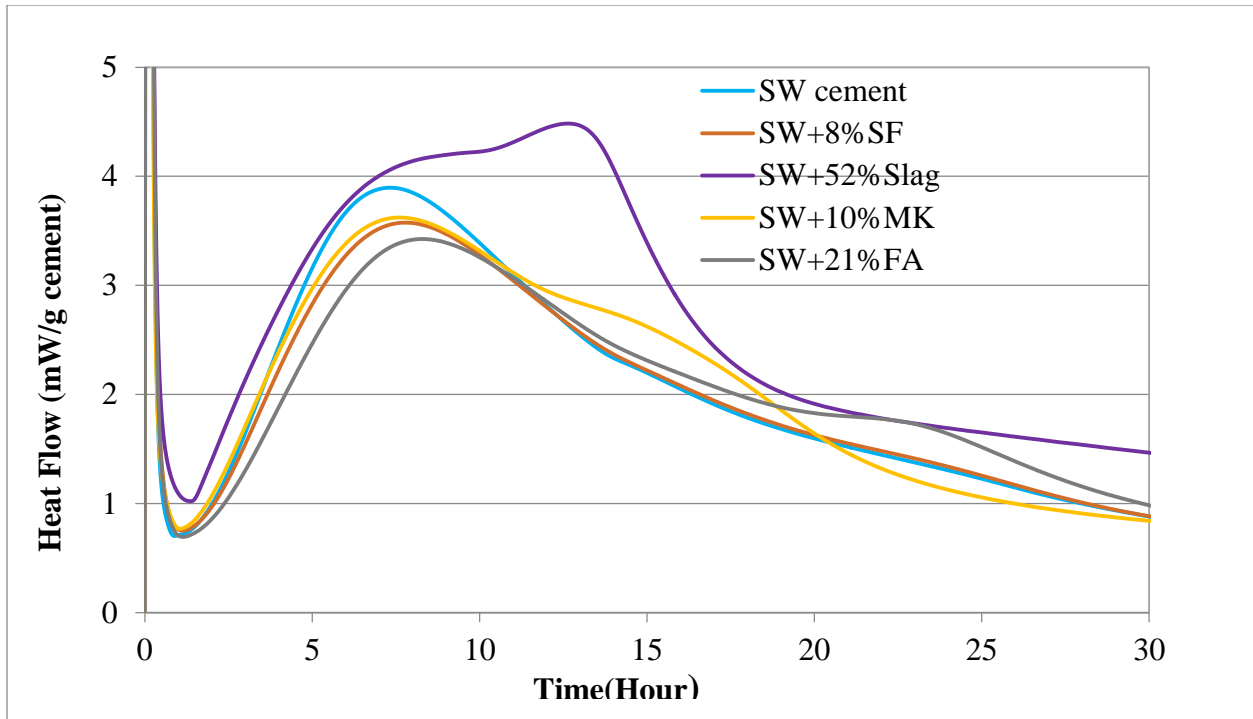


Figure 9: Measured Heat Flow of Cement and Mineral Admixture Samples Normalized by Mass of Cement (Internal Mixing, w/c= 0.485)

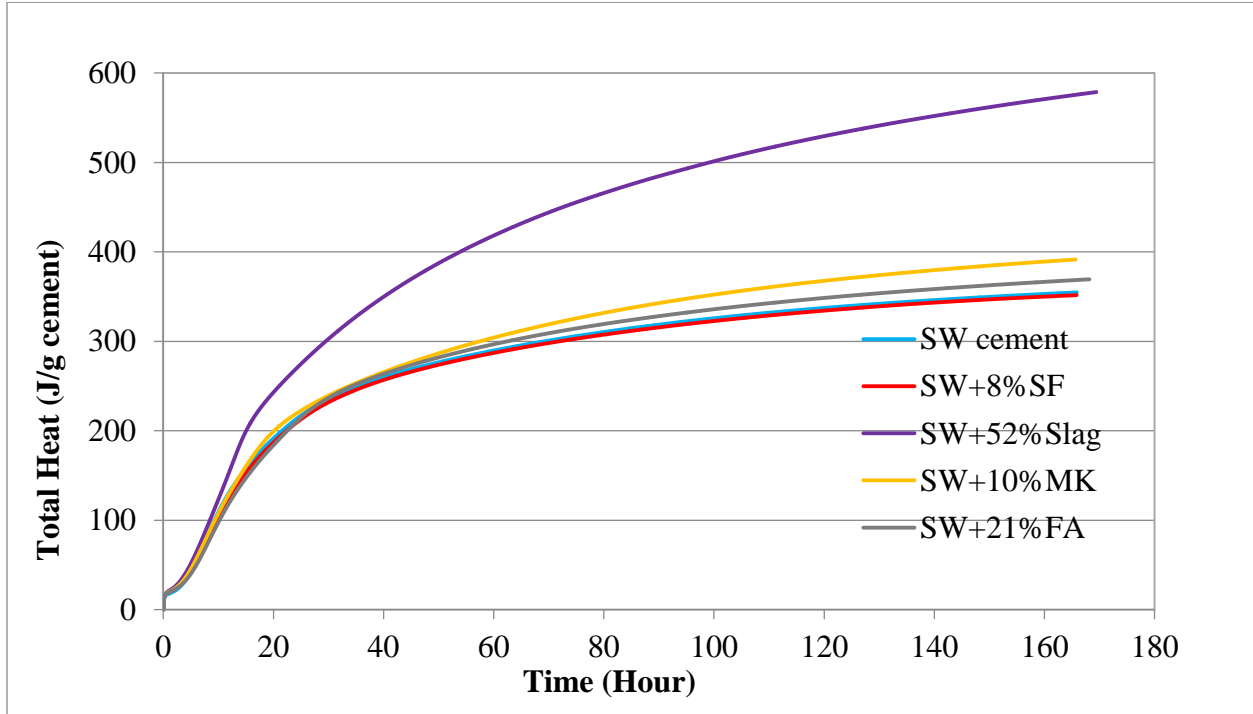


Figure 10: Total Heat of Cement and Mineral Admixture Samples Normalized by Mass of Cement (Internal Mixing, w/c= 0.485)

External mixing of the cement-mineral admixture binary mixtures of common dosage used in construction at a w/c ratio of 0.42 (Figure 11) showed slightly different heat flow trends from those tested following the internal mixing protocol with a w/c ratio of 0.485 (Figure 9). With external mixing, the main hydration peak of all cement-mineral admixture combinations occurred earlier and had higher intensity compared to internal mixing. This is attributed to better dispersion of mineral admixtures with the external mixing procedure even at a lower w/c ratio of 0.42. As for the total heat, both external (Figure 12) and internal (Figure 10) mixing protocols produced similar trends for slag and metakaolin in that slag showed the highest total heat at 72 hours followed by metakaolin. SF showed similar total heat to FA at 72 hours in external mixing while lower than FA in internal mixing. Again, this is confirming that internal mixing might pose an issue for HOH studies for SF in absence of dispersion agents such as SP or WRA.

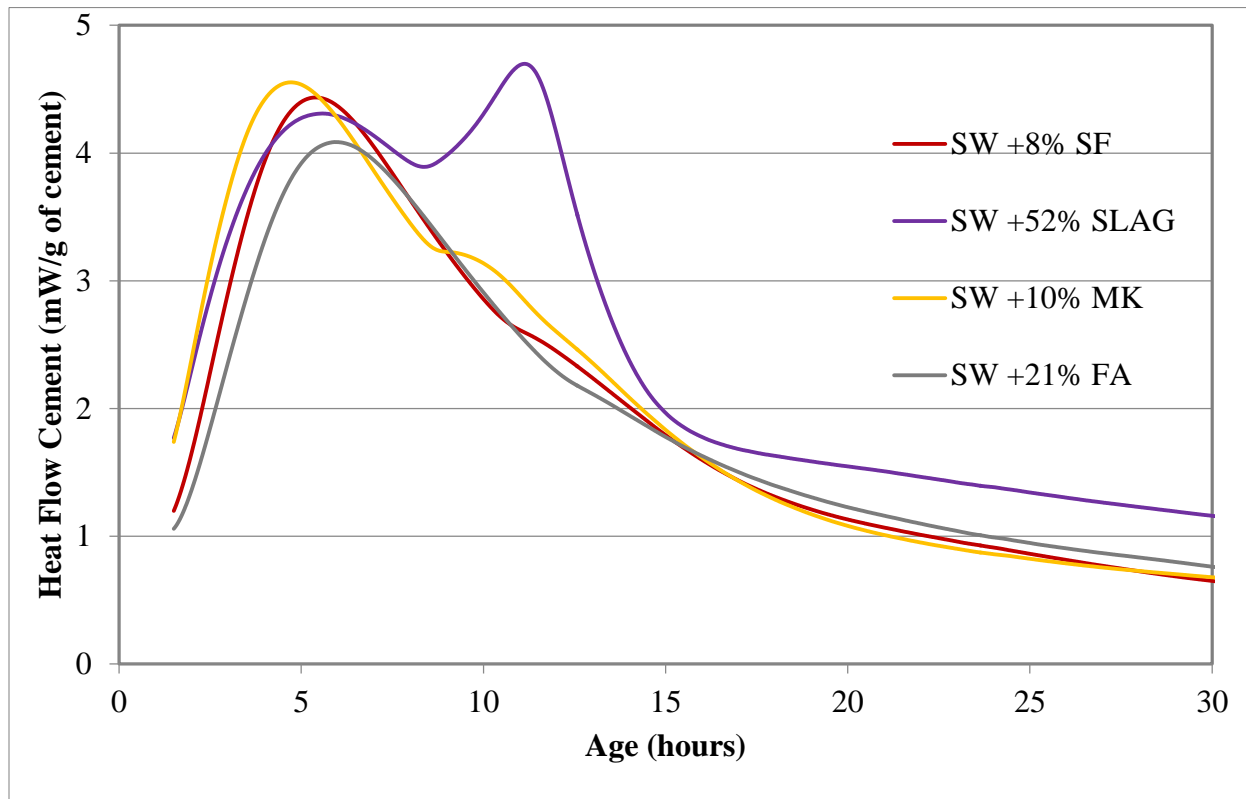


Figure 11: Measured Heat Flow of OPC and OPC/Mineral Admixture Pastes Normalized by Mass of Cement (External Mixing, w/c= 0.42)

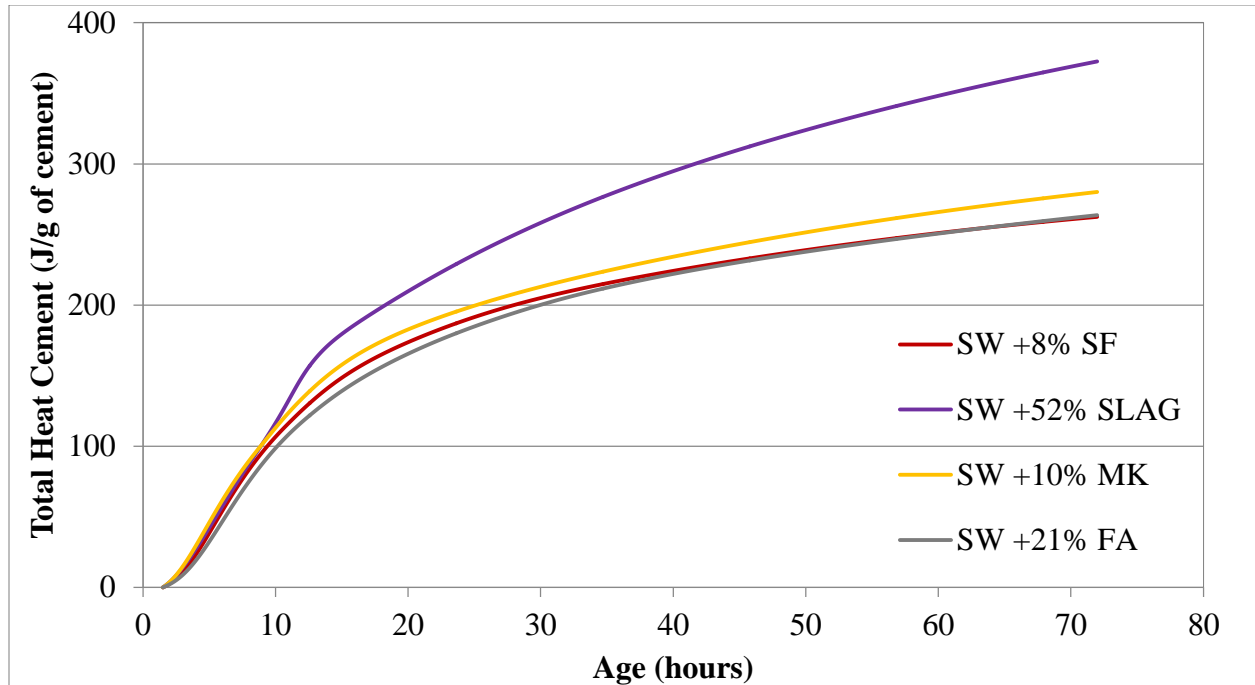


Figure 12: Total Heat of Mineral Admixture Samples Normalized by Mass of Cement (External Mixing, w/c= 0.42)

4.1.1 Effect of Fly Ash Content

Figure 13 and Figure 14 illustrate the effect of Class F fly ash dosage on heat flow and total heat, respectively, using external mixing and a w/c ratio of 0.485. It is clear that at cement replacement levels below 30% there is no effect on cement hydration. This is not surprising, as Class F fly ash is expected to be non-reactive during the first week [13]. Even at 30% replacement, the timing and magnitude of the silicate hydration peak remains unaffected as reported in the literature [17], [86], [103]. The only difference observed at 30% replacement level is the presence of the fourth peak, which was observed with internal mixing at 21% fly ash replacement. As discussed previously, the nature of this peak remains undetermined.

When normalized by the mass of total cementitious content, both the heat flow (Figure 15) and total heat (Figure 16) decrease with increasing cement replacement level. Since fly ash is not reactive at such early ages, the decreased heat is due to the reduction of cement content.

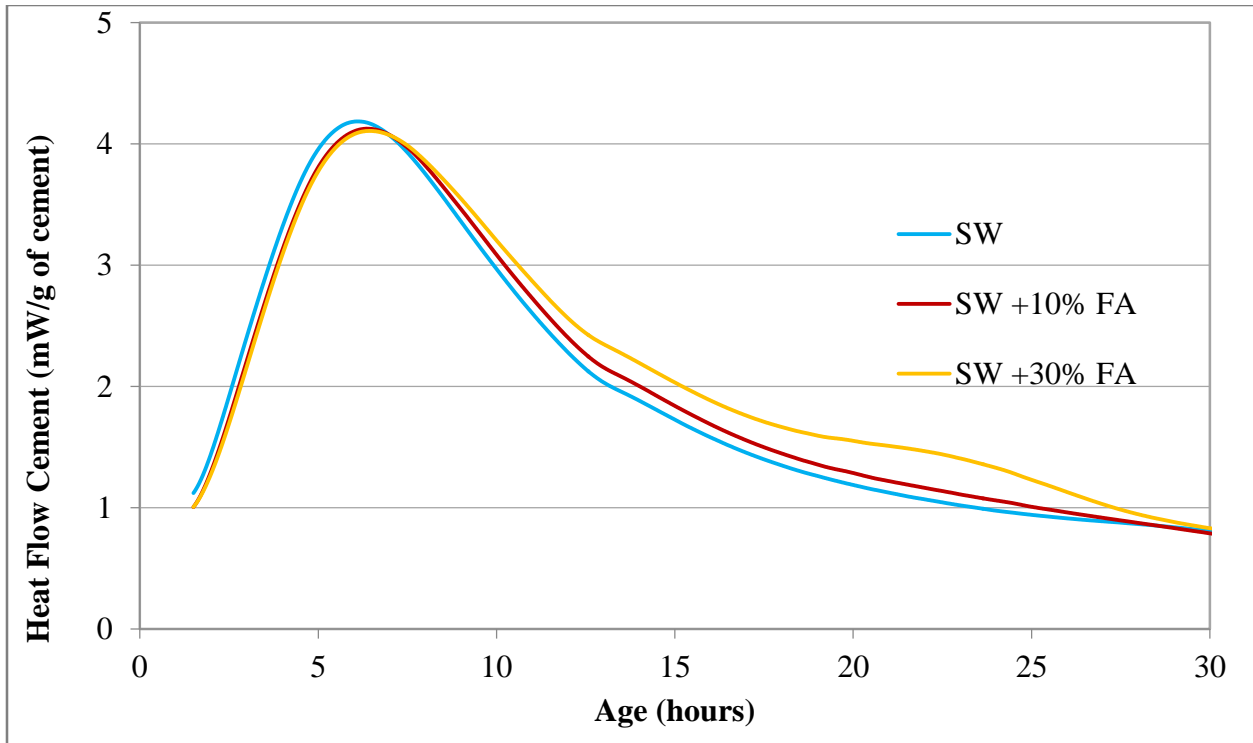


Figure 13: Measured Heat Flow of Cement/Fly Ash Pastes Normalized by Mass of Cement (External Mixing, w/c= 0.485)

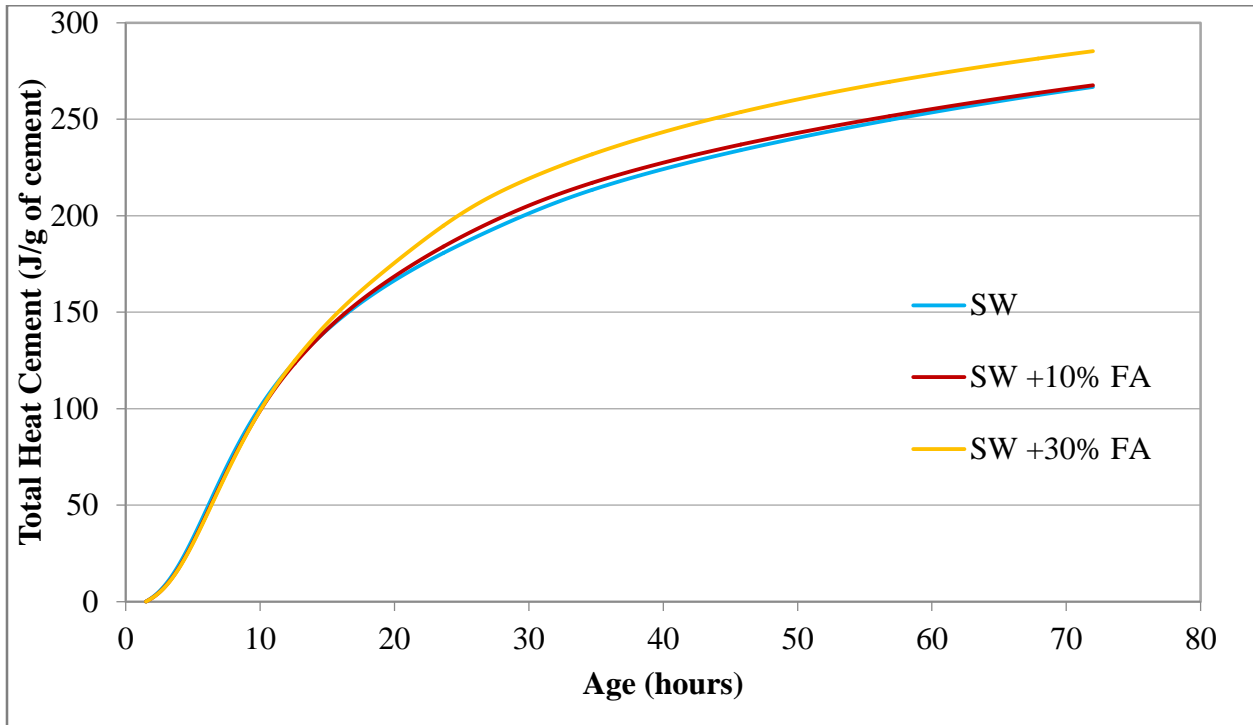


Figure 14: Total Heat of Cement/Fly Ash Pastes Normalized by Mass of Cement (External Mixing, w/c= 0.485)

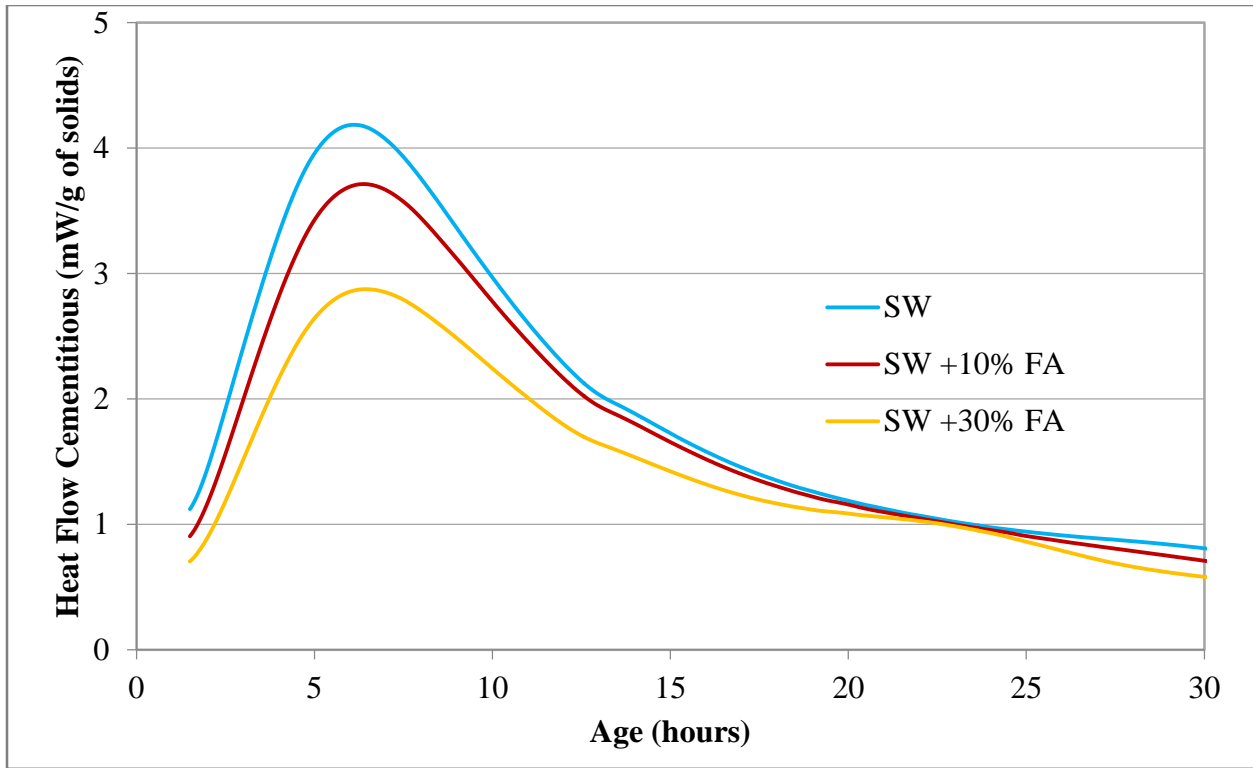


Figure 15: Measured Heat Flow of Cement/Fly Ash Pastes Normalized by Mass of Cementitious Materials (External Mixing, w/c= 0.485)

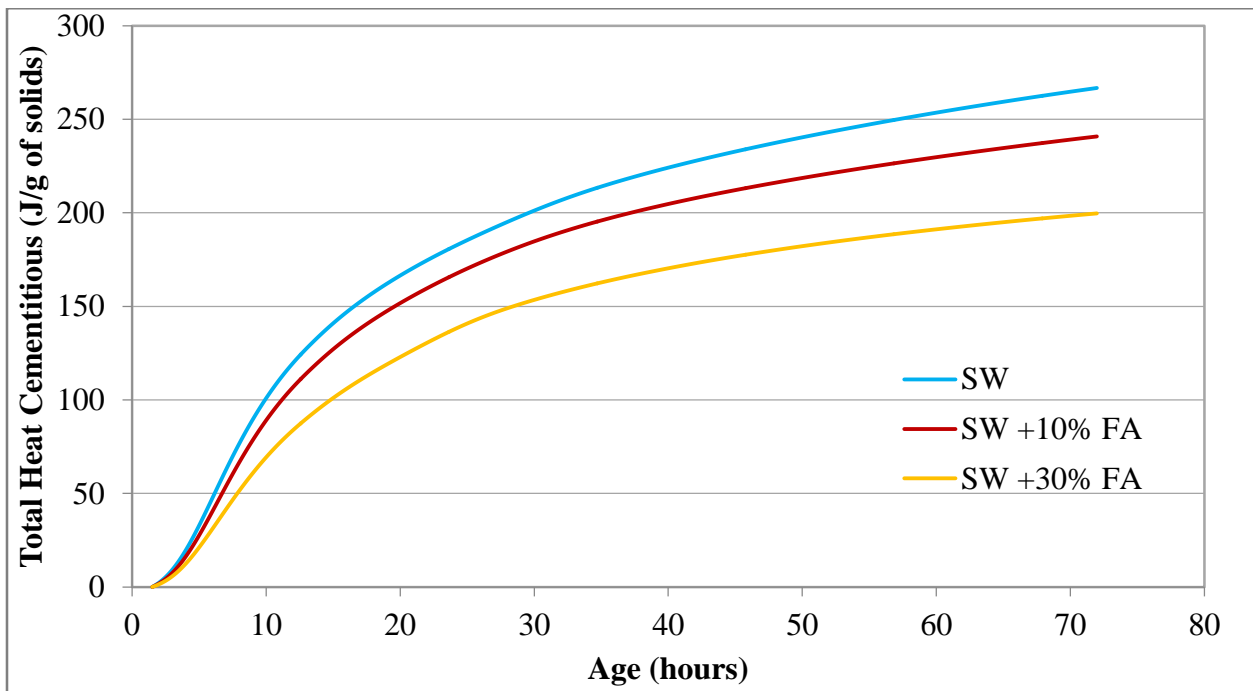


Figure 16: Total Heat of Cement/Fly Ash Pastes Normalized by Mass of Cementitious Materials (External Mixing, w/c= 0.485)

4.1.2 Effect of Blast Furnace Slag Content

Unlike fly ash, the effect of slag content on cement heat flow was observed to be dosage-dependent (Figure 17). There is an increase in the magnitude of the aluminate peak with increasing slag dosage that is possibly due to the reaction of amorphous alumina supplied by BFS. Although the reactivity of different slags varies [98], [99], reactivity of slag activated by Portland cement has been generally compared to that of C_2S [22]. Brunet et al. [102] also reported that in slags the reactivity of alumina is higher than that of silica. This can explain the greater effect of slag addition on the aluminate hydration compared to the reaction of silicates. Increased heat flow also translates to increase in total heat when normalized by mass of cement (Figure 18) with increasing slag content. The effect of high slag content on the main hydration peak needs to be studied further to understand better if this phenomenon reflects on durability and to what extent.

Normalizing heat flow by mass of cementitious materials reveals that both heat flow (Figure 19) and total heat (Figure 20) generally decrease with increasing slag content. It is interesting to note that at 10% cement replacement with slag, the total heat curve is very similar to that of the plain cement mix. It appears that at 10% replacement there is sufficient acceleration of cement hydration by slag (possibly coupled with the reaction of slag itself) to offset the effect of decreased cement content in terms of heat generation. Also, heat flow and total heat curves (normalized by mass of cementitious materials) for 21% and 30% slag are very similar despite variable cement replacement levels. Comparing Figure 17 and Figure 19 reveals that although the sulfate depletion point in the two samples occurs at the same time, it occurs at a higher heat flow value in the 30% slag paste (Figure 17), which points to a higher reactivity of aluminates.

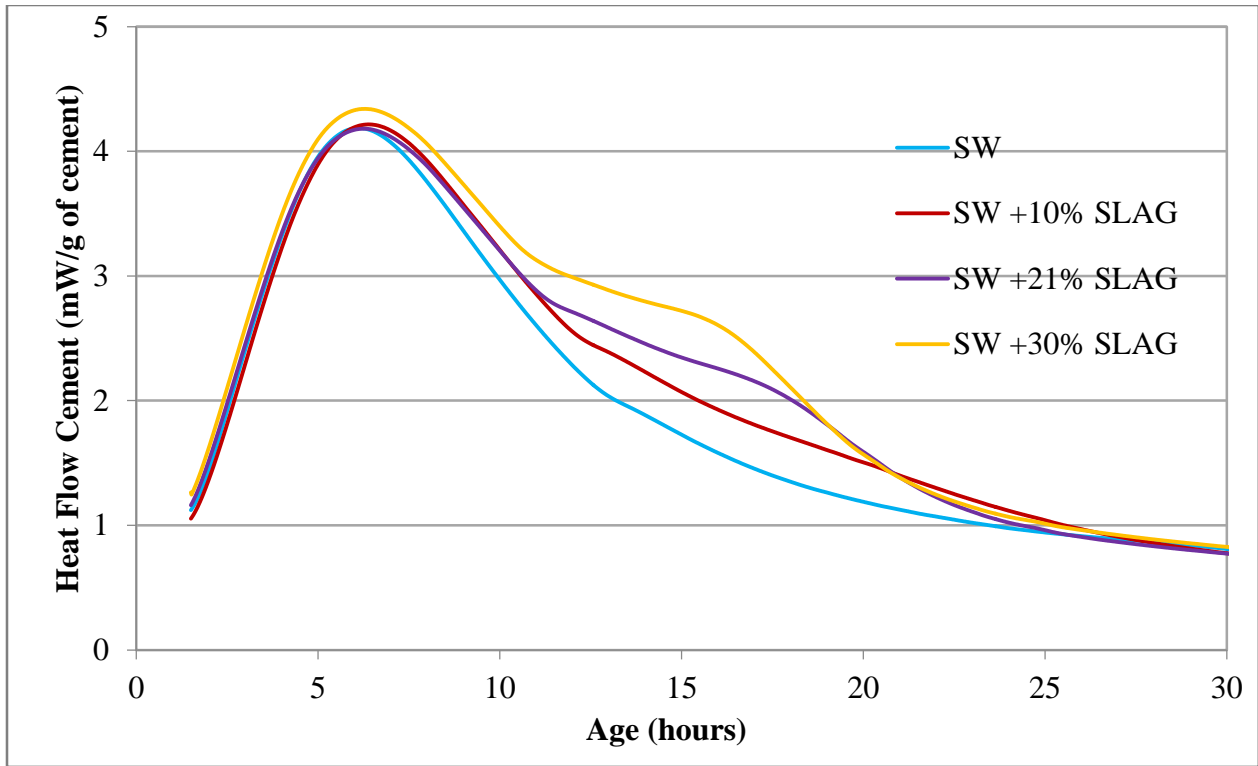


Figure 17: Measured Heat Flow of Cement/Slag Pastes Normalized by Mass of Cement (External Mixing, w/c= 0.485)

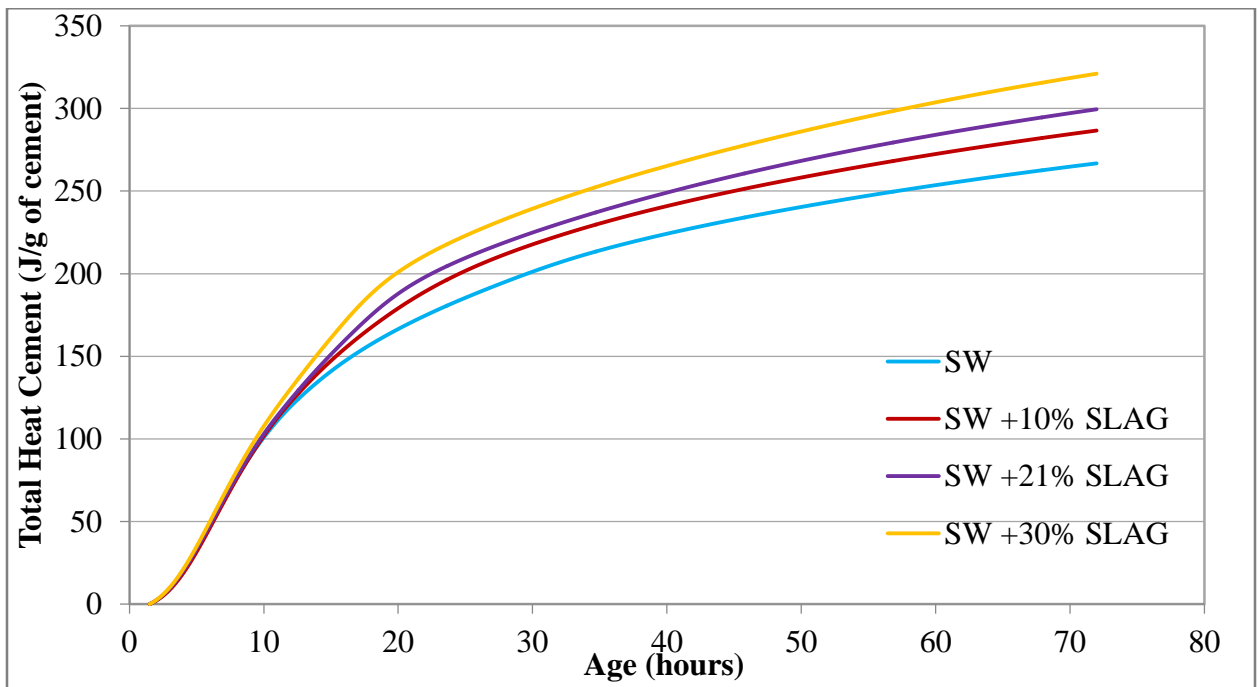


Figure 18: Total Heat of Cement/Slag Pastes Normalized by Mass of Cement (External Mixing, w/c= 0.485)

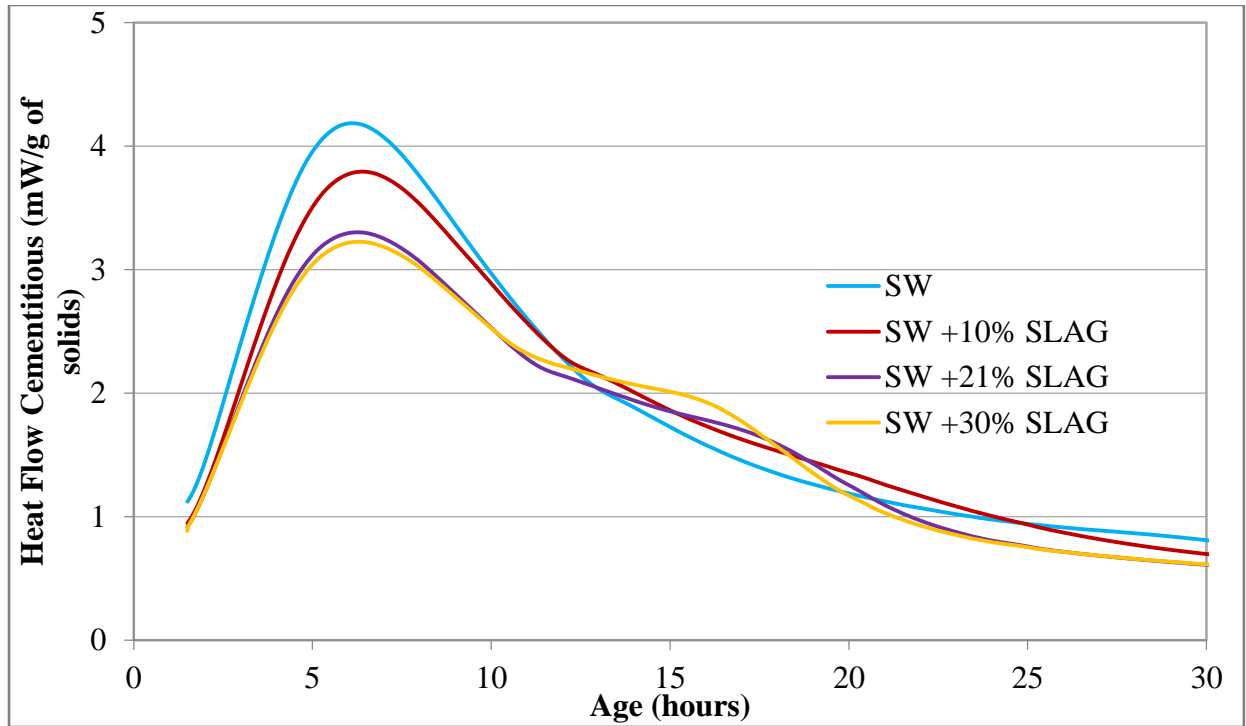


Figure 19: Measured Heat Flow of Cement/Slag Pastes Normalized by Mass of Cementitious Materials (External Mixing, w/c= 0.485)

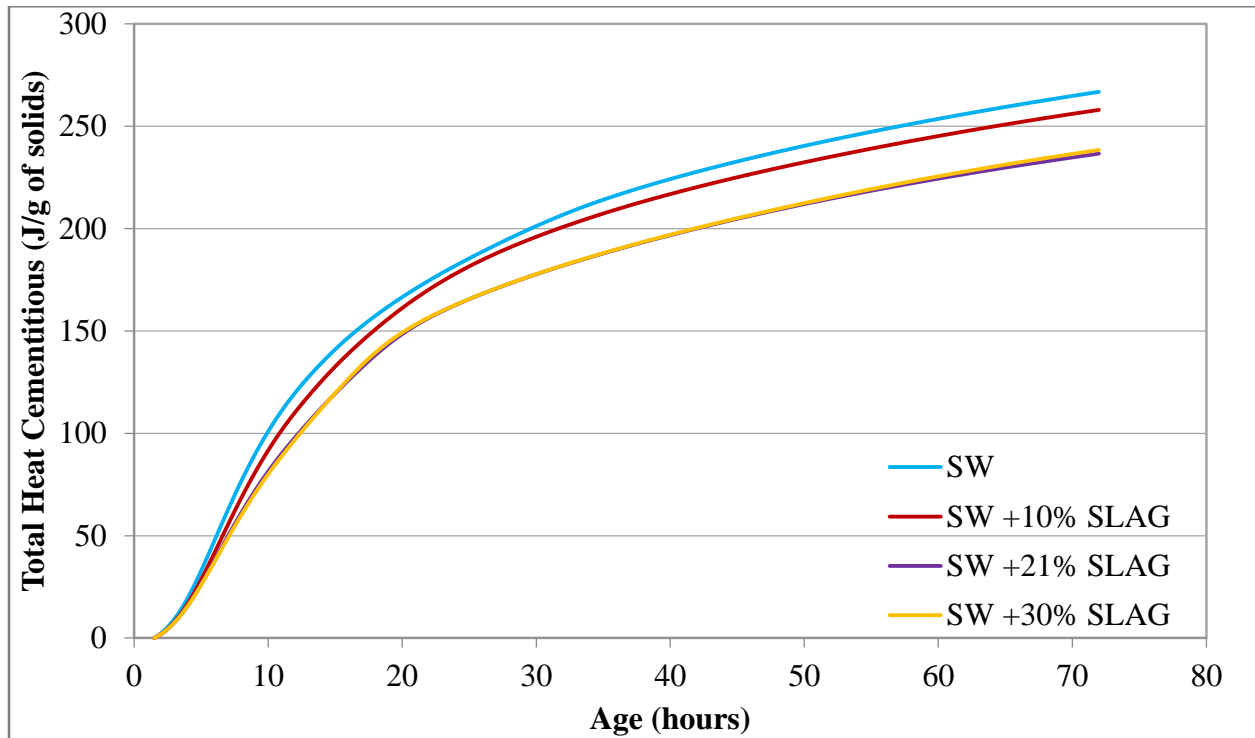


Figure 20: Total Heat of Cement/Slag Pastes Normalized by Mass of Cementitious Materials (External Mixing, w/c= 0.485)

4.1.3 Effect of Silica Fume Content

In terms of cement reactivity, silica fume addition affects both the silicate peak and the sulfate depletion point at all replacement levels (Figure 21). With the main hydration peak, peak magnitude increases with increasing SF dosage. There is also a slight shift to the left with 10% SF addition; however, peak position remains essentially unchanged at subsequently higher dosages. As for the sulfate depletion peak, both its magnitude and timing are accelerated by increasing silica fume replacement levels. Several researchers have discounted the possibility of silica fume reaction during the first 24 hours [85], [92], therefore, the accelerating effect is most likely due to heterogeneous nucleation. It is interesting that cement heat flow continues to increase with increasing silica fume content of up to 30% indicating that the saturation limit where addition of extra nucleation sites does not result in increased hydration rate has not been reached. Total heat also increases with increasing SF dosages when normalized by mass of cement (Figure 22), which is somewhat contrary to [92], who observed a decrease in total heat at 30% SF replacement.

Normalizing by total cementitious content showed that heat flow decreases as silica fume content increases (Figure 23) and that total heat decreases as well (Figure 24). The same effect was observed for the fly ash and slag; however, in the case of silica fume this decrease is significantly lower. This points to significant acceleration of cement hydration.

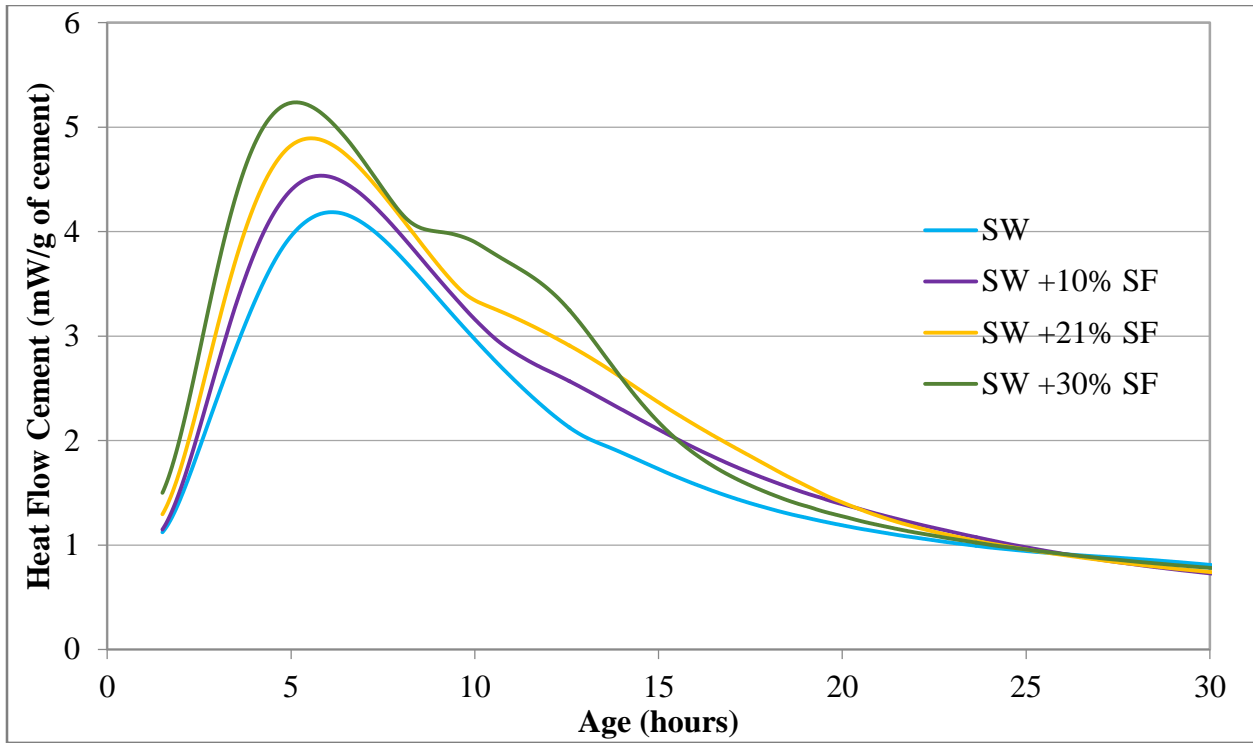


Figure 21: Measured Heat Flow of Cement/Silica Fume Pastes Normalized by Mass of Cement (External Mixing, w/c= 0.485)

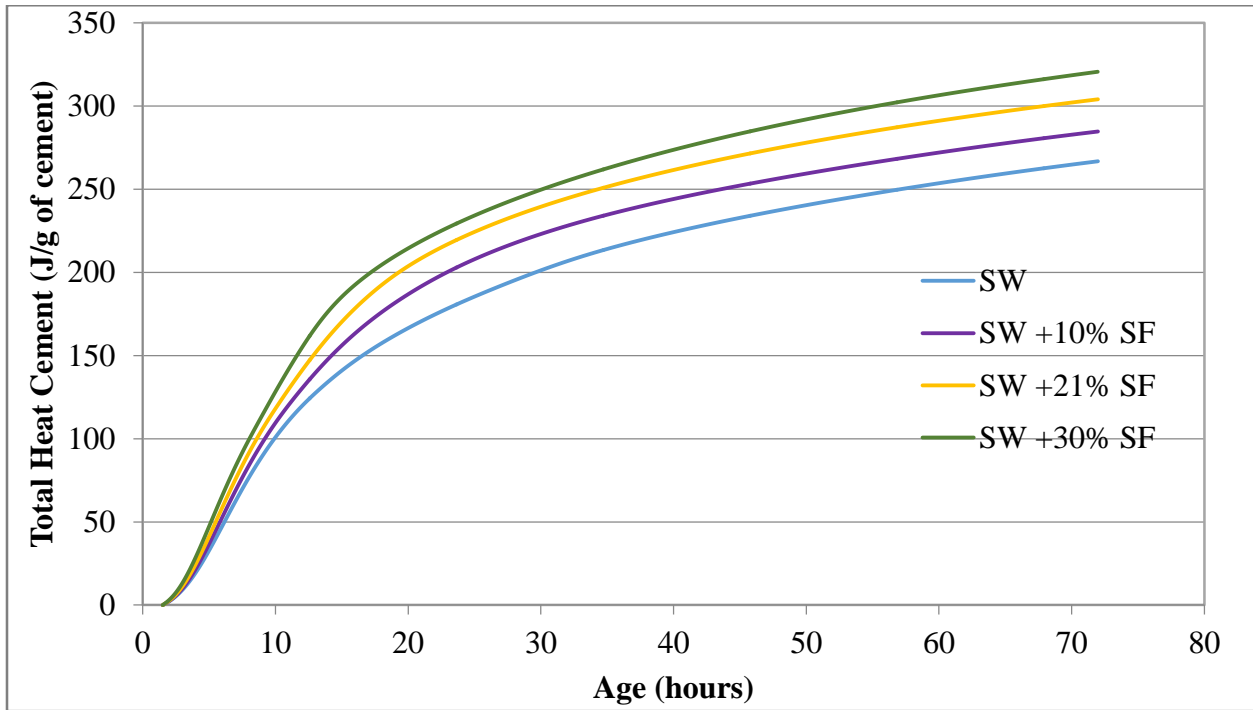


Figure 22: Total Heat of Cement/Silica Fume Pastes Normalized by Mass of Cement (External Mixing, w/c= 0.485)

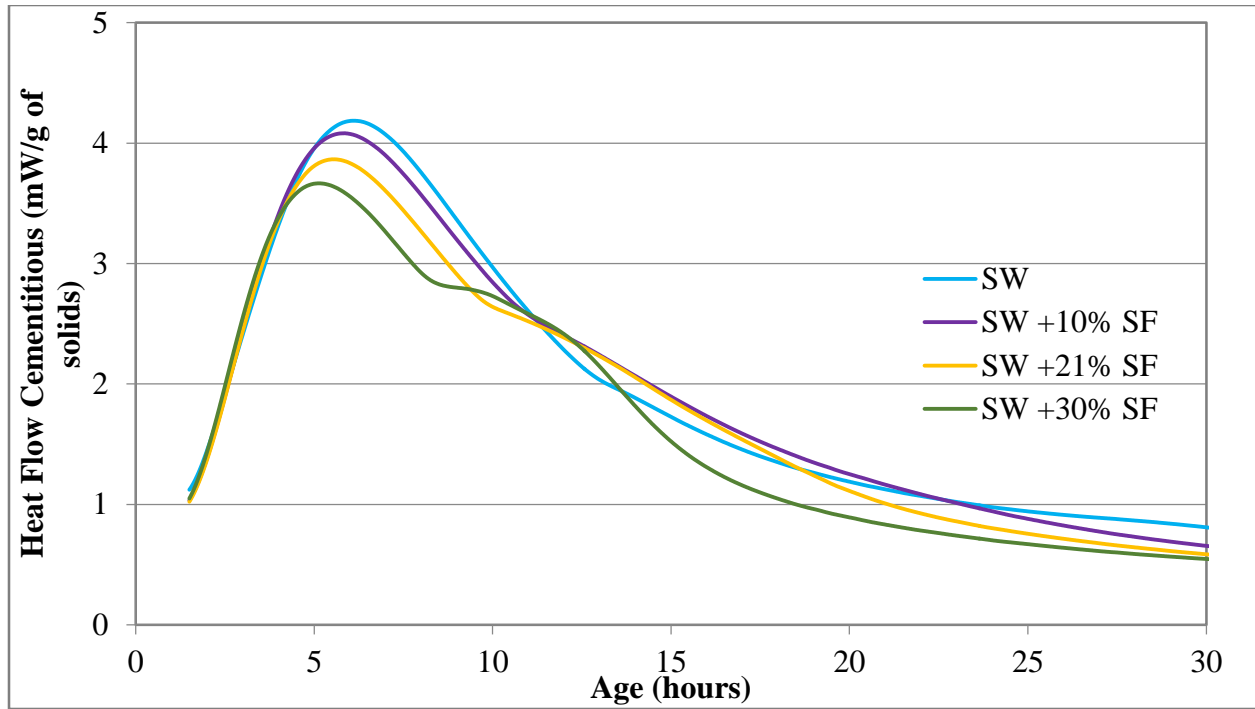


Figure 23: Measured Heat Flow of Cement/Silica Fume Pastes Normalized by Mass of Cementitious Materials (External Mixing, w/c= 0.485)

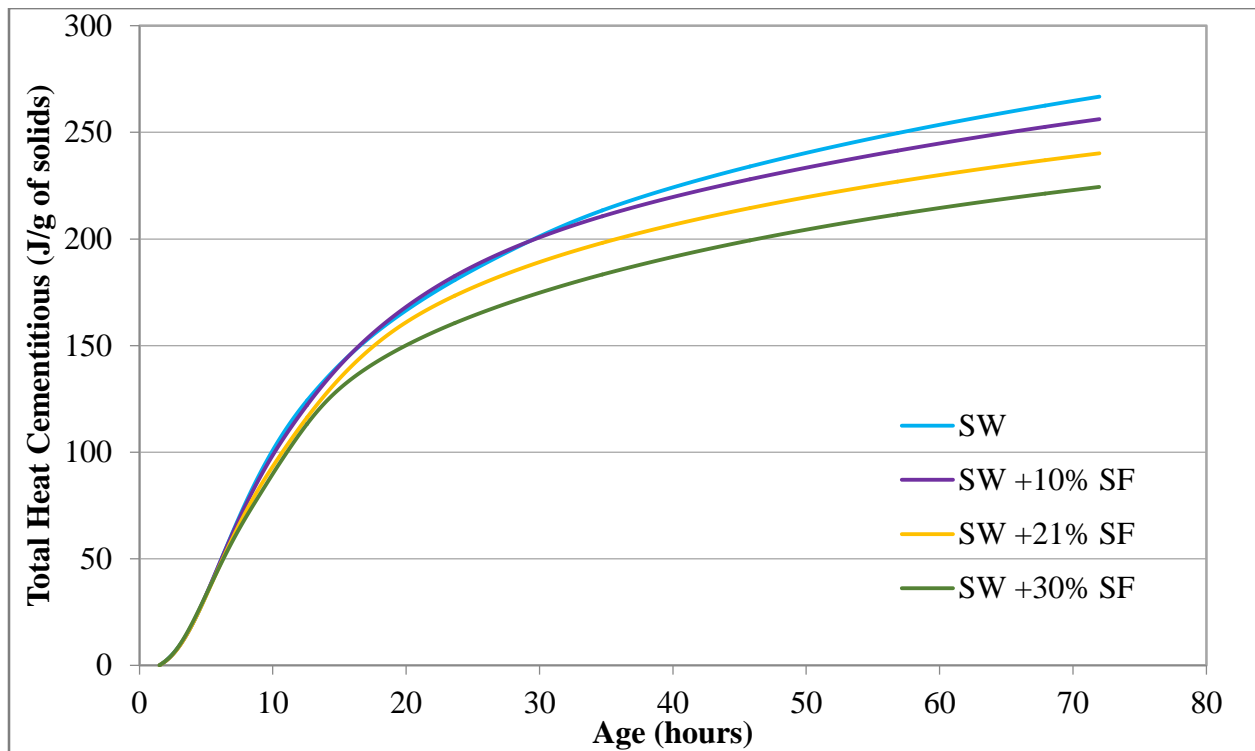


Figure 24: Total Heat of Cement/Silica Fume Pastes Normalized by Mass of Cementitious Materials (External Mixing, w/c= 0.485)

4.1.4 Effect of Metakaolin Content

Similarly to silica fume, initial addition of metakaolin shifts the main hydration peak to the left, with subsequent additions not affecting the peak position (Figure 25). The magnitude of the silicate peak increases with 21% MK addition; however, at 30% replacement there is no further increase in peak magnitude. If the silicate hydration is accelerated by MK through heterogeneous nucleation, it may be possible that at 21% MK the maximum effective number of nucleation seeds have been reached and further increase does not affect silicate reactivity. Unlike the silicate peak, both the timing and magnitude of the aluminate peak is accelerated by increasing MK dosage. It appears that reaction of aluminates supplied by MK may be contributing to this acceleration. MK is known to be reactive at early ages [88], [94]; Frias et al. [88] reported measureable pozzolanic activity as early as 2 hours. As for the total heat, there is a significantly larger effect shown by 21% and 30% additions (Figure 26).

Figure 27 and 28 show the heat flow and total heat curves pastes with metakaolin normalized by the mass of total cementitious materials. Maximum heat flow remains unaffected at 21% cement replacement by metakaolin (silicate peak), while at 30% replacement the maximum heat is increased (aluminate peak). Figure 28 shows that all the pastes regardless of cement replacement levels had the same total heat up to 10 hours, after which the sample with 30% MK started to show lower total heat. Total heat for the rest of the samples continued to be the same up to 15 hours, after which total heat was higher in the plain cement mix.

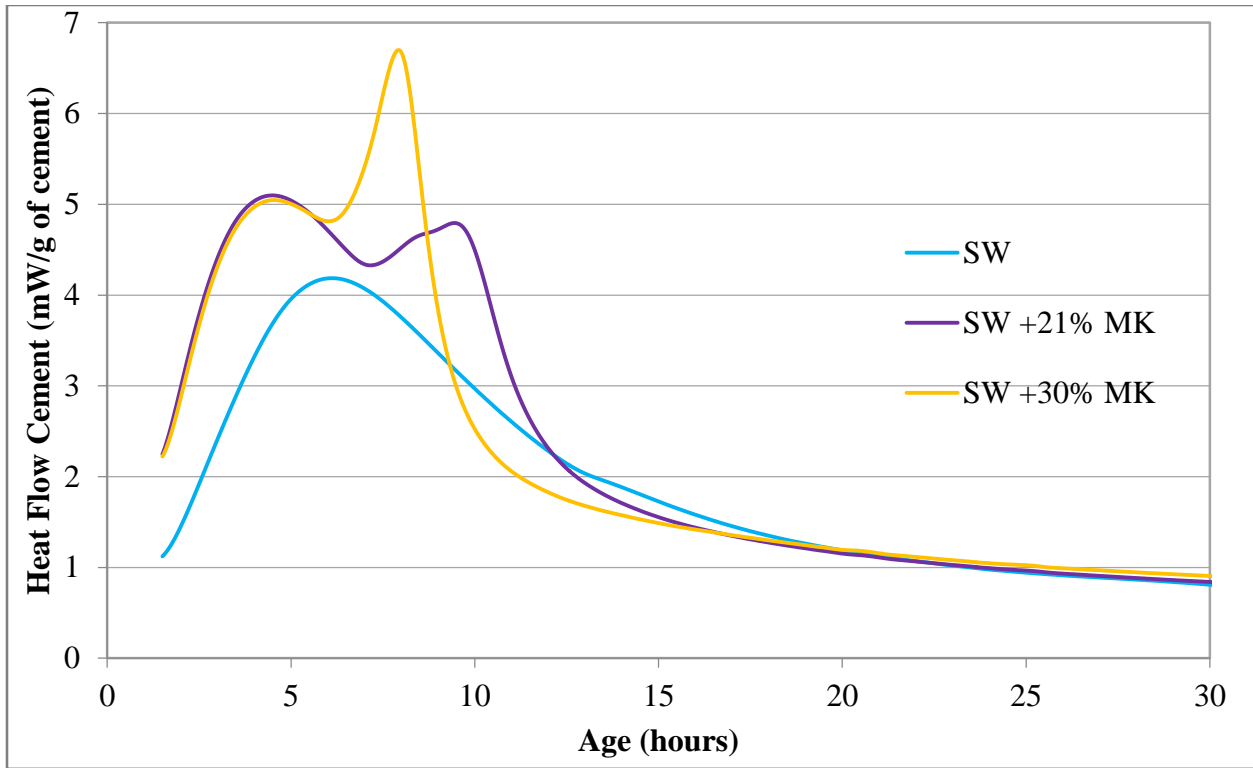


Figure 25: Measured Heat Flow of Cement/Metakaolin Pastes Normalized by Mass of Cement (External Mixing, w/c= 0.485)

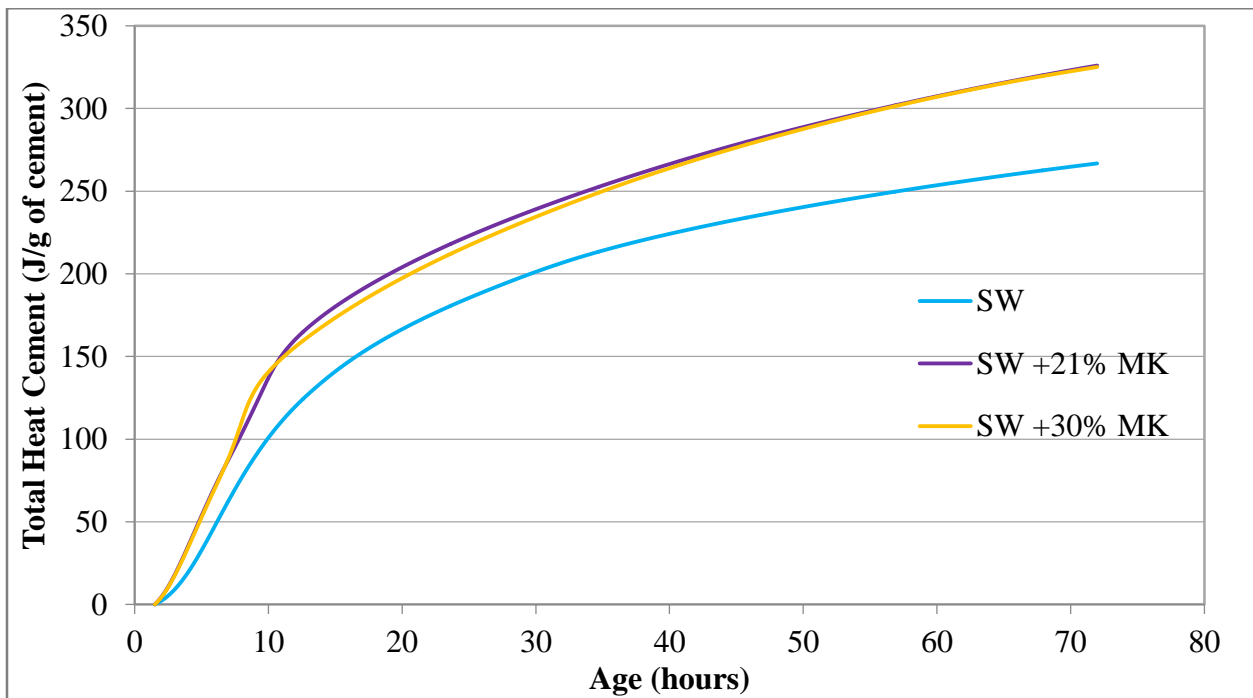


Figure 26: Total Heat of Cement/Metakaolin Pastes Normalized by Mass of Cement (External Mixing, w/c=0.485)

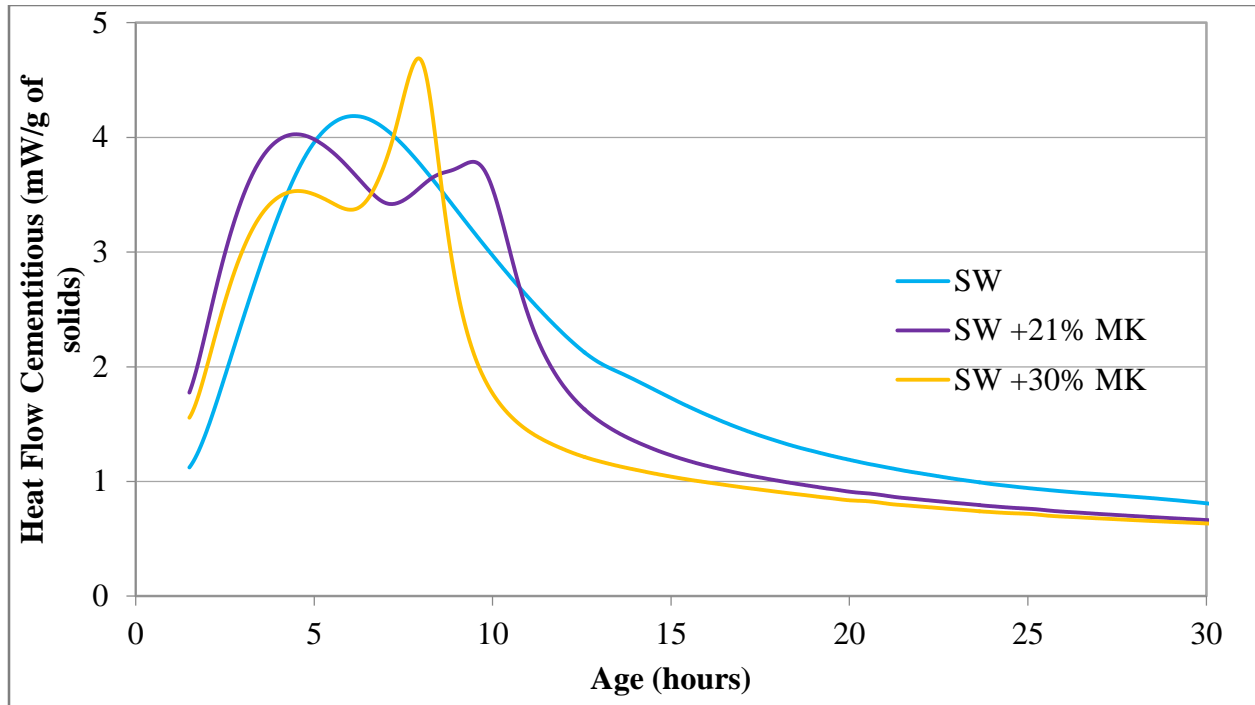


Figure 27: Measured Heat Flow of Cement/Metakaolin Pastes Normalized by Mass of Cementitious Materials (External Mixing, w/c= 0.485)

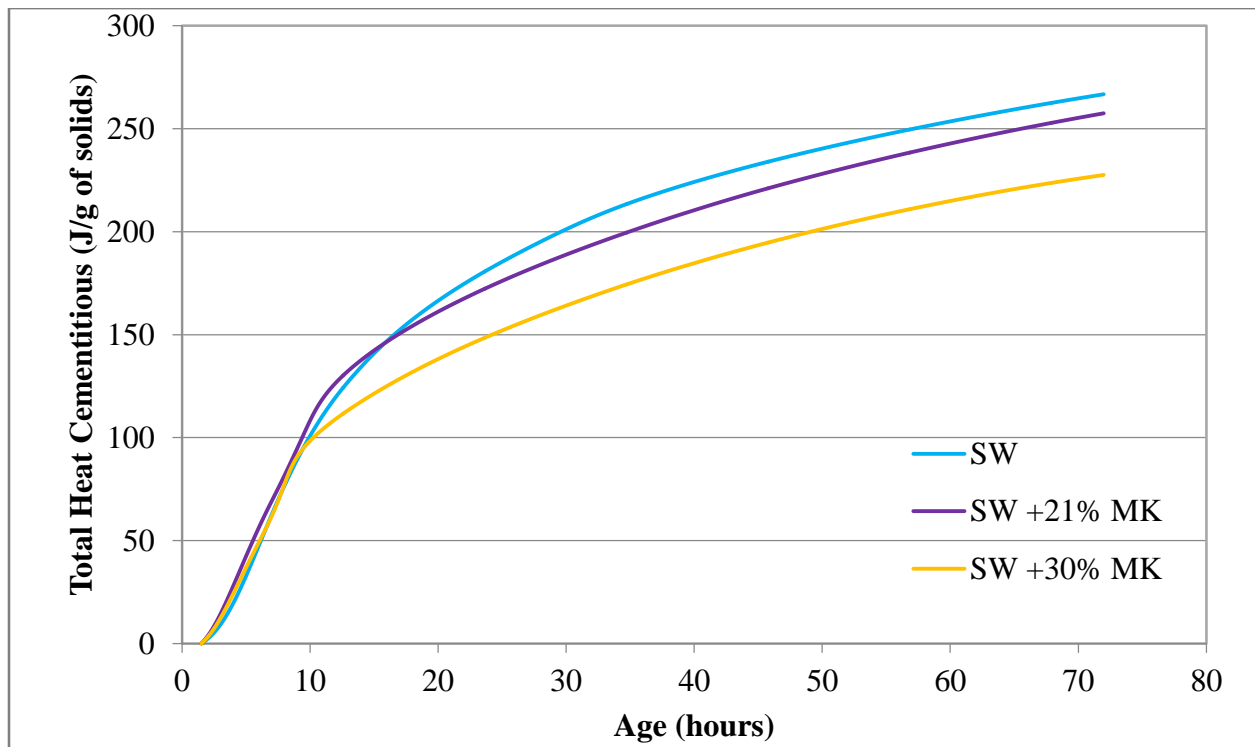


Figure 28: Total Heat of Cement/Metakaolin Pastes Normalized by Mass of Cementitious Materials (External Mixing, w/c= 0.485)

4.1.5 Effect of Chemical Admixtures

In the case of cement-chemical admixture combinations (Figure 29), addition of AEA did not have any effect on cement hydration while WRA had a retarding effect. It was also observed that SP1 had a retarding effect exceeding that of WRA. AEA and WRA did not have a significant effect on the total heat of hydration up to 7 days; addition of SP1, however, decreased the total heat compared to the rest of the mixes up to approximately 15 hours, after which the total heat generated by the SP1 paste exceeded the rest of the pastes. At 7 days, the heat evolved by the SP1 mixture was higher by approximately 17 J/g of cement. In addition to retarding the main hydration peak, both WRA and SP1 accelerated the occurrence of the sulfate depletion point.

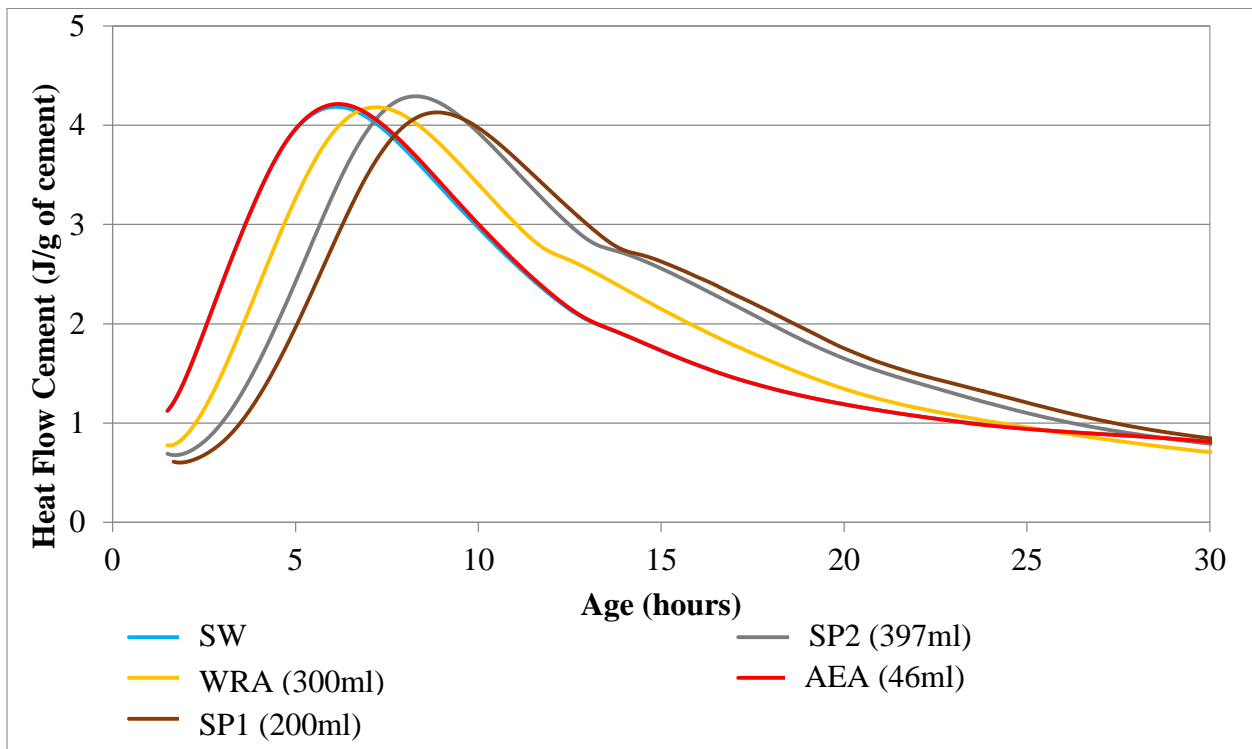


Figure 29: Measured Heat Flow of OPC and OPC/Chemical Admixture Pastes Normalized by Mass of Cement (External Mixing, w/c= 0.485)

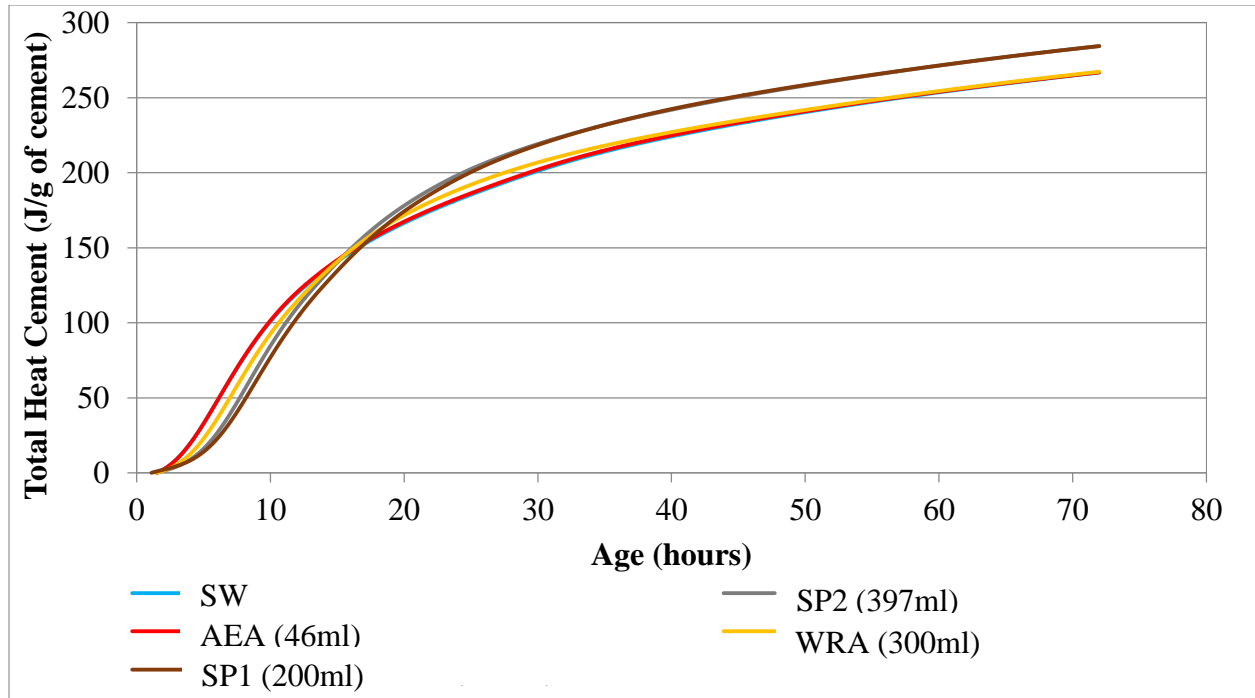


Figure 30: Measured Total Heat of OPC and OPC/Chemical Admixture Pastes Normalized by Mass of Cement (External Mixing, w/c= 0.485)

4.2 Setting Time

Setting time was determined on mortar mixes incorporating different mineral admixtures to determine their effect on setting properties. In studying the effects of different mineral admixtures on the setting time, the same chemical admixtures were used in sample preparation as discussed previously in Chapter 3, so that the only variable to consider is the mineral admixture. Setting time measurements were conducted according to ASTM C807-13 [1] which requires working on mortar of normal consistency. The amount of sand used in each mixture to achieve normal consistency for each mixture is presented in Table 17 and Table 18.

Table 17: Amount of Sand Used for Normal Consistency for Mixtures with Varying Mineral Admixtures

Mix ID	Sand (g)
SW+Admix(SP1)	2235
SW+Admix(SP2)	2150
10MK	1985
20MK	1435
10SF	2100
10FA	2175
21FA	2100
30FA	2100
21Slag	2175
30Slag	2175
52Slag	2225

Table 18: Amount of Sand Used for Normal Consistency for Mixtures with Varying Chemical Admixtures

Mix ID	Sand (g)
SW+100SP1	2235
SW+100SP2	2150
10MK+100SP1	2000
10SF+100SP2	2125
21FA+100SP2	2175
52Slag+100SP2	2250
SW+170SP1	2255
SW+170SP2	2150
10MK+170SP1	2050
10SF+170SP2	2175
21FA+170SP2	2175
52Slag+170SP2	2275

4.2.1 Metakaolin

The effect of metakaolin replacement for cement on setting time is depicted in Figure 31 where it can be seen that metakaolin decreases the setting time and the effect is more pronounced at 21% replacement level. The results are consistent with the heat of hydration calorimetric measurements where the main hydration peak, defining final set, experienced a shift in its position to shorter time. However, the main hydration peak timing did not show noticeable shift beyond 21% MK and therefore the 30 % replacement level was not considered here. A left shift in the in the main hydration peak or a reduction in the setting time indicates that MK addition has the effect of accelerating silicates hydration.

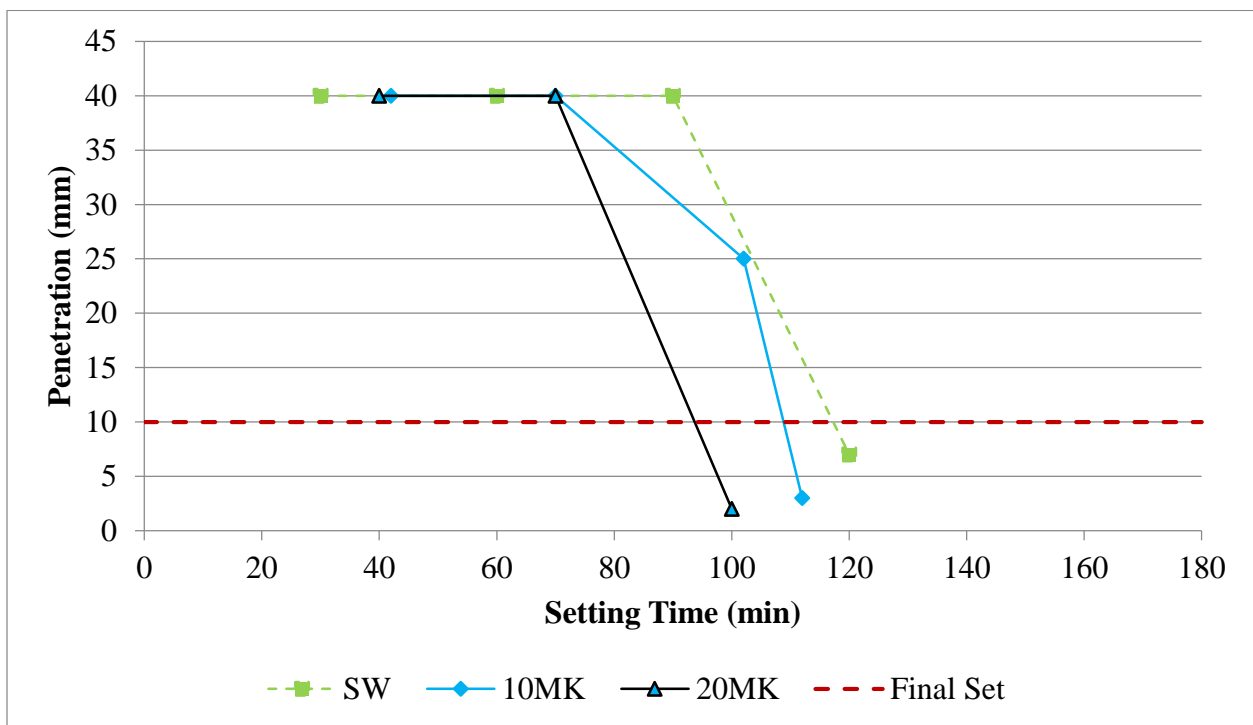


Figure 31: Mortar Setting Time for Metakaolin Mixtures

The results are consistent with Li and Ding [35] findings in that metakaolin mixtures had a shorter setting time than the control. Li and Ding determined the setting time of paste at normal

consistency. According to Li and Ding, since metakaolin contains amorphous silica and alumina, it reacts with the cement to form C-S-H gel during early hydration.

4.2.2 Silica Fume

Silica fume was evaluated at a replacement of 10% on setting time and the results are presented in Figure 32. The results show that silica fume has no significant impact on setting time at a replacement level of 10% silica fume. This is consistent with Rao [44] findings where final setting time was not influence by silica fume. If heat of hydration analysis is also considered here, both tests are indicating the same findings, which is that at a level of replacement of 10%, silica fume appears not to have significant effect on setting time or kinetics of early hydration. Previously it was indicated that lack of acceleration or retardation with addition of silica fume at the levels used here could be due to opposing effects of dilution and pozzolanic reaction of silica fume.

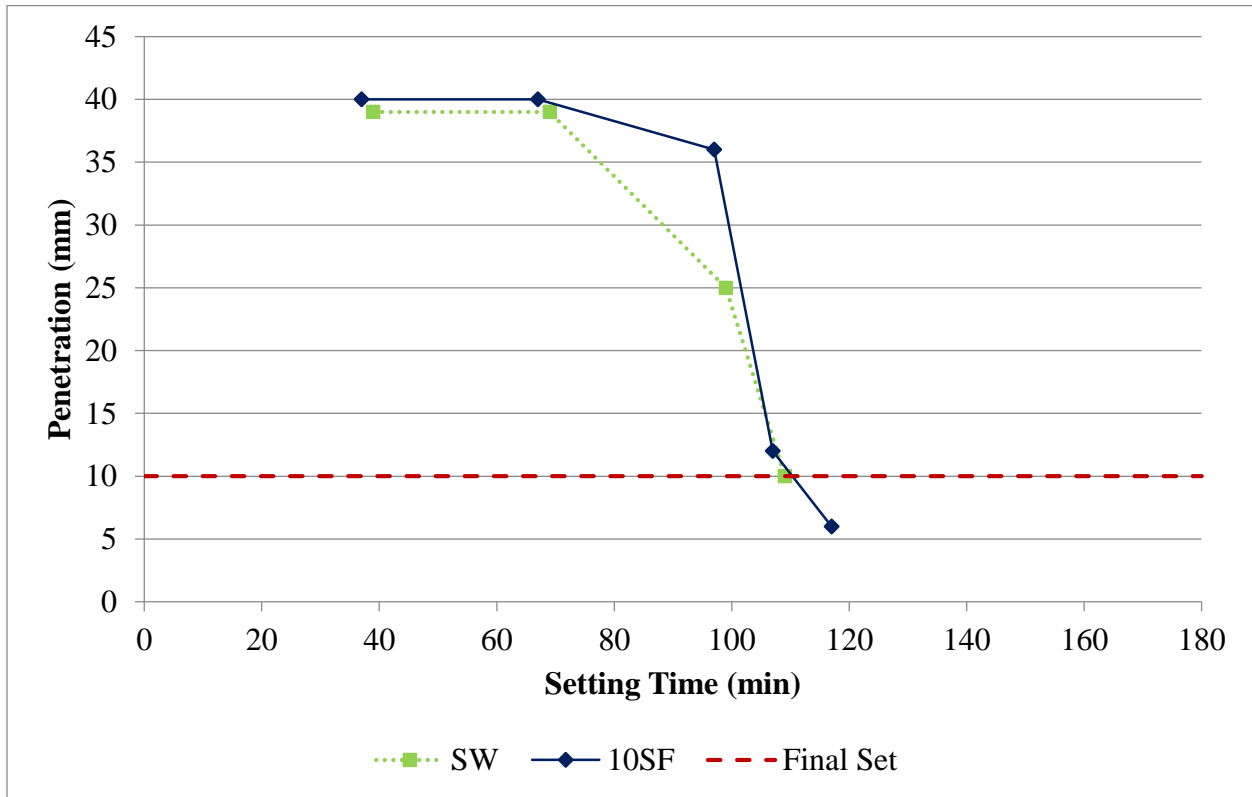


Figure 32: Mortar Setting Time for Silica Fume Mixtures

4.2.3 Fly Ash

Fly Ash setting properties was examined at three different replacement levels of 10, 21, and 30 %. The results show that at low fly ash content of 10%, no significant effects could be observed on the setting properties, a finding that is also consistent with heat of hydration measurements. However, on increasing the level of replacement to 21% a retardation effect could be observed that increases with replacement level. The results are consistent with the findings of Kocak and Nas [52] as well as Brooks et al. [34]. The retardation effect is primarily due to dilution effect and the slow reactivity of fly ash as a pozzolan in addition to this particular fly ash with its lower amorphous content of 72%.

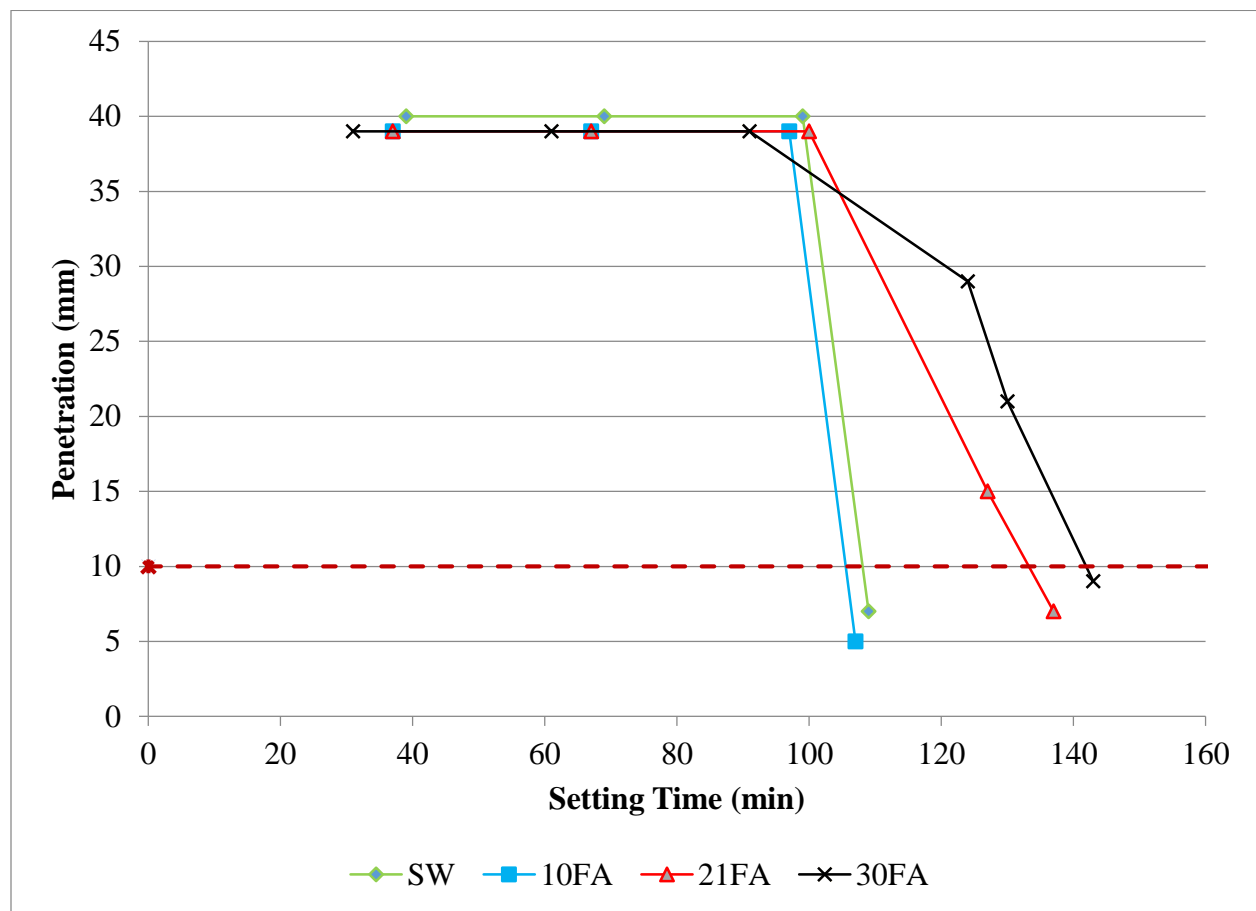


Figure 33: Mortar Setting Time for Fly Ash Mixtures

4.2.4 Blast Furnace Slag

Slag was investigated at three different replacement levels of 21, 30, and 52 %. Figure 34 shows the results for mortar setting time of the slag mixtures. The results indicate that at all replacement levels, slag increases the setting time from the control mixture, with the retardation effect independent of the replacement level. Similar to the heat of hydration curves, increasing slag content from 0 to 30%, there was no visible effect on silicate hydration kinetics. Setting time for the 52% replacement shows a slight drop when compared to lower replacement levels but the setting time of the 52% slag mix was still notably retarded compared to the control. This is believed to be due to the action of the chemical admixtures on the setting behavior of the slag mixtures, which was apparent at all levels of replacement.

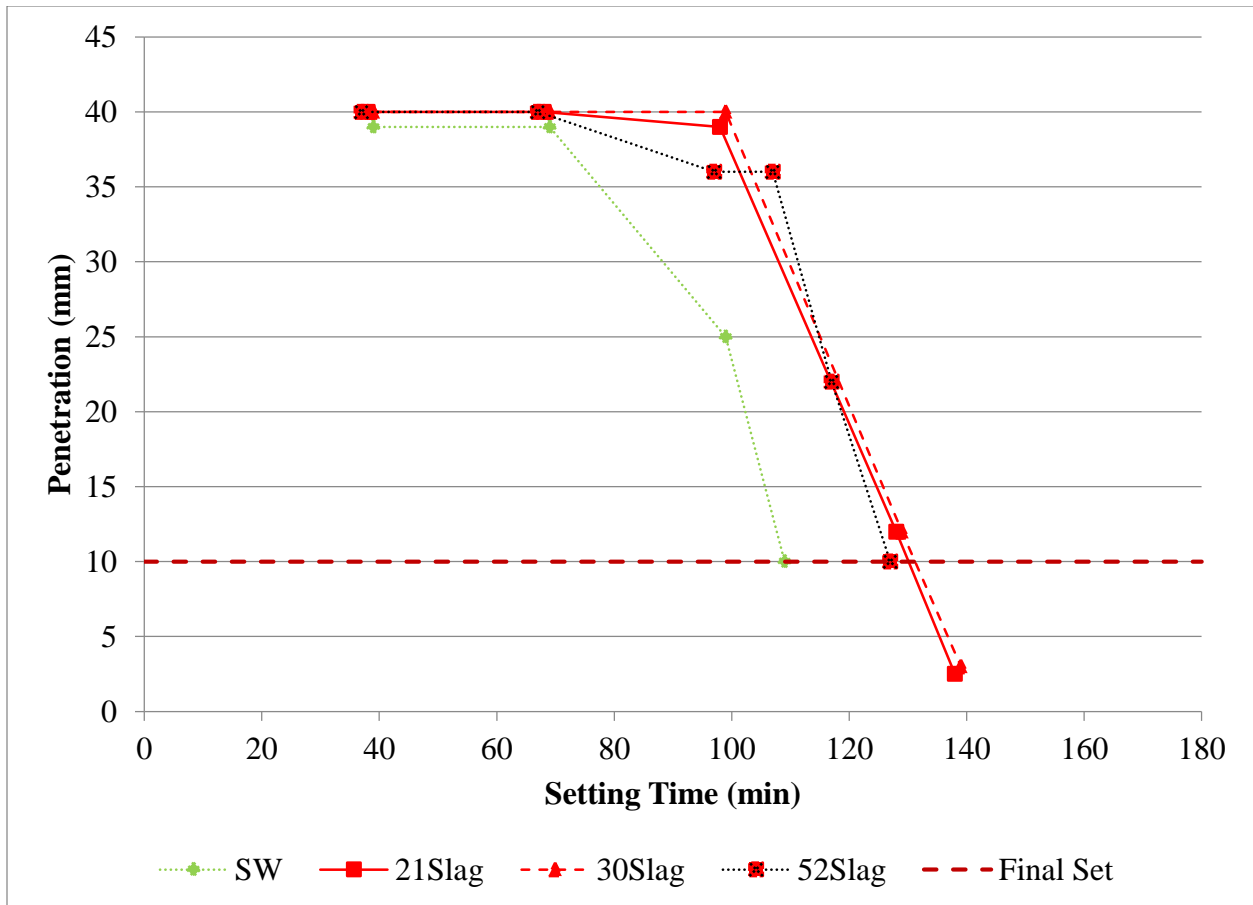


Figure 34: Mortar Setting Time for Slag Mixtures

4.2.5 Varying SP1 Dosage

There was two SPs used throughout this study with metakaolin mixture using SP1 and the other mineral admixtures using SP2. Setting time was also determined on mortar by varying the dosage of the used SP. For each SP, the dosage was varied between 100 and 170 ml per 100 kg cementitious material. Figure 35 shows the effect of varying SP1 dosage on setting time for SW with no mineral admixture replacement.

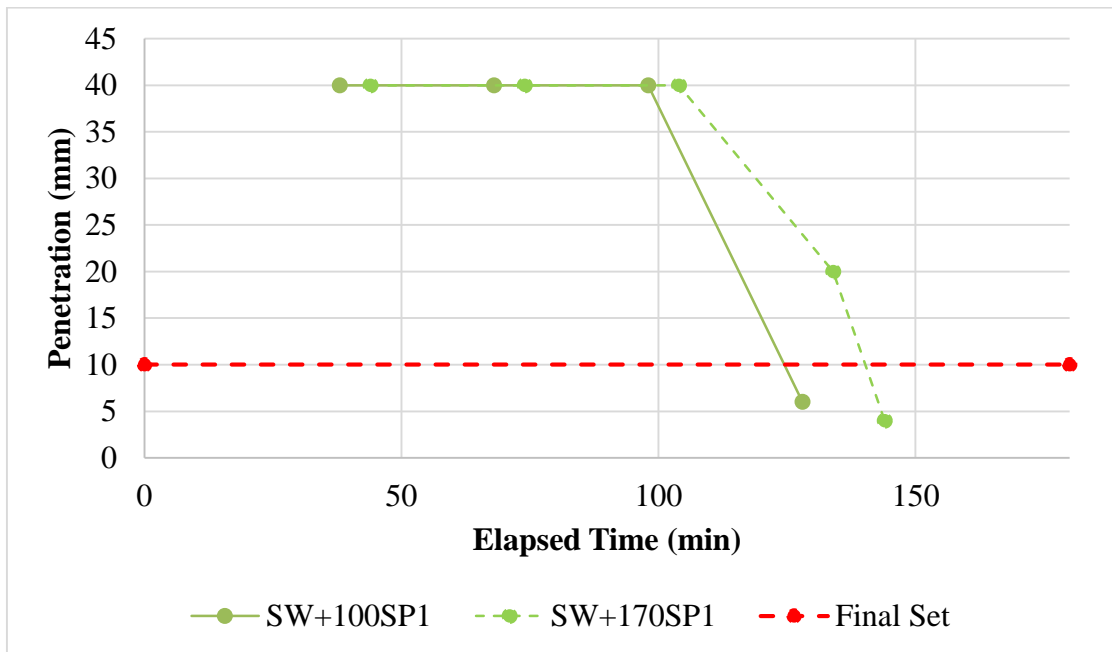


Figure 35: Mortar Setting Time for Varying SP1 Dosage with No Mineral Admixture Replacement

Considering the binary systems incorporating MK, Figure 36, it can be observed that increasing the dosage of the HRWR SP1 increases the final setting time. It is also noted that for the same superplasticizer dosage, metakaolin mixtures have a shorter setting time than the control mixture (Figure 35).

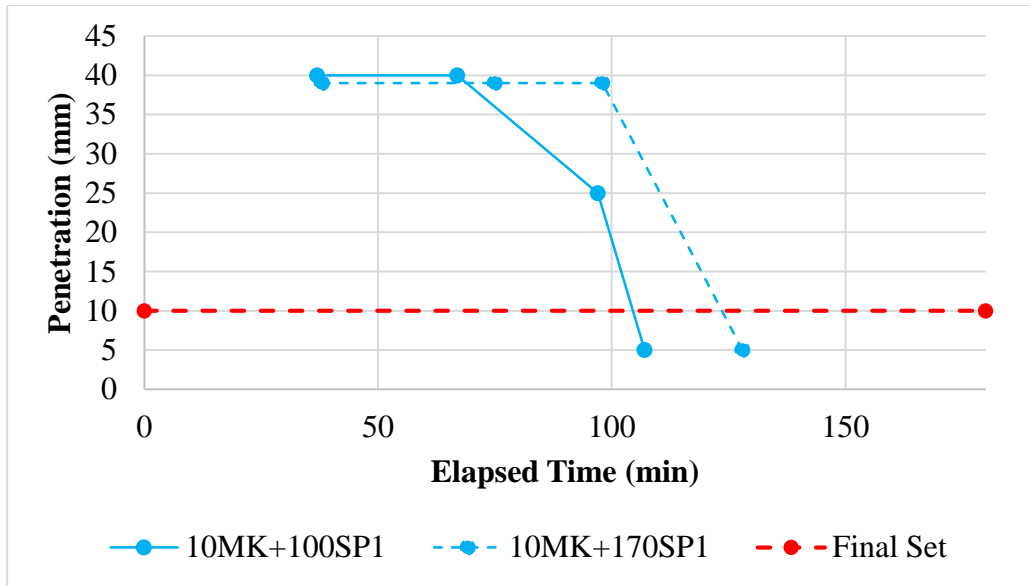


Figure 36: Mortar Setting Time for Varying SP1 Dosage for Metakaolin Mixtures

4.2.6 Varying SP2 Dosage

For cementitious mixtures incorporating silica fume, blast-furnace slag and fly ash, a different superplasticizer “SP2” was used to be consistent with the most commonly used admixture combination in Florida mixtures. Again, an upper and a lower range, similar to SP1 were used here and the effect on setting time was studied for different cementitious systems. The superplasticizer dosage was varied between 100 and 170 ml per 100 kg cementitious material. Figure 37 to 40 shows the results on the effect of varying SP2 dosage on setting time. The results show that for the range of SP2 used here, the effect of using SP2 on setting time was a slight delay in the final set. Similarly, for the cementitious systems studied here, the effect was a slight increase in final set between 10 to 21 minutes with FA the least affected (8 minutes) and slag experiencing the longest delay (21 minutes).

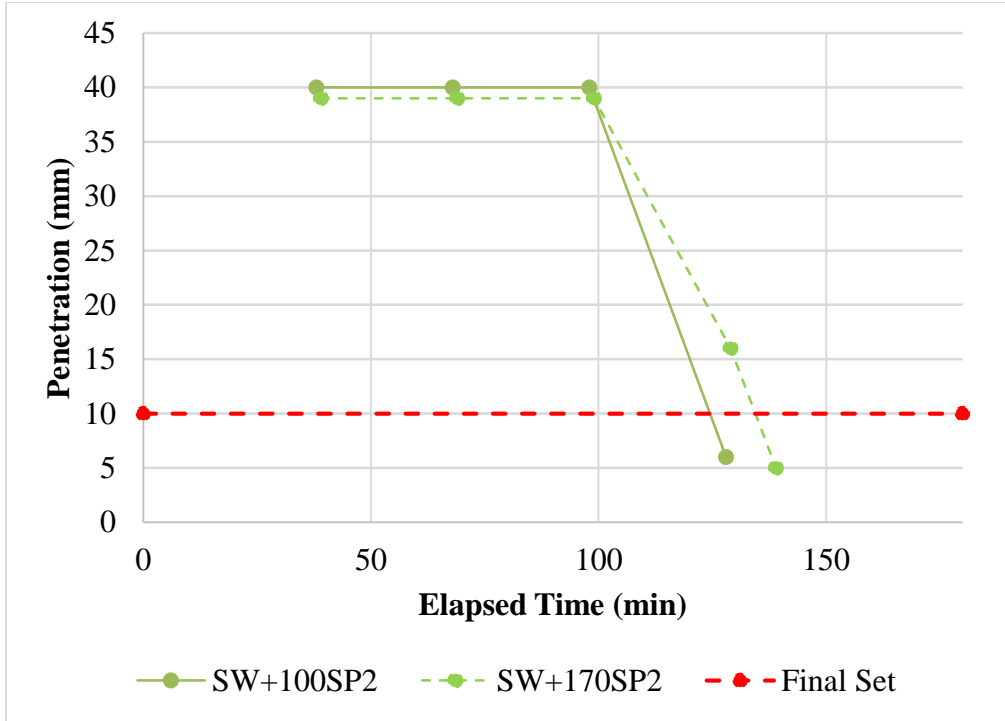


Figure 37: Mortar Setting Time for Varying SP2 Dosage with No Mineral Admixture Replacement

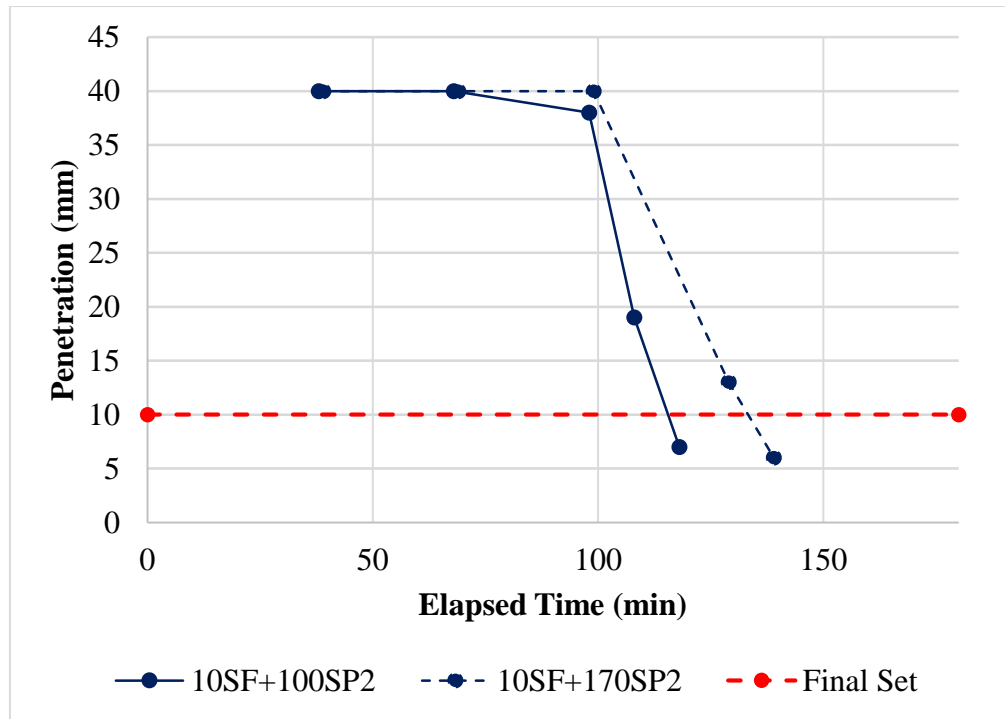


Figure 38: Mortar Setting Time for Varying SP2 Dosage for Silica Fume Mixtures

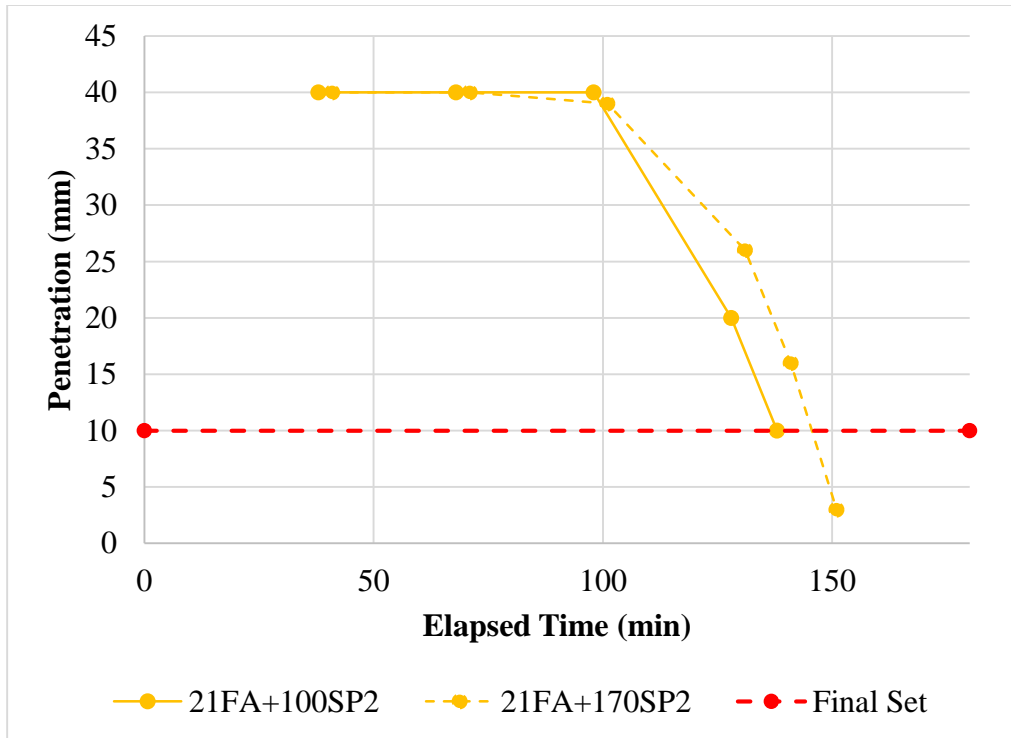


Figure 39: Mortar Setting Time for Varying SP2 Dosage for Fly Ash Mixtures

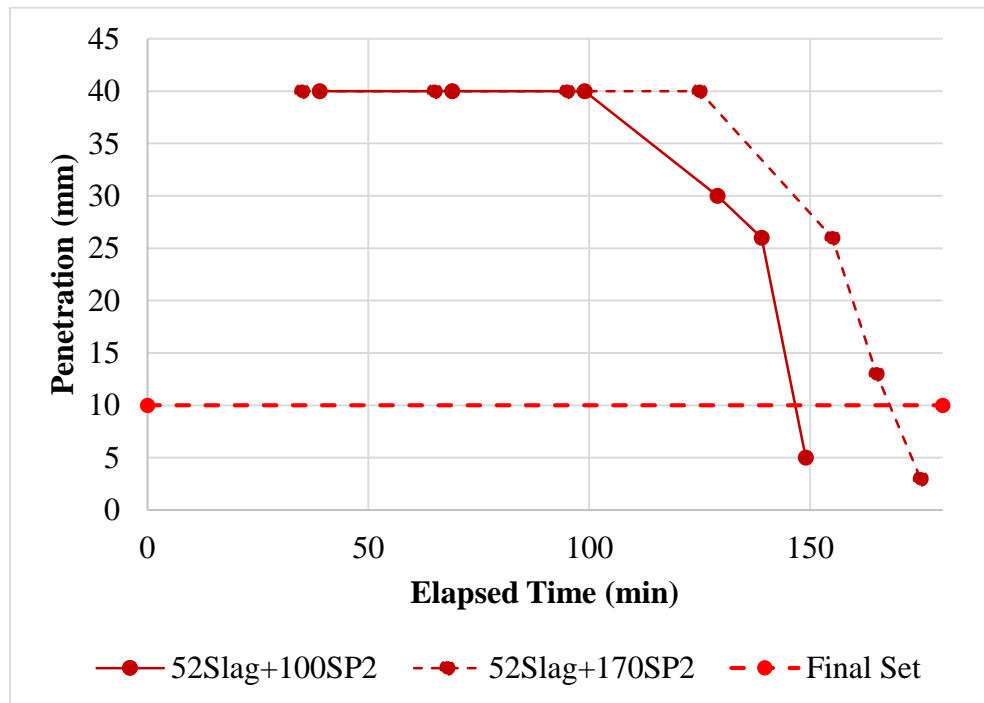


Figure 40: Mortar Setting Time for Varying SP2 Dosage for Slag Mixtures

In conclusion, superplasticizers from the polycarboxylate-polyether family appear to consistently delay or retard setting of the all cementitious mixtures studied here. This is expected due to their effect on tricalcium silicate hydration [104].

4.3 Compressive Strength

4.3.1 Metakaolin

Metakaolin was evaluated at two different replacement levels: 10 and 21%. Figure 41 shows the compressive strength results for MK mixtures where it can be seen that as the replacement level increases, the early age strength decreases. At 28 days, the 10% metakaolin mixture had the highest compressive strength but the 21% metakaolin has the highest rate of strength gain between 7 and 28 days. This is consistent with the results of Poon et al. [36] in which 10% metakaolin had the highest compressive strength.

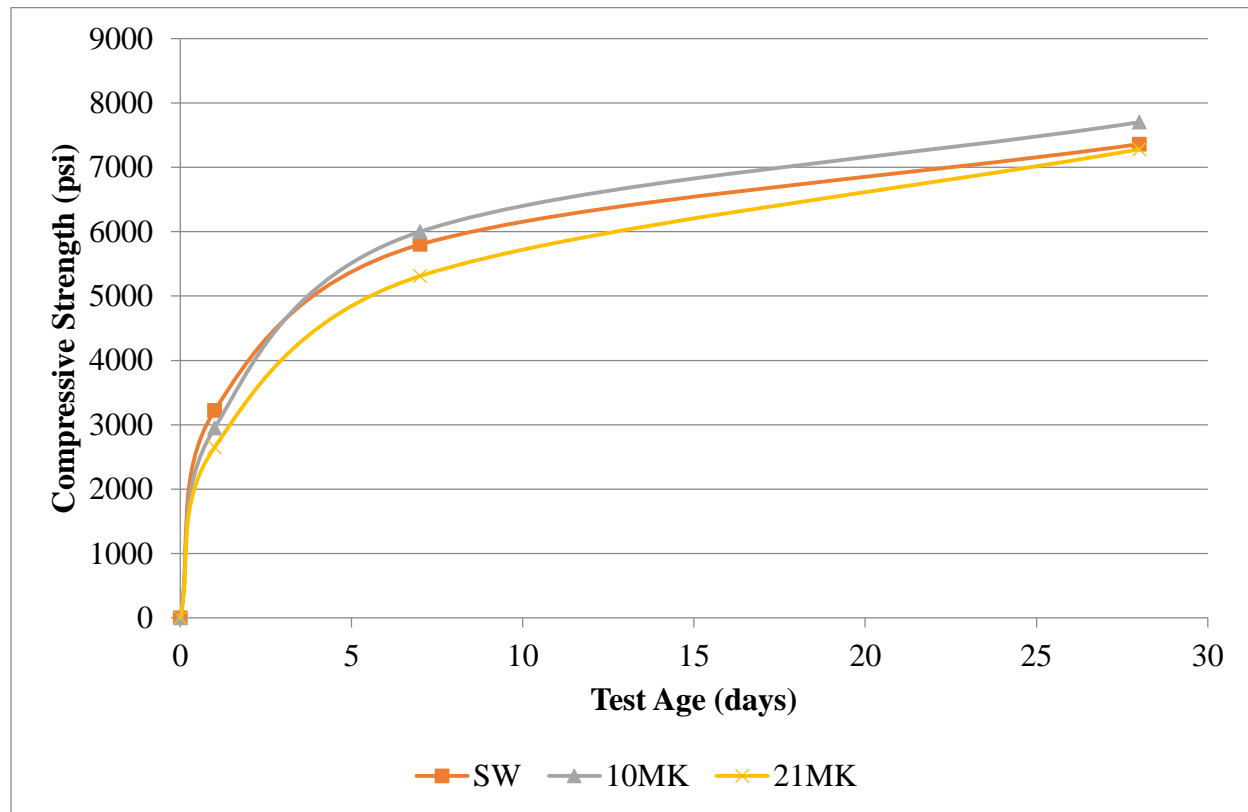


Figure 41: Compressive Strength of Metakaolin Mixtures

4.3.2 Silica Fume

SF was evaluated at a 10% mass replacement. Figure 42 shows the results for the compressive strength results for silica fume mixture. The results show that the addition of silica fume increased the 28 day compressive strength, whereas the control mixture had the highest early-age strength. The lower early age strength can be attributed to the dilution effect (lower cement content) while the higher 28 day strength can be attributed to the pozzolanic reaction as well as the packing of finer silica particles at the interfacial transition zone. This is consistent with the results of Toutanji et al. [45], Erdem and Kirca [47], and Gesoğlu et al [48].

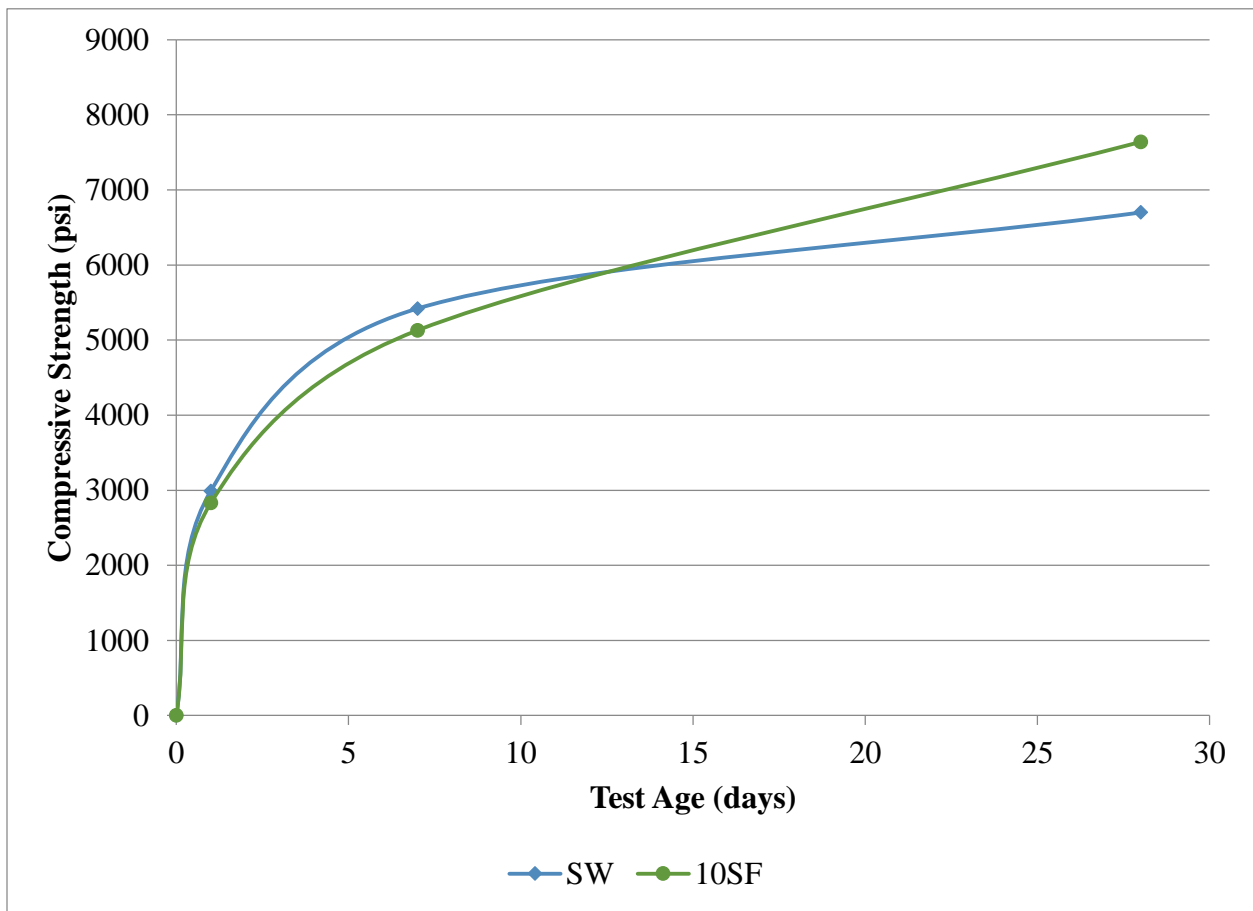


Figure 42: Compressive Strength of Silica Fume Mixtures

4.3.3 Fly Ash

Fly ash was evaluated at three different replacement levels: 10, 21, and 30%. Figure 43 shows the results for compressive strength for the fly ash mixtures where it can be seen that increasing fly ash content results in a decrease in compressive strength. This is consistent with the results by Liu et al. [54], Roy et al. [39], and Gesoğlu et al [48]. According to Liu et al, the decrease in strength is attributed to fly ash having little effect on the chemical activity at early ages. The FA used in this current study had an amorphous content of approximately 72% which represents the lowest amount of amorphous content among the mineral admixtures studied here.

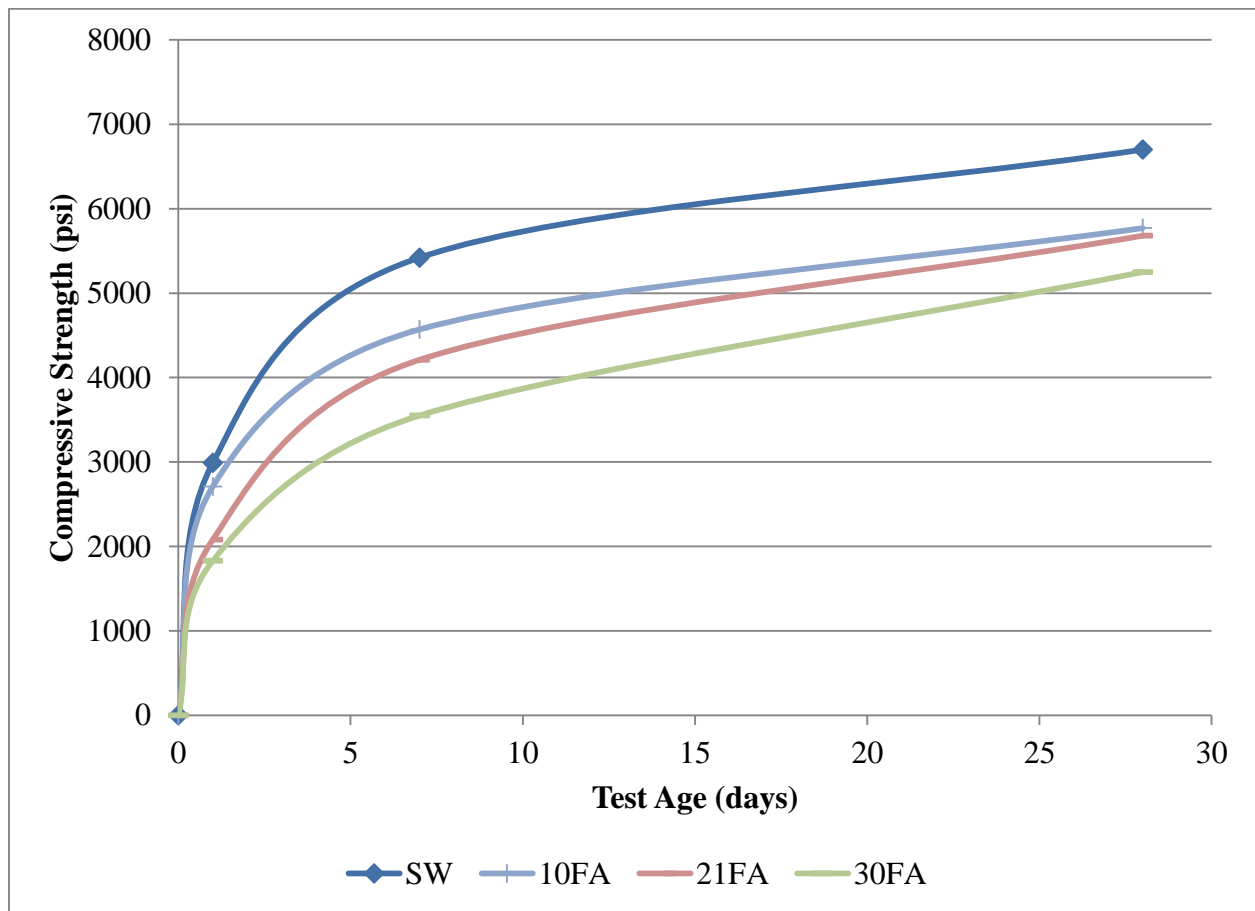


Figure 43: Compressive Strength of Fly Ash Mixtures

4.3.4 Slag

Slag was evaluated at three different replacement levels: 21, 30, and 52%. Figure 44 shows the compressive strength results for the slag mixtures where it can be seen that the early-age strength decreases as the replacement level of slag increases. At 28 days, the 30% slag mix had a compressive strength higher than the control. This is consistent with the results by Menendez [60] and Aldea et al. [61]. Menendez found that at 90 day, the 30% slag mixture had a higher compressive strength than the control. Aldea et al. noted that the replacement level of 25% has the optimum. While the optimum slag replacement level can vary with the characteristics of the slag and the age considered, the slag used here shows the highest rate of strength gain between 7 and 28 days for the 30% replacement but then the rate of strength gain drops when the slag replacement increases to 52%.

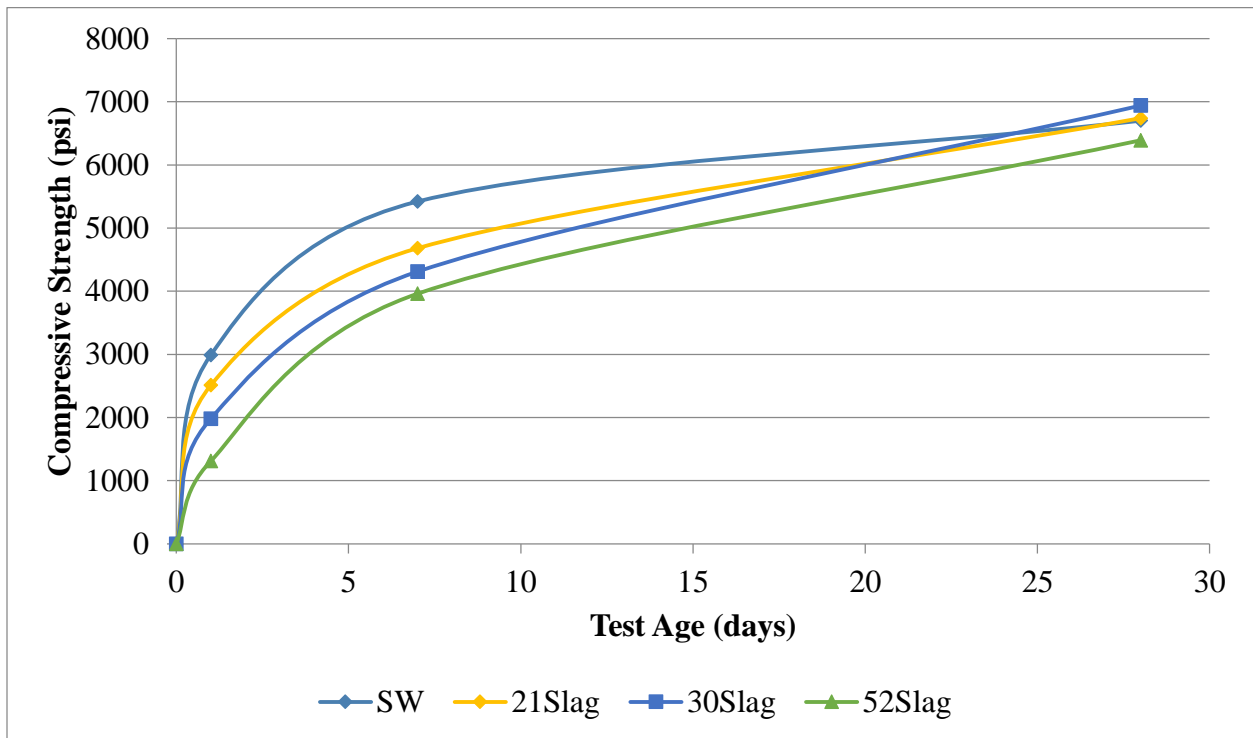


Figure 44: Compressive Strength of Slag Mixtures

4.3.5 Varying SP1 Dosages

There was two SP used throughout this study with metakaolin mixture using SP1 and the others using SP2. Compressive strength was also determined on mortar by varying the dosage of SP. Each SP dosage was varied between 100 and 170 ml per 100 kg cementitious material. The compressive strength results of varying SP1 is shown on Figure 45 and 46. The results indicate that for mixtures containing SP1, (the control containing SP1 at 2 levels and 10% metakaolin with two different levels of SP1), increasing the superplasticizer dosage while maintaining the w/cementitious ratio constant results in an increase in the 7 and 28day strength. This could be due to better dispersion of MK using SP1. This is consistent with the findings of Xiao et al. [105] where it was noted that the increase in dosages leads to an increase in compressive strength until 0.35%.

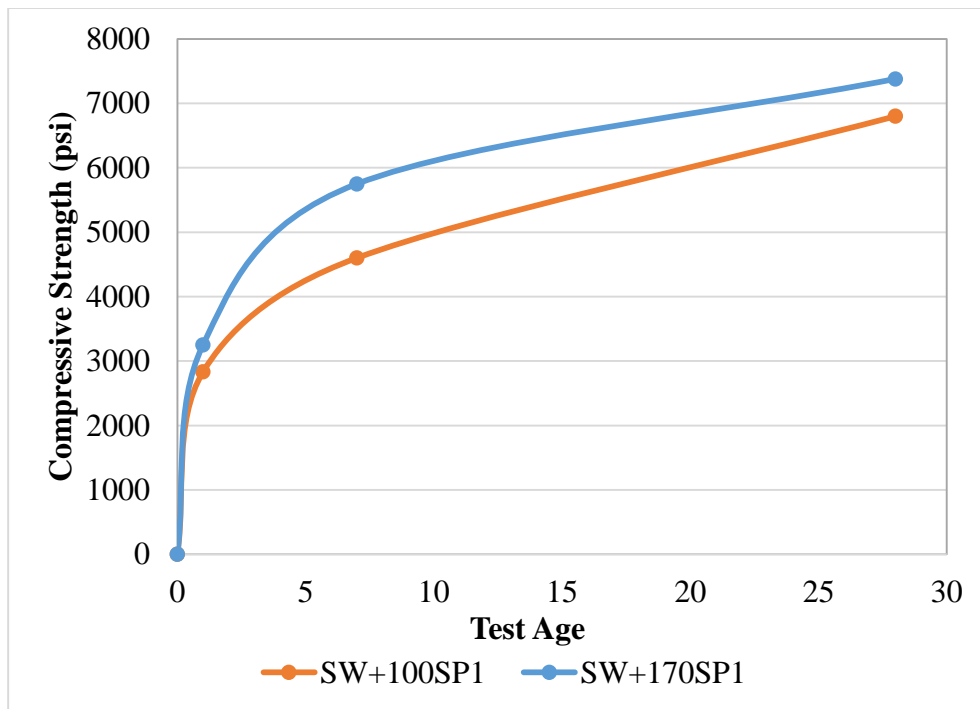


Figure 45: Compressive Strength of Control Mixtures with Varying SP1 Dosage

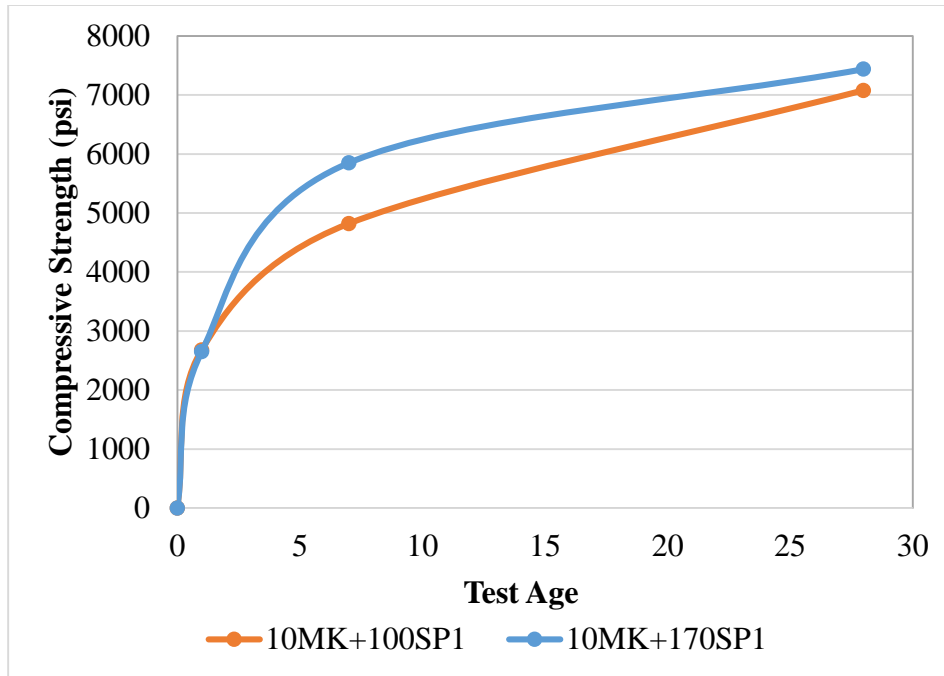


Figure 46: Compressive Strength of Metakaolin Mixtures with Varying SP1 Dosage

4.3.6 Varying SP2 Dosages

Compressive strength was also determined on mortar by varying the dosage of SP2 between 100 and 170 ml per 100 kg cementitious material. The compressive strength results of varying SP2 is shown on Figure 47 to 50. For the control mixture, increasing the superplasticizer dose increased strength at all ages but the effect is negligible at 1 day. For mixtures containing mineral admixtures, the 28 day compressive strength was consistently higher when SP2 dose was increased. The 7-day strength of the 10% SF mixture showed a significantly lower value when the superplasticizer dosage was increased. While similar trends were noticed with the fly ash mixture, but to a lesser extent, the slag mixture showed a consistent increase in compressive strength at all ages with increasing superplasticizer dosage.

The results indicate that superplasticizers interact differently with mineral admixtures. This is not surprising as different mineral admixtures have differences in their chemical composition. Thus, it is critical that before selecting a superplasticizer for a concrete mixture incorporating

mineral admixtures, the effectiveness of the selected superplasticizer and its compatibility with the cementitious system has to be studied thoroughly.

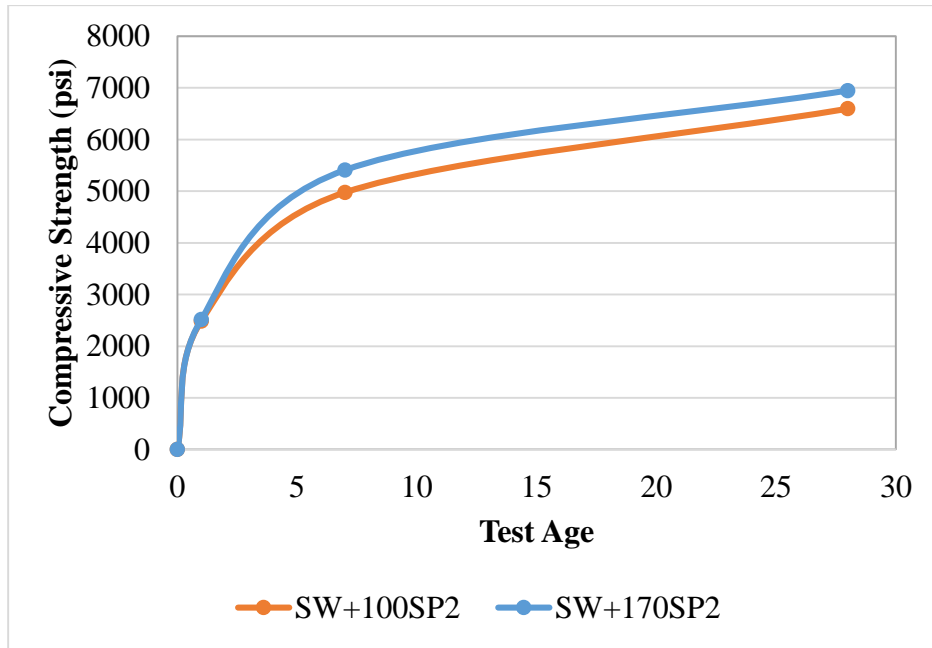


Figure 47: Compressive Strength of Control Mixtures with Varying SP2 Dosage

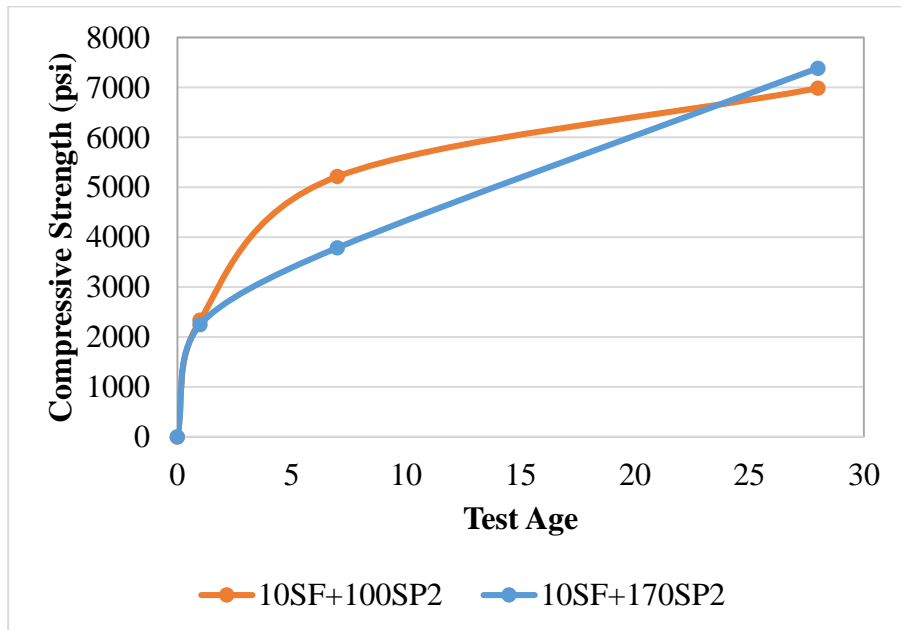


Figure 48: Compressive Strength of Silica Fume Mixtures with Varying SP2 Dosage

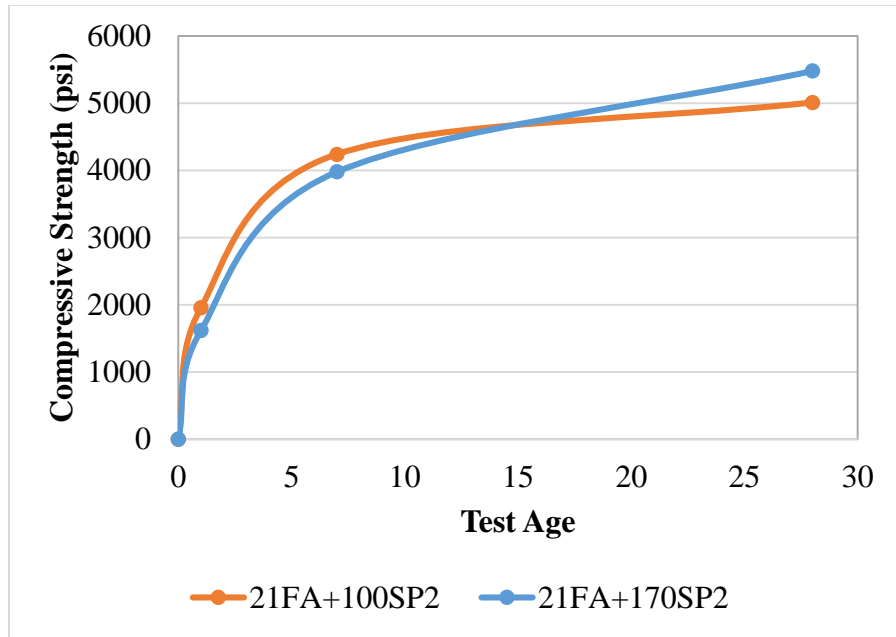


Figure 49: Compressive Strength of Fly Ash Mixtures with Varying SP2 Dosage

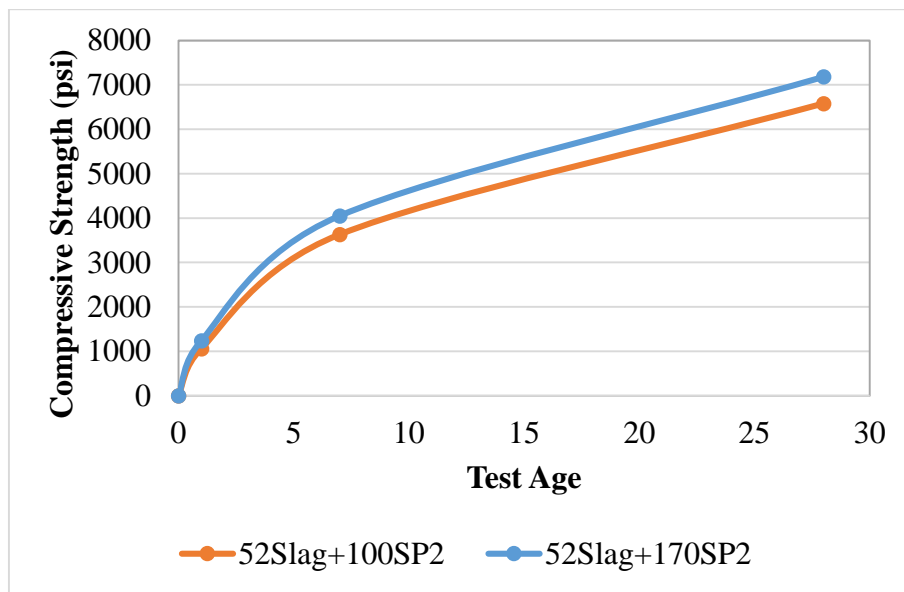


Figure 50: Compressive Strength of Slag Mixtures with Varying SP2 Dosage

4.4 Sulfate Durability

Mineral admixtures are typically used in concrete mixtures in order to improve sulfate durability. Sulfate durability of different cementitious mixtures incorporating chemical admixtures were studied here using sodium sulfate as the exposure media. The mixtures proportions used here

are the same as those used for compressive strength and setting properties. The details of the mixtures proportions were previously provided in Chapter 3 of this document. In general, chemical admixtures were fixed for all mixtures in their type and amount to be able to compare primarily the performance of different mineral admixtures in a sulfate environment. However, the metakaolin mixture and its control were prepared with a different superplasticizer, SP1, to be consistent with mixtures used in the state of Florida. Fly ash, silica fume, blast furnace slag and their control mixture were all prepared with the same chemical admixtures used in the metakaolin mix and its control except for the superplasticizer type. The superplasticizer used in the former was SP2. Sulfate durability of the cementitious systems was studied in a sodium sulfate solution. The results show that one mixture disintegrated before the 6 month period and that mixtures containing silica fume showed the highest sulfate resistance. Replacement level of 21% fly ash also showed high sulfate resistance. Slag mixtures are shown to not pass the criteria set by ASTM C-989-13 [66] for high sulfate resistance.

4.4.1 Effect of Superplasticizer Type

Figure 51 shows the sulfate expansion results for mortar mixed with the two superplasticizers used in this study, SP1 and SP2, together with a control mixture that has no superplasticizers. From the results, both superplasticizers mixtures qualify for moderate sulfate resistance. The difference between the two mixtures is 0.01% expansion, with SP1 having a slight advantage in sulfate resistance.

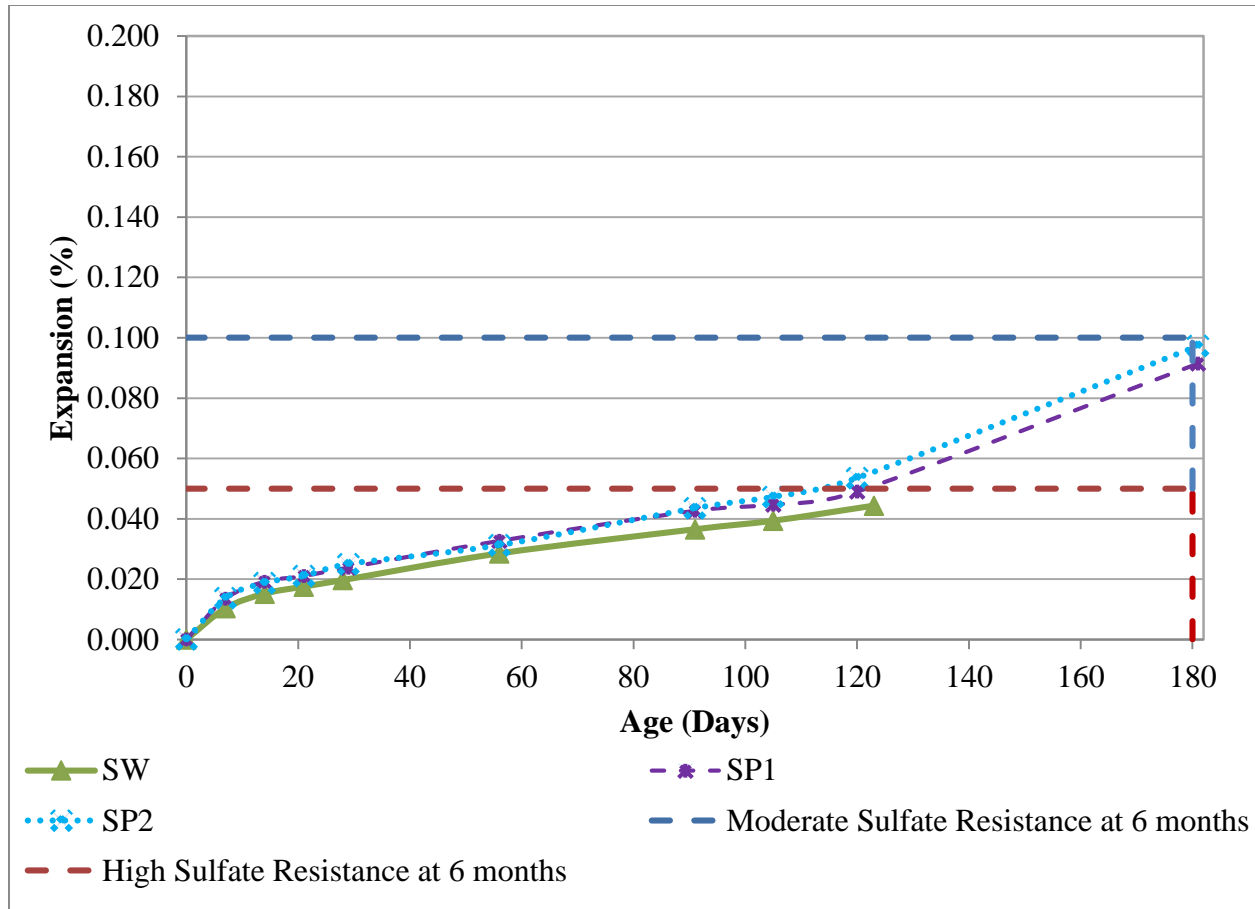


Figure 51: Effect of SP on Length Change of Mortar Sample in 5% Na₂SO₄ Solution

4.4.2 Effect of Metakaolin

Figure 52 shows the sulfate expansions results for the effect of metakaolin in 5% Na₂SO₄ solution at 2 replacement levels. During the induction period, the higher metakaolin mixture shows higher expansion, but at 120 days, it appears that the trend might potentially change. The 10% metakaolin mixture shows the highest rate of expansion compared to the 20% replacement or even the control mixture. Longer exposure times are required prior to establishing a concluding trend on the effectiveness of metakaolin as a mineral admixture in enhancing sulfate durability of cementitious mixtures.

According to the results, the 10% metakaolin sample showed an expansion of 0.045% at 120 days while the 20% metakaolin sample showed an expansion of 0.043% at 120 days. No

conclusive remarks can be stated here until the data is collected to 180 days. Al-Akhras [32]. Al-Akhras investigated up to 15% metakaolin and found that 15% had the best results, with an improvement of 0.03% from the 10% metakaolin results. This was attributed to the decrease in cement content by the pozzolans that reduces the C₃A in the cement as well as the pozzolanic reaction of forming C-S-H.

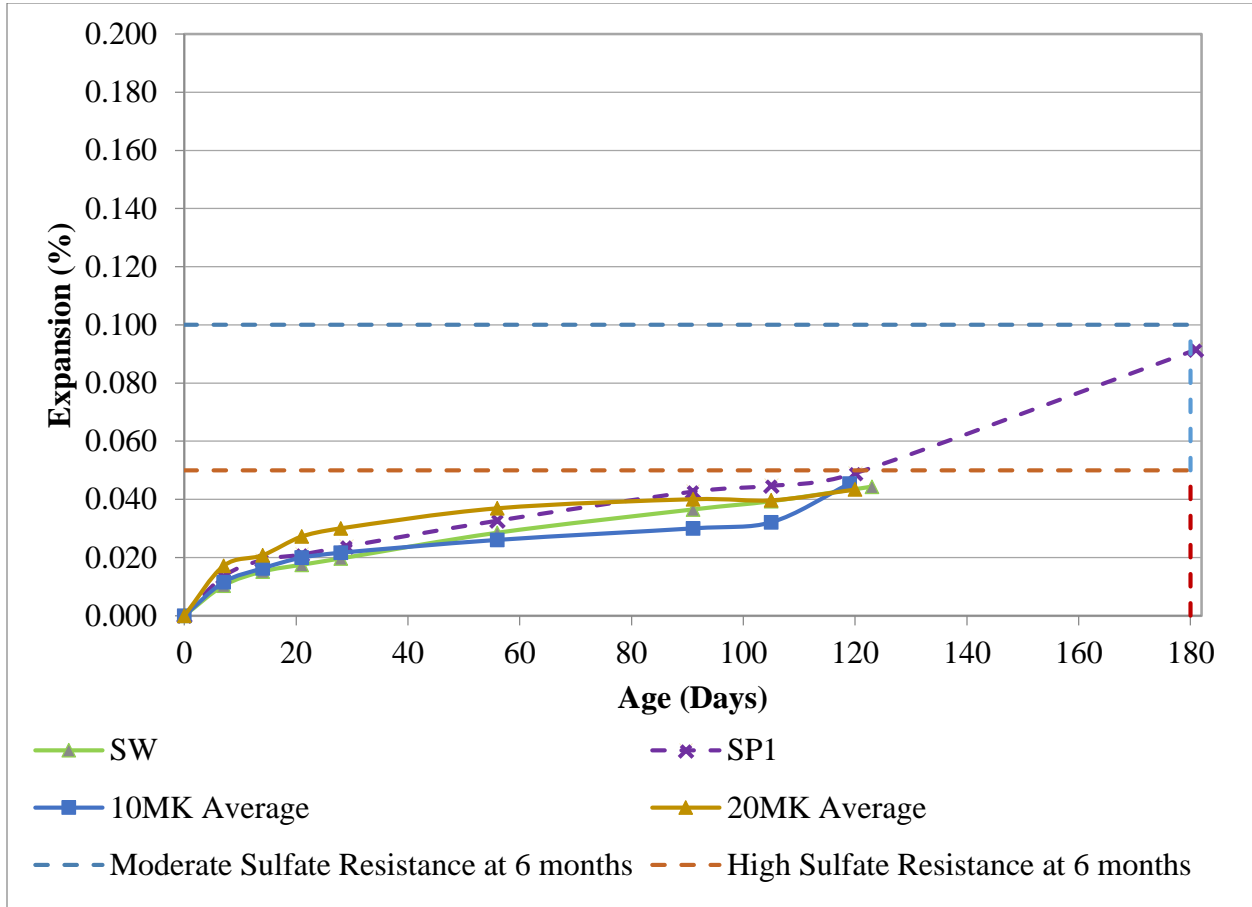


Figure 52: Effect of Metakaolin on Length Change of Mortar Sample in 5% Na₂SO₄ Solution

4.4.3 Effect of Silica Fume

Figure 53 shows the sulfate expansion results for silica fume in 5% Na₂SO₄ solution. The results clearly indicate that 10% silica fume improves the sulfate resistance of mortar bars for the period reported here. According to ASTM C1240-14 [106], silica fume mixtures can be classified

as “High sulfate resistance”. This is consistent with the results of Hooton [49], Mardani-Aghabaglou, and Cohen and Bentur [51]. Silica fume has a higher surface area and pozzolanic activity among the mineral admixtures studied here. Its contribution to mortar strength was as highest among the mineral admixtures studied here with the exception of metakaolin. However, while silica fume has a higher silica content, metakaolin has a higher alumina content. This could explain why the 10% metakaolin mixture experienced almost double the expansion of the silica fume mixture at 120 days of exposure to the sodium sulfate solution.

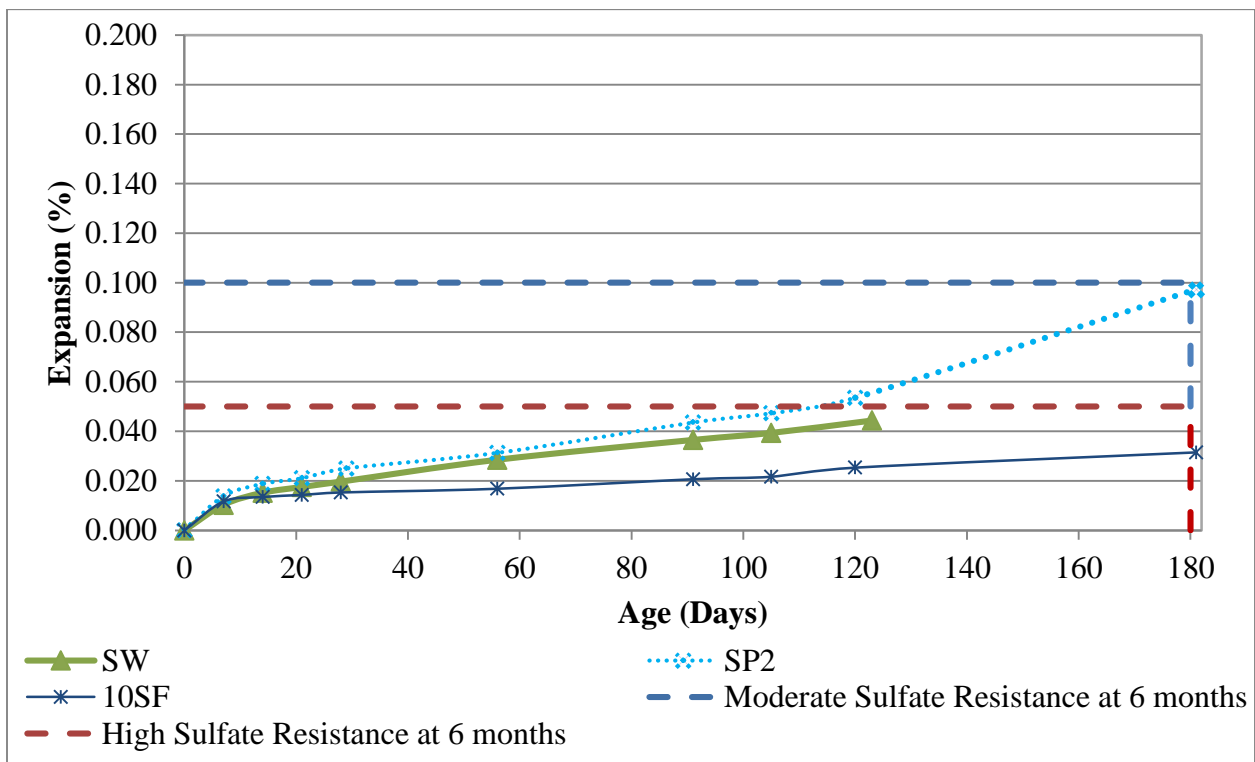


Figure 53: Effect of Silica Fume on Length Change of Mortar Sample in 5% Na₂SO₄ Solution

4.4.4 Effect of Fly Ash

Figure 54 shows the sulfate expansions for the fly ash mixture in 5% Na₂SO₄ solution. Though the class F fly ash used in this study had a low amorphous content and low strength gain, it enhanced sulfate durability of the mixture when compared to the control mixture. At six months,

fly ash improves the sulfate resistance of mortar bars as it showed a 0.05% expansion versus the control mixture expansion of 0.1%. According to ASTM criteria, the fly ash mixture is considered “high sulfate resistance” with an expansion of 0.05% at 6 months. This is consistent with the results by Ghafoori [58] who investigate the effect of class F fly ash on sulfate resistance and concluded that the addition of fly ash to mixture improves sulfate durability. When comparing fly ash mixture with the 20% metakaolin, the fly ash mixture showed lower expansion than the metakaolin at 120 days of exposure. However, silica fume performance is still better than either metakaolin or fly ash though silica fume was only used at 10 % replacement level.

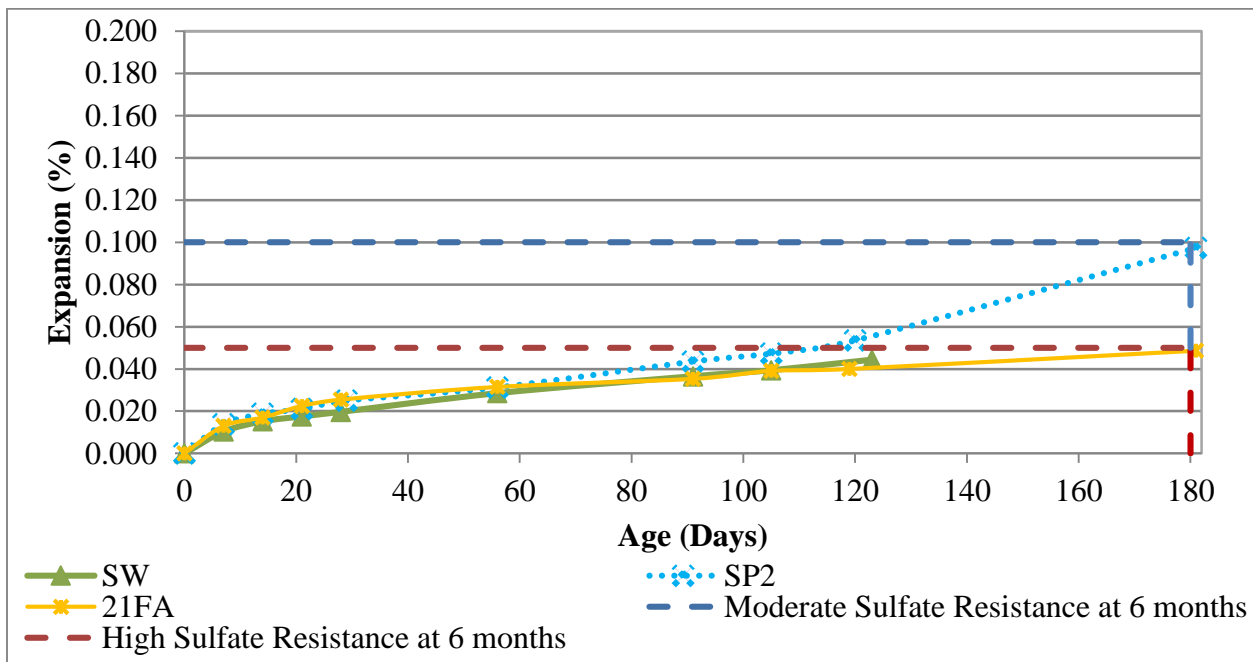


Figure 54: Effect of Fly Ash on Length Change of Mortar Sample in 5% Na₂SO₄ Solution

4.4.5 Effect of Blast Furnace Slag

Figure 55 shows the sulfate expansions results for the effect of slag in 5% Na₂SO₄ solution. The results show that 52% slag did not improve the sulfate resistance of the mortars bars. Before the 6 month expansion measurement, the mortar bar had disintegrated. This result differs from the results by Ekolu and Ngwenya [62] and Kandasamy and Shehata [57]. Ekolu and Ngwenya

investigated the sulfate durability of slag with an alumina content of 13.4%. Ekolu and Ngwenya found that the slag mixture containing 30% slag showed some expansion while the 50 and 70% slag mixture showed relatively no expansion. The mixtures in their study was moist-cured for 21 days before immersion into sulfate solution. Kandasamy and Shehata investigated the sulfate durability of slag with an alumina content of 7.4%. They found that mixtures containing 30 and 40% replacement level of slag enhanced sulfate durability. According to Kandasamy and Shehata, sulfate resistance is improved through the C-S-H ability to incorporate Al^{3+} ions. Yu et al. [63] investigated the sulfate durability of 0, 40, and 70% slag in a 3, 10, and 30 Na_2SO_4 solution with an alumina content of 15.85% and found that 70% slag had the best results. It was found that the 70% slag mixture in 30 g/L solution experience breakage before 180 days and in a 10g/L solution experience a breakage at 240 days. Ogawa et al. [64] investigated an unmodified slag as well as an optimized slag on sulfate durability. The unmodified slag had an alumina content of 15.0% and was used at a mass replacement of 40%. The modified slag had its chemical composition optimized and was used at a mass replacement of 40% to make a slag cement with an alumina content of 7.7%. It was determined that the unmodified slag showed expansion after 25 weeks and experience breakage at 38 weeks. The optimized slag performed excellent even after 104 weeks. Ogawa et al. [65] also investigated on how to improve sulfate durability of high alumina slag and found that addition of limestone powder as well as increasing the calcium sulfate content will improve sulfate durability. The addition of limestone powder is believed to have limited improvement of sulfate resistance as the formation of monocarboaluminates would only slowly convert to ettringite. The increase in calcium sulfate would increase the amount of ettringite formed initially therefore decreasing the potential for monosulfate formations.

The reason for the disintegration of the 50% slag mixture needs to be further examined to understand better why this particular mixture experienced failure when exposed to sodium sulfate solution.

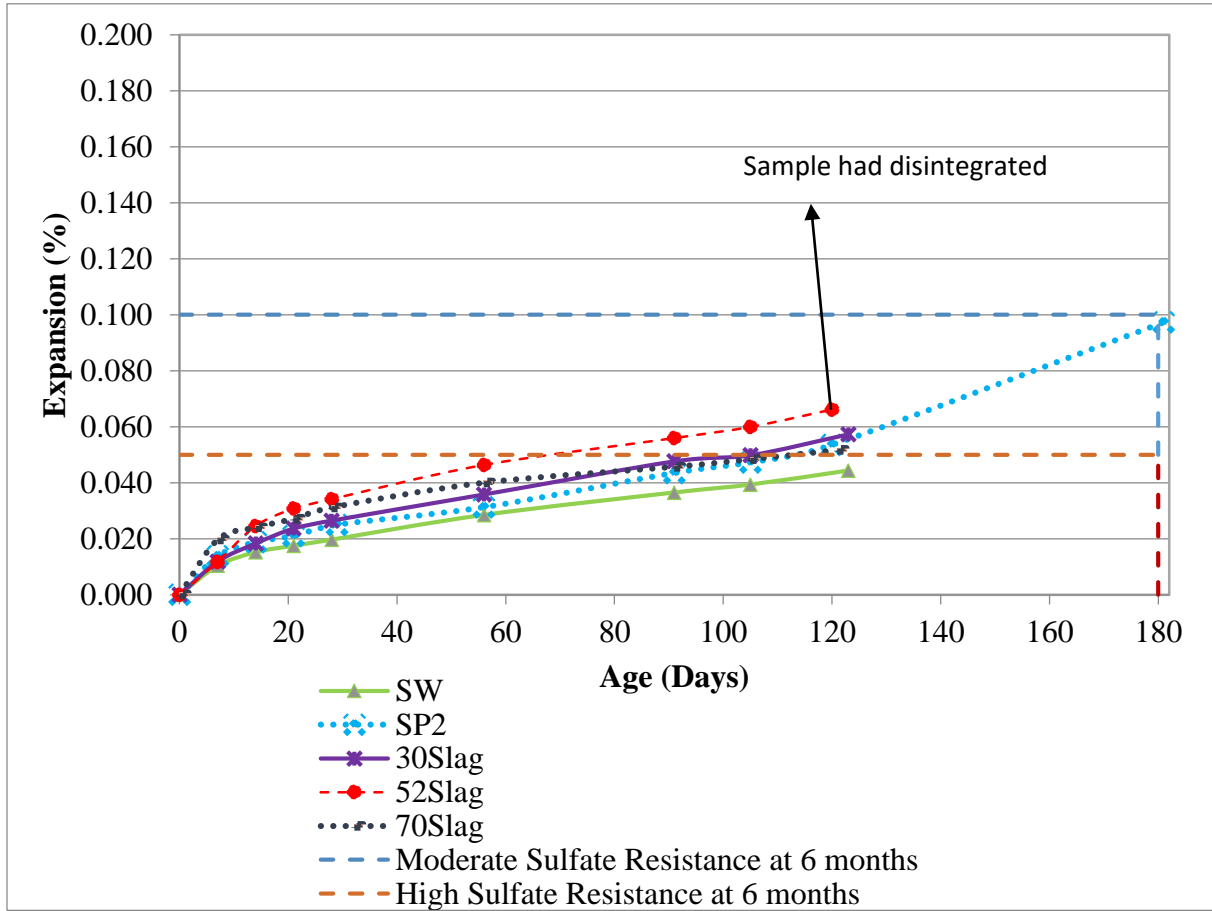


Figure 55: Effect of Slag on Length Change of Mortar Sample in 5% Na₂SO₄ Solution

4.5 XRD Analysis

In order to have a better understanding as to why 52% slag sample disintegrated, phase analysis was conducted using x-ray diffraction on the 52% slag mortar bar. Two paste samples were analyzed to identify phases present in the control and 52% slag mixture prior to exposure to the sulfate media. The paste samples were prepared to match the cementitious content mixture proportions in the mortar bars and were examined at an age of 1 day. The results, Table 19 and 20, indicate that at 1 day the control sample shows the presence of portlandite, complete consumption

of gypsum and the presence of ettringite but no monosulfates. The 52% slag paste, however, shows mixtures of monosulfoaluminate, ettringite and hemicarboaluminate. So at the time of exposure to the sulfate solution, the slag sample showed the presence of phases that could undergo phase transformation to the higher sulfate compound, ettringite, if exposed to a source of sulfate.

Table 19: Phase Constituents of SW Paste at 1 Day

Phase ID	Amount (w/o)
Quartz	0.6
Calcite	2.5
Gypsum	-
Alite	6
Belite	14.9
Aluminate	2.6
Ferrite	3.9
Ettringite	8
Portlandite	10.3
Monosulfate	-
Hemicarboaluminate	-
Bassanite	-
Amorphous	51.2

Table 20: Phase Constituents of 52% Slag Paste at 1 Day

Phase ID	Amount (w/o)
Quartz	1.1
Calcite	2.8
Gypsum	-
Alite	1.5
Belite	6.2
Aluminate	0.2
Ferrite	0.7
Ettringite	4
Portlandite	3.7
Monosulfate	3.1
Hemicarboaluminate	2.1
Bassanite	-
Amorphous	74.6

Analysis of mortar bars for the 52% slag specimen that has disintegrated when exposed to sodium sulfate solution together with the control are presented in Figure 56. It can be seen that the outer surface of the 52% slag mortar bar has more than double the ettringite content that the inner core showed. While the control showed an increase in the ettringite content between the surface and the inner core, the increase is modest compared to the 52% Slag bar. It is plausible that this concentration differential might be contributing to the failure of the 52% slag mixture.

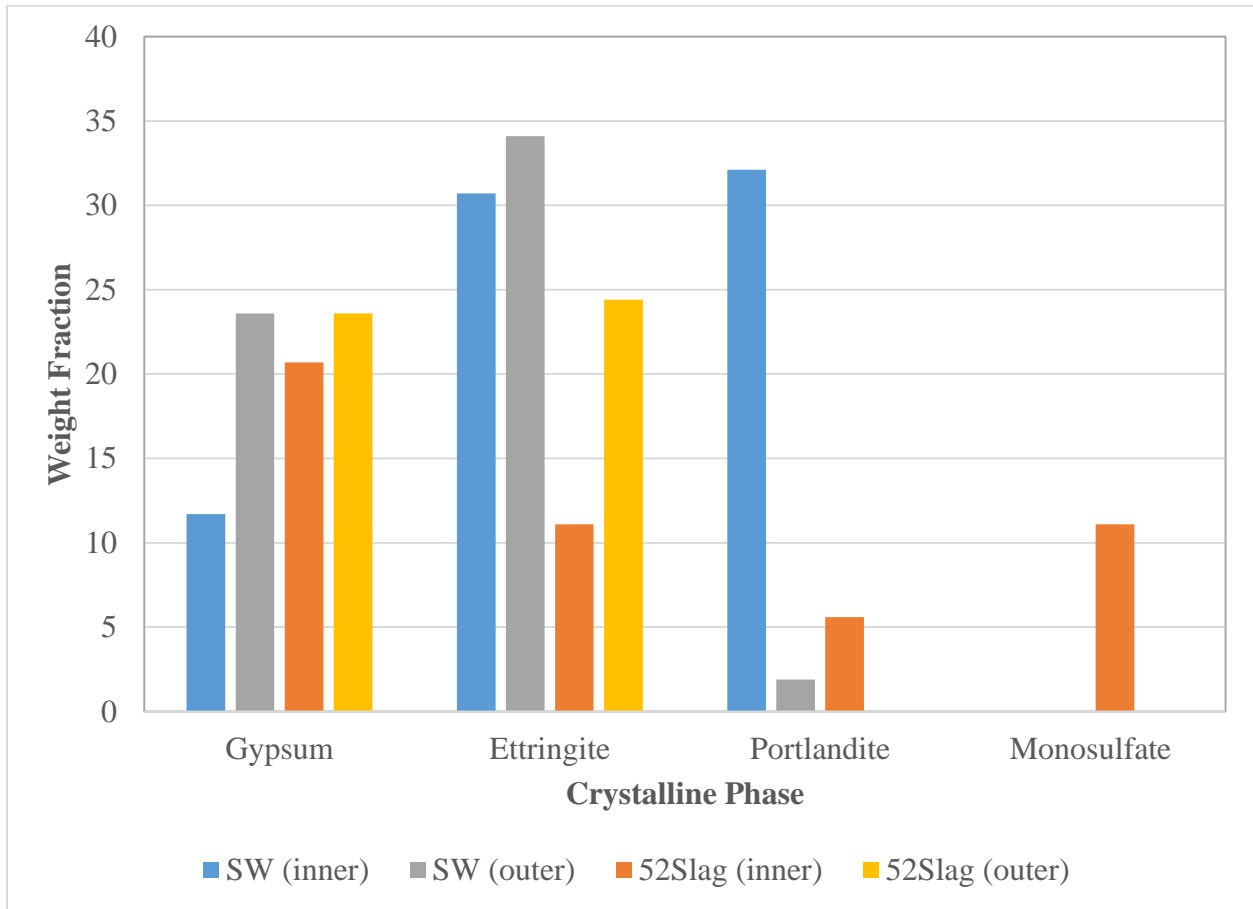


Figure 56: XRD Analysis of 52% Slag at Time of Disintegration and the Control

CHAPTER 5: CONCLUSIONS AND FURTHER RESEARCH

In the present study, the effect of different mineral and chemical admixtures and their combinations on durability was investigated. The chapter presents the conclusions from this study as well as recommendations for future research.

5.1 Conclusions

The conclusions drawn from this study are as follows:

1. Silica fume is beneficial for durability at a replacement level as low as 10%. It outperformed the other mineral admixtures studied here regarding sulfate durability and heat generation.
2. Heat of hydration measurements indicate that incorporation of slag or metakaolin affect the sulfate depletion point in the cementitious system. It is also noted that they increase the heat of hydration if the rate of heat evolution or total heat is expressed per gram of cement. Both of those mixtures appear to be undersulfated.
3. The amorphous content of fly ash can be seen to affect the trends in this study.
4. Higher dosages of SP lead to an increase in setting time and compressive strength.
5. The alumina content of mineral admixtures are important in sulfate durability.

5.2 Recommendations for Future Research

The recommendations for future research are as follows:

1. Varying a higher dosage of SP can be explored to determine how it affects chemical and mechanical properties.

2. Strength tests can be conducted for a longer time and in a sulfate media to better understand the strength evolution of mixtures in a sulfate environment.
3. XRD and SEM can be used for an in depth study on the effects of mineral and chemical admixtures on durability.
4. Cracking potential can be investigated to determine the thermal effects of mineral and chemical admixtures combinations on cracking tendencies.

REFERENCES

- [1] ASTM C807, “Standard Test Method for Time of Setting of Hydraulic Cement Mortar by Modified,” *ASTM Int.*, vol. i, pp. 1–3, 2013.
- [2] ASTM C109/C109M, “Standard test method for compressive strength of hydraulic cement mortars (Using 2-in. or cube specimens),” *ASTM Int.*, pp. 1–10, 2013.
- [3] ASTM C1012/C1012M, “Standard Test Method for Length Change of Hydraulic-Cement Mortars Exposed to a,” *ASTM Int.*, no. c1012, pp. 1–7, 2012.
- [4] F. Jackson, “The durability of concrete in service,” *ACI J. Proc.*, vol. 43, no. 165, pp. 165–180, 1946.
- [5] W. Lerch, “The influence of gypsum on the hydration and properties of Portland cement pastes,” 1946.
- [6] L. Roberts and P. Taylor, “Understanding cement-SCM-admixture interaction issues,” *Concr. Int.*, pp. 33–41, 2007.
- [7] L. Meyer and W. Perenchio, “Theory of Concrete Slump Loss Related to the Use of Chemical Admixtures,” 1980.
- [8] C. Bedard and N. Mailvaganam, “The Use of Chemical Admixtures in Concrete. Part I: Admixture-Cement Compatibility,” *J. Perform. Constr. Facil.*, vol. 19, no. 4, pp. 263–267, 2005.
- [9] ACI Committee 212, *Chemical Admixtures for Concrete*. Detroit, MI: American Concrete Institute, 1991.
- [10] R. Rixom and N. Mailvaganam, *Chemical Admixtures for Concrete*, 3rd ed. New York, NY: Routledge, 1999.
- [11] ASTM C 125, “Standard Terminology Relating to Concrete and Concrete Aggregates,” in *Annual Book of ASTM Standards, V. 04.02*, ASTM International, 2011.
- [12] ASTM C494, “Standard Specification for Chemical Admixtures for Concrete,” *ASTM Int.*, pp. 1–9, 2013.
- [13] A. M. Neville, *Properties of Concrete*, 4th ed. Harlow, England: Pearson Education Limited, 2006.

- [14] I. Soroka and D. Ravina, “Hot Weather Concreting with Admixtures,” *Cem. Concr. Compos.*, vol. 20, no. 3, pp. 129–136, 1998.
- [15] J. Cheung, a. Jeknavorian, L. Roberts, and D. Silva, “Impact of admixtures on the hydration kinetics of Portland cement,” *Cem. Concr. Res.*, vol. 41, no. 12, pp. 1289–1309, Dec. 2011.
- [16] P. Sandberg and L. Roberts, “Studies of cement-admixture interactions related to aluminate hydration control by isothermal calorimetry,” in *Seventh CANMET/ACI International Conference on Superplasticizers and Other Chemical Admixtures in Concrete*, 2003, pp. 529–542.
- [17] H. Wang, C. Qi, H. Farzam, and J. I. M. Turici, “Interaction of Materials Used in Concrete,” *Concr. Int.*, vol. 28, no. 4, pp. 47–52, 2006.
- [18] V. Ramachandran, “Influence of triethanolamine on the hydration characteristics of tricalcium silicate,” *J. Appl. Chem. Biotechnol.*, vol. 22, no. 11, pp. 1125–1138, 1972.
- [19] M. Heikal, M. S. Morsy, and I. Aiad, “Effect of polycarboxylate superplasticizer on hydration characteristics of cement pastes containing silica fume,” *Ceram. - Silikaty*, vol. 50, no. 1, pp. 5–14, 2006.
- [20] F. Puertas, H. Santos, M. Palacios, and S. Martínez-Ramírez, “Polycarboxylate superplasticiser admixtures: effect on hydration, microstructure and rheological behaviour in cement pastes,” *Adv. Cem. Res.*, vol. 17, no. 2, pp. 77–89, 2005.
- [21] J. G. Jang, N. K. Lee, and H. K. Lee, “Fresh and hardened properties of alkali-activated fly ash/slag pastes with superplasticizers,” *Constr. Build. Mater.*, vol. 50, pp. 169–176, 2014.
- [22] S. Mindess, J. F. Young, and D. Darwin, *Concrete*, 2nd ed. Upper Saddle River, NJ: Prentice Hall, 2003.
- [23] A. Shvarzman, K. Kovler, G. . Grader, and G. . Shter, “The effect of dehydroxylation/amorphization degree on pozzolanic activity of kaolinite,” *Cem. Concr. Res.*, vol. 33, no. 3, pp. 405–416, Mar. 2003.
- [24] C. Bich, J. Ambroise, and J. Péra, “Influence of degree of dehydroxylation on the pozzolanic activity of metakaolin,” *Appl. Clay Sci.*, vol. 44, no. 3–4, pp. 194–200, May 2009.
- [25] G. Kakali, T. Perraki, S. Tsivilis, and E. Badogiannis, “Thermal treatment of kaolin: the effect of mineralogy on the pozzolanic activity,” *Appl. Clay Sci.*, vol. 20, no. 1–2, pp. 73–80, Sep. 2001.
- [26] T. Ramlochan, M. Thomas, and K. a Gruber, “The effect of metakaolin on alkali–silica reaction in concrete,” *Cem. Concr. Res.*, vol. 30, no. 3, pp. 339–344, Mar. 2000.

- [27] J. Ambroise, S. Maximilien, and J. Pera, "Properties of metakaolin blended cements," *Adv. Cem. Based Mater.*, vol. 1, no. 4, pp. 161–168, 1994.
- [28] M. Murat, "Hydration reaction and hardening of calcined clays and related minerals. I. Preliminary investigation on metakaolinite," *Cem. Concr. Res.*, vol. 13, no. 2, pp. 259–266, 1983.
- [29] G. Batis, P. Pantazopoulou, S. Tsivilis, and E. Badogiannis, "The effect of metakaolin on the corrosion behavior of cement mortars," *Cem. Concr. Compos.*, vol. 27, no. 1, pp. 125–130, Jan. 2005.
- [30] C.-S. Poon, L. Lam, S. . Kou, Y.-L. Wong, and R. Wong, "Rate of pozzolanic reaction of metakaolin in high-performance cement pastes," *Cem. Concr. Res.*, vol. 31, no. 9, pp. 1301–1306, Sep. 2001.
- [31] W. Aquino, D. A. Lange, and J. Olek, "The influence of metakaolin and silica fume on the chemistry of alkali - silica reaction products," *Cem. Concr. Compos.*, vol. 23, pp. 485–493, 2001.
- [32] N. M. Al-Akhras, "Durability of metakaolin concrete to sulfate attack," *Cem. Concr. Res.*, vol. 36, no. 9, pp. 1727–1734, Sep. 2006.
- [33] L. Courard, A. Darimont, M. Schouterden, F. Ferauche, X. Willem, and R. Degeimbre, "Durability of mortars modified with metakaolin," *Cem. Concr. Res.*, vol. 33, no. 9, pp. 1473–1479, 2003.
- [34] J. J. Brooks, M. A. M. Johari, and M. Mazloom, "Effect of admixtures on the setting times of high-strength concrete," *Cem. Concr. Compos.*, vol. 22, pp. 293–301, 2000.
- [35] Z. Li and Z. Ding, "Property improvement of Portland cement by incorporating with metakaolin and slag," *Cem. Concr. Res.*, vol. 33, no. 4, pp. 579–584, Apr. 2003.
- [36] C. S. Poon, S. C. Kou, and L. Lam, "Compressive strength, chloride diffusivity and pore structure of high performance metakaolin and silica fume concrete," *Constr. Build. Mater.*, vol. 20, pp. 858–865, 2006.
- [37] S. Wild, J. M. Khatib, and A. Jones, "Relative Strength, Pozzolanic Activity and Cement Hydration in Superplasticised Metakaolin Concrete," *Cem. Concr. Res.*, vol. 26, no. 10, pp. 1537–1544, 1996.
- [38] E.-H. Kadri, S. Kenai, K. Ezziane, R. Siddique, and G. De Schutter, "Influence of metakaolin and silica fume on the heat of hydration and compressive strength development of mortar," *Appl. Clay Sci.*, vol. 53, no. 4, pp. 704–708, 2011.

- [39] D. M. Roy, P. Arjunan, and M. R. Silsbee, "Effect of silica fume, metakaolin, and low-calcium fly ash on chemical resistance of concrete," *Cem. Concr. Res.*, vol. 31, no. 12, pp. 1809–1813, Dec. 2001.
- [40] A. Mardani-Aghabaglou, G. İnan Sezer, and K. Ramyar, "Comparison of fly ash, silica fume and metakaolin from mechanical properties and durability performance of mortar mixtures view point," *Constr. Build. Mater.*, vol. 70, pp. 17–25, 2014.
- [41] J. M. Khatib and S. Wild, "Sulphate Resistance of Metakaolin Mortar," *Cem. Concr. Res.*, vol. 28, no. 1, pp. 83–92, 1998.
- [42] Z. Wu and J. Young, "The hydration of tricalcium silicate in the presence of colloidal silica," *J. Mater. Sci.*, vol. 19, no. 11, pp. 3477–3486, 1984.
- [43] R. F. Feldman and H. Cheng-yi, "Properties of Portland cement-silica fume pastes II. Mechanical properties," *Cem. Concr. Res.*, vol. 15, no. 6, pp. 943–952, 1985.
- [44] G. A. Rao, "Investigations on the performance of silica fume-incorporated cement pastes and mortars," *Cem. Concr. Res.*, vol. 33, no. 11, pp. 1765–1770, Nov. 2003.
- [45] H. A. Toutanji and Tahar El-Korchi, "The Influence of Silica Fume on the Compressive Strength of Cement Paste and Mortar," *Cem. Concr. Res.*, vol. 25, no. 7, pp. 1591–1602, 1995.
- [46] H. A. Mohamed, "Effect of fly ash and silica fume on compressive strength of self-compacting concrete under different curing conditions," *Ain Shams Eng. J.*, vol. 2, no. 2, pp. 79–86, 2011.
- [47] T. K. Erdem and Ö. Kirca, "Use of binary and ternary blends in high strength concrete," *Constr. Build. Mater.*, vol. 22, pp. 1477–1483, 2008.
- [48] M. Gesoğlu, E. Güneyisi, and E. Özbay, "Properties of self-compacting concretes made with binary, ternary, and quaternary cementitious blends of fly ash, blast furnace slag, and silica fume," *Constr. Build. Mater.*, vol. 23, pp. 1847–1854, 2009.
- [49] R. D. Hooton, "Influence of silica fume replacement of cement on physical properties and resistance to sulfate attack, freezing and thawing, and alkali-silica reactivity," *ACI Mater. J.*, vol. 90, no. 2, pp. 143–151, 1993.
- [50] W. Kunther, B. Lothenbach, and J. Skibsted, "Influence of the Ca/Si ratio of the C–S–H phase on the interaction with sulfate ions and its impact on the ettringite crystallization pressure," *Cem. Concr. Res.*, vol. 69, pp. 37–49, 2015.
- [51] M. D. Cohen and a Bentur, "Durability of Portland Cement - Silica Fume Pastes in Magnesium Sulfate and Sodium Sulfate Solutions," *ACI Mater. J.*, vol. 85, no. 3, pp. 148–157, 1988.

- [52] Y. Kocak and S. Nas, “The effect of using fly ash on the strength and hydration characteristics of blended cements,” *Constr. Build. Mater.*, vol. 73, pp. 25–32, Dec. 2014.
- [53] Y. Fan, S. Yin, Z. Wen, and J. Zhong, “Activation of fly ash and its effects on cement properties 1,” *Cem. Concr. Res.*, vol. 29, no. December 1997, pp. 467–472, 1999.
- [54] J. Liu, Y. Zhang, R. Liu, and B. Zhang, “Effect of fly ash and silica fume on hydration rate of cement pastes and strength of mortars,” *J. Wuhan Univ. Technol. Sci. Ed.*, vol. 29, pp. 1225–1228, 2014.
- [55] C. S. Poon, L. Lam, and Y. L. Wong, “A study on high strength concrete prepared with large volumes of low calcium fly ash,” *Cem. Concr. Res.*, vol. 30, pp. 447–455, 2000.
- [56] J. Tangpagasit, R. Cheerarot, C. Jaturapitakkul, and K. Kiattikomol, “Packing effect and pozzolanic reaction of fly ash in mortar,” *Cem. Concr. Res.*, vol. 35, no. 6, pp. 1145–1151, 2005.
- [57] S. Kandasamy and M. H. Shehata, “Durability of ternary blends containing high calcium fly ash and slag against sodium sulphate attack,” *Constr. Build. Mater.*, vol. 53, pp. 267–272, 2014.
- [58] N. Ghafoori, M. Najimi, H. Diawara, and M. S. Islam, “Effects of class F fly ash on sulfate resistance of Type V Portland cement concretes under continuous and interrupted sulfate exposures,” *Constr. Build. Mater.*, vol. 78, pp. 85–91, 2015.
- [59] S. Kourounis, S. Tsivilis, P. E. Tsakiridis, G. D. Papadimitriou, and Z. Tsibouki, “Properties and hydration of blended cements with mineral alunite,” *Constr. Build. Mater.*, vol. 37, no. 2, pp. 815–822, 2007.
- [60] G. Menéndez, V. Bonavetti, and E. F. Irassar, “Strength development of ternary blended cement with limestone filler and blast-furnace slag,” *Cem. Concr. Compos.*, vol. 25, pp. 61–67, 2003.
- [61] C. M. Aldea, F. Young, K. Wang, and S. P. Shah, “Effects of curing conditions on properties of concrete using slag replacement,” *Cem. Concr. Res.*, vol. 30, pp. 465–472, 2000.
- [62] S. O. Ekolu and A. Ngwenya, “Sulphate resistance of concrete made with moderately high alumina slag,” *Constr. Mater. Struct.*, pp. 797–805, 2014.
- [63] C. Yu, W. Sun, and K. Scrivener, “Degradation mechanism of slag blended mortars immersed in sodium sulfate solution,” *Cem. Concr. Res.*, vol. 72, pp. 37–47, 2015.
- [64] S. Ogawa, H. Hyodo, H. Hirao, K. Yamada, A. Matsui, and D. Hooton, “Sulfate Resistance Improvement of Blended Cement Based on Ground Granulated Blast Furnace Slag,” *3rd ACF Int. Conf.*, pp. 499–506, 2008.

- [65] S. Ogawa, T. Nozaki, K. Yamada, H. Hirao, and R. D. Hooton, "Improvement on sulfate resistance of blended cement with high alumina slag," *Cem. Concr. Res.*, vol. 42, no. 2, pp. 244–251, 2012.
- [66] ASTM C989, "Standard Specification for Slag Cement for Use in Concrete and Mortars," *ASTM Int.*, pp. 1–8, 2013.
- [67] ASTM C1017/C1017M, "Standard Specification for Chemical Admixtures for Use in Producing Flowing Concrete," *ASTM Int.*, pp. 1–9, 2013.
- [68] ASTM C260, "Standard Specification for Air-Entraining Admixtures for Concrete 1," *ASTM Int.*, pp. 1–4, 2010.
- [69] ASTM Standard C114 2011b, *Standard Test Method for Chemical Analysis of Hydraulic Cement*. West Conshohocken, Pa.: ASTM International, 2012.
- [70] ASTM C150/C150M, "Standard Specification for Portland Cement," *ASTM Int.*, pp. 1–9, 2012.
- [71] ASTM C778, "Standard Specification for Standard Sand," *ASTM Int.*, pp. 1–3, 2013.
- [72] ASTM C1702, "Standard Test Method for Measurement of Heat of Hydration of Hydraulic Cementitious Materials Using Isothermal Conduction Calorimetry," *ASTM Int.*, pp. 1–7, 2009.
- [73] A. C. . Muller, K. L. Scrivener, A. M. Gajewicz, and P. J. McDonald, "Use of bench-top NMR to measure the density, composition and desorption isotherm of C-S-H in cement paste," *Microporous Mesoporous Mater.*, vol. 178, pp. 99–103, 2013.
- [74] ASTM C305, "Standard practice for mechanical mixing of hydraulic cement pastes and mortars of plastic consistency," *ASTM Int.*, pp. 1–3, 2014.
- [75] ASTM C1365, "Standard Test Method for Determination of the Proportion of Phases in Portland Cement and Portland-Cement Clinker Using X-Ray Powder Diffraction Analysis," *ASTM Int.*, pp. 1–10, 2011.
- [76] H. F. W. Taylor, *Cement Chemistry*, 2nd ed. London, UK: Thomas Telford Publishing, 1997.
- [77] F. Lagier and K. E. Kurtis, "Influence of Portland cement composition on early age reactions with metakaolin," *Cem. Concr. Res.*, vol. 37, no. 10, pp. 1411–1417, Oct. 2007.
- [78] A. Quennoz and K. L. Scrivener, "Interactions between alite and C3A-gypsum hydrations in model cements," *Cem. Concr. Res.*, vol. 44, pp. 46–54, Feb. 2013.

- [79] I. Odler, "Hydration, Setting and Hardening of Portland Cement," in *Lea's Chemistry of Cement and Concrete*, 4th ed., P. C. Hewlett, Ed. New York, NY: Arnold, 1998, pp. 241–297.
- [80] V. Kocaba, "Development and Evaluation of Methods to Follow Microstructural Development of Cementitious Systems Including Slags," Ecole Polytechnique Federale de Lausanne, 2009.
- [81] P. Lawrence, M. Cyr, and E. Ringot, "Mineral admixtures in mortars. Effect of inert materials on short-term hydration," *Cem. Concr. Res.*, vol. 33, no. 12, pp. 1939–1947, Dec. 2003.
- [82] D. P. Bentz, "Powder additions to mitigate retardation in high-volume fly ash mixtures," *ACI Mater. J.*, vol. 107, no. 5, pp. 508–514, 2010.
- [83] S. Dittrich, J. Neubauer, and F. Goetz-Neunhoeffler, "The influence of fly ash on the hydration of OPC within the first 44 h - A quantitative in situ XRD and heat flow calorimetry study," *Cem. Concr. Res.*, vol. 56, pp. 129–138, Feb. 2014.
- [84] G. Baert, S. Hoste, G. Schutter, and N. Belie, "Reactivity of fly ash in cement paste studied by means of thermogravimetry and isothermal calorimetry," *J. Therm. Anal. Calorim.*, vol. 94, no. 2, pp. 485–492, Sep. 2008.
- [85] B. Lothenbach, K. Scrivener, and R. D. Hooton, "Supplementary cementitious materials," *Cem. Concr. Res.*, vol. 41, no. 12, pp. 1244–1256, Dec. 2011.
- [86] K. Riding, J. Poole, K. J. Folliard, M. C. G. Juenger, and A. K. Schindler, "Modeling Hydration of Cementitious Systems," *ACI Mater. J.*, vol. 109, no. 2, pp. 225–234, 2012.
- [87] A. K. Schindler and K. J. Folliard, "Heat of Hydration Models for Cementitious Materials," *ACI Mater. J.*, vol. 102, pp. 24–33, 2005.
- [88] M. Frías, M. S. de Rojas, and J. Cabrera, "The effect that the pozzolanic reaction of metakaolin has on the heat evolution in metakaolin-cement mortars," *Cem. Concr. Res.*, vol. 30, pp. 209–216, 2000.
- [89] V. Lilkov, E. Dimitrova, and O. Petrov, "Hydration process of cement containing fly ash and silica fume: the first 24 hours," *Cem. Concr. Res.*, vol. 27, no. 4, pp. 577–588, 1997.
- [90] B. W. Langan, K. Weng, and M. A. Ward, "Effect of silica fume and fly ash on heat of hydration of Portland cement," *Cem. Concr. Res.*, vol. 32, pp. 1045–1051, 2002.
- [91] E.-H. Kadri and R. Duval, "Hydration heat kinetics of concrete with silica fume," *Constr. Build. Mater.*, vol. 23, no. 11, pp. 3388–3392, Nov. 2009.

- [92] J. Zelić, D. Rušić, D. Veža, and R. Krstulović, “The role of silica fume in the kinetics and mechanisms during the early stage of cement hydration,” *Cem. Concr. Res.*, vol. 30, no. 10, pp. 1655–1662, 2000.
- [93] M. Alexander and B. Magee, “Durability performance of concrete containing condensed silica fume,” *Cem. Concr. Res.*, vol. 29, no. 6, pp. 917–922, 1999.
- [94] J. Cabrera and M. F. Rojas, “Mechanism of hydration of the metakaolin–lime–water system,” *Cem. Concr. Res.*, vol. 31, no. 2, pp. 177–182, Feb. 2001.
- [95] R. Siddique and J. Klaus, “Influence of metakaolin on the properties of mortar and concrete: A review,” *Appl. Clay Sci.*, vol. 43, no. 3–4, pp. 392–400, Mar. 2009.
- [96] M. Antoni, J. Rossen, F. Martirena, and K. Scrivener, “Cement substitution by a combination of metakaolin and limestone,” *Cem. Concr. Res.*, vol. 42, no. 12, pp. 1579–1589, Dec. 2012.
- [97] N. Bouzoubaâ, A. Bilodeau, V. Sivasundaram, B. Fournier, and D. M. Golden, “Development of Ternary Blends for High- Performance Concrete,” no. 101, pp. 19–29, 2004.
- [98] P. K. Mehta and P. J. M. Monteiro, *Concrete: Microstructure, Properties and Materials*, 3rd ed. New York, NY: McGraw-Hill, 2006.
- [99] R. Siddique and M. I. Khan, *Supplementary Cementing Materials*, vol. 37. Berlin, Germany: Springer Berlin Heidelberg, 2011.
- [100] J. . Escalante, L. . Gómez, K. . Johal, G. Mendoza, H. Mancha, and J. Méndez, “Reactivity of blast-furnace slag in Portland cement blends hydrated under different conditions,” *Cem. Concr. Res.*, vol. 31, no. 10, pp. 1403–1409, Oct. 2001.
- [101] X. Feng, E. J. Garboczi, D. P. Bentz, P. E. Stutzman, and T. O. Mason, “Estimation of the degree of hydration of blended cement pastes by a scanning electron microscope point-counting procedure,” *Cem. Concr. Res.*, vol. 34, no. 10, pp. 1787–1793, Oct. 2004.
- [102] F. Brunet, T. Charpentier, C. N. Chao, H. Peycelon, and a. Nonat, “Characterization by solid-state NMR and selective dissolution techniques of anhydrous and hydrated CEM V cement pastes,” *Cem. Concr. Res.*, vol. 40, no. 2, pp. 208–219, Feb. 2010.
- [103] A. Schindler and K. Folliard, “Heat of hydration models for cementitious materials,” *ACI Mater. J.*, vol. 102, no. 1, pp. 24–33, 2005.
- [104] B. Lothenbach, F. Winnefeld, and R. Figi, “The influence of superplasticizers on the hydration of Portland cement,” *Proc. 12th Ina. Congr. Chem. Cem.*, pp. 9–12, 2007.

- [105] L. Xiao, Z. Li, and X. Wei, "Selection of superplasticizer in concrete mix design by measuring the early electrical resistivities of pastes," *Cem. Concr. Compos.*, vol. 29, no. 5, pp. 350–356, 2007.
- [106] ASTM C1240, "Standard Specification for Silica Fume Used in Cementitious Mixtures," *ASTM Int.*, pp. 1–7, 2014.

APPENDIX A: PERMISSION


Below is the permission for the usage of Tables 1 - 3 from Chapter 3 from the FDOT reports.

 **Victor Tran** <tranv@mail.usf.edu>
to Harvey.DeFord  Oct 27 (7 days ago) ☆  

Dear Dr. DeFord,

This is Victor Tran from USF. I am writing to ask for permission to use the technical data from FDOT contract:BDV25-977-01 and contract:BDV25-977-02 for my thesis. As per university requirements, I am required to ask for permission for any previously-published articles, tables, figures, etc.

Thank you,
Victor Tran

 **DeFord, Harvey**
to Research, me  5:03 PM (19 hours ago) ☆  

Victor – you may use the data for your thesis.

Sorry for the delay – too many interruptions.

Dale

Dale DeFord, PhD
Structural Materials Research Specialist
Office: [352-955-6671](tel:352-955-6671), Fax: [850-412-8355](tel:850-412-8355)
Office Hours: M-Th 7:00 AM-5:30 PM
harvey.deford@dot.state.fl.us

Note: Most written communications to or from state officials are public records available to the public and media upon request (Florida Statute, Chapter 119).